Investigation of the Greenland Atmospheric Boundary Layer over Summit 2002 (IGLOS). Field Phase report
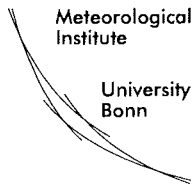
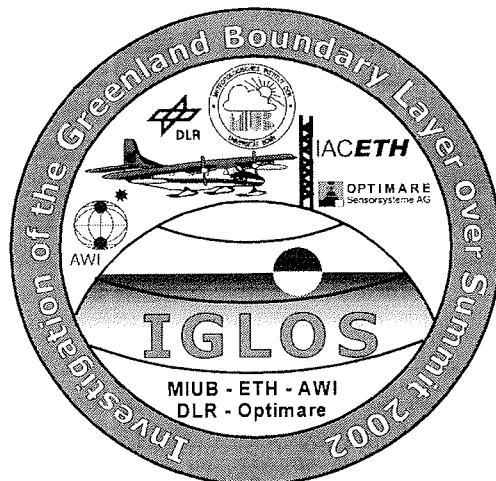## Clemens Drüe and Günther Heinemann

Meteorological
Institute

University
Bonn

Meteorological Institute of Bonn University, 2003

Corresponding authors address:
Dr. Clemens Drüe
Meteorologisches Institut Uni Bonn
Auf dem Hügel 20
D-53121 Bonn, Germany
email: clemens@uni-bonn.de

Contents

ii

Abstract

The aircraft-based meteorological field experiment IGLOS (Investigation of the Greenland boundary Layer Over Summit) was conducted in June/July 2002 over the summit region of the Greenland ice sheet. It was focused on the investigation of the stable boundary layer (SBL) over flat, homogenous snow surfaces. Such surfaces are typical for the ice sheets of the Arctic and the Antarctic. Hence, further knowledge about such SBLs is important for better understanding of the weather and climate in the polar regions.

The main tool used for IGLOS was the German research aircraft POLAR2 that is owned by the Alfred-Wegener-Institut (AWI) and is operated by the Deutsches Zentrum für Luft- und Raumfahrt (DLR). The plane was equipped with ski gear and thereby was able to operate from both, fixed runways and skiways. It was based at Kangerlussuaq in West Greenland and was transferred to Summit Camp for special observation periods (SOPs). The actual flight missions were performed from Summit Camp. The aircraft was instrumented with meteorological and radiation sensors and with the turbulence measurement system METEOPOD, which is operated by Optimare. The METEOPOD allows the determination of turbulence characteristics and turbulent heat and momentum fluxes. Furthermore, the plane was carrying a high-resolution laser altimeter that allows the determination of surface roughness structures.
At Summit Camp, the Eidgenössische Technische Hochschule Zürich (ETH) performed radiosonde ascends up to every 3 hours and operated a 50 m tower measuring mean and turbulent atmospheric quantities as well as radiation fluxes at multiple levels. 10 km south of Summit Camp, a second turbulence measurement station was set up during IGLOS to assess horizontal gradients and to yield a second independent ground truth.

A total of six flight missions have been conducted successfully. These missions cover a variety of synoptic situations. The surface inversion strength was typically in the range 10 to 20 K, the SBL heights typically ranged from 75 to 300 m. In all cases a low level jet (LLJ) could be observed. The maximum wind speed of this LLJ typically ranged from 7 to 12 ms^{-1}. The turbulence activity in general was low, SBL wave motions and periods of intermittent turbulence were observed repeatedly.

iv

1 Introduction

1.1 Goals

The experiment IGLOS (Investigation of the Greenland boundary Layer Over Summit) was conducted in June and July 2002 in central Greenland. The experiment focuses on investigations of the stable boundary layer (SBL) over the inner part of the inland ice sheet. An improved understanding of the structures of and applicable parameterizations for such stable boundary layers are of high relevance for numerical models used for weather and climate prediction as well as for air pollutant dispersion. The main goals of IGLOS are in particular:

- investigation of the 3D structures and transport processes in the SBL

- investigation of the coupling between the SBL and both, the snow surface and the free atmosphere

- creation of a dataset for validation and/or improvement of SBL parameterizations for numeric models

1.2 Scientific background

The exchange processes of energy and momentum at the snow-atmosphere interface of the polar ice sheets are key factors of the polar climate system. Throughout most of the year, the planetary boundary layer (PBL) over the polar ice sheets exhibits a stable stratification. The realistic parameterization of transport processes in the SBL is still a great challenge for numeric simulations. The inadequate formulation of SBL processes in current weather and climate models causes significant problems e.g. to recreate the energy and mass budget of the polar ice sheets in the models. This applies both, to Greenland and central Antarctica. The structure of the SBL and processes within the SBL over the ice sheets are dominated by the overlying synoptic forcing and by the forcing at the snow surface. For a better understanding of the SBL, it is therefore essential to study the relevant processes at the snow surface (energy and momentum exchange, snowdrift), in the SBL (turbulence structures, profiles of net radiation) as well in the free atmosphere (wind forcing, clouds). A short overview of SBL research aspects and recent field studies on ice sheets is given in the following, in order to point out the possible contributions of IGLOS.

Parameterizations of turbulent fluxes at the snow surface   The current parameterizations for the transport of momentum, sensible and latent heat at the snow-atmosphere interface are based on Monin-Obukhov similarity theory. Since models usually calculate surface fluxes from the lowest model level and simulated surface properties, it is usually necessary to prescribe values for the surface roughness with respect to momentum and heat (z_0 and z_T). For z_0 a number of studies is available in literature, e.g. by Heinemann (1989) or König (1985).

The estimation of z_T nevertheless is still an open question. According to Andreas (1987) z_T is *smaller* than z_0. A contrasting study of Cassano et al. (2001) for the Brunt shelf in Antarctica (near Halley) concludes that z_T seems to be about a factor 80 *above* z_0. In the same study, seven parameterizations taken from current weather and climate models are tested. It turns out that these show in general a tendency to underestimate the surface turbulent heat fluxes in the presence of strong stability. Although the study comprises a total of 45 month of measurements at Halley Station, Antarctica, between February 1995 and October 1998, strongly stable stratification occurred only in quite rare cases.

This also applies for a four-week period in the southern summer 1994, when turbulence measurements were carried out at the Georg-von-Neumayer station (Handorf, 1996, Handorf et al., 1999). In this experiment, the stability parameter z/L at 2 m height exceeded the value of 1.6 only one single time.

Therefore, Cassano et al. (2001) recommend the conduction of similar experiments on the inner Antarctic plateau, which applies to the inner part of the Greenlandic inland ice sheet, too.

Past studies of the SBL over Greenland concentrated on the lowest part of the PBL. To contribute to the improvement of numerical models, it is necessary to incorporate processes in the upper portion of the SBL, where the PBL is coupled with the free atmosphere. Furthermore, the stratification of the free atmosphere above the PBL has to be considered for several parameterizations based on Monin-Obukhov similarity theory or the SBL height (Zilitinkevich and Mironov, 1996; Zilitinkevich and Calanca, 2000). Under extremely stable conditions, transports by gravity waves and the modification of the similarity functions by radiation processes have to be considered, too (Forrer and Rotach, 1997). As an example, in Figure 1 measured data are compared to the formulation of Högström (1988), Webb (1970) and the scheme used in the ECHAM numerical models. The plot shows considerable differences between observation and calculation even at moderate Richardson numbers $(Ri \approx 0.07)$.

Parameterizations of turbulent transports in the SBL   For the description of turbulence structures within the SBL, the concept of local scaling has proven to be a useful tool for mid-latitude conditions. This concept was introduced by Nieuwstadt (1984) using measurements of the 200 m tower in Cabauw (Netherlands). The main advantage of this kind of SBL scaling is the fact that scaled variables from different experiments are comparable, and a deeper understanding of the SBL can be achieved by combining different data sets. Recent studies (Forrer, 1999; Heinemann, 2002) have indicated that this concept can also be applied to the SBL over polar ice sheets.

The validation of the local scaling behavior of the SBL and the derivation of appropriate similarity functions require turbulence measurements extending over the full SBL height. This requirement was fulfilled by the KABEG experiment (see below), while only the lower part of the SBL was covered by turbulence measurements in most cases by Forrer (1999). An example of the KABEG results is given in Figure 2, which displays the scaled standard deviation of the vertical wind as a function of the local stability over the whole stability range of the KABEG
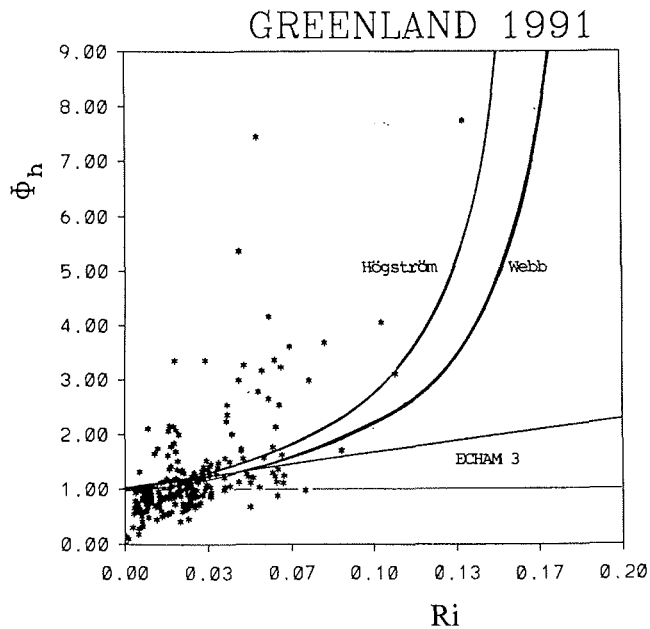
GREENLAND 1991

Figure 1.: Plot of ϕ_h against the gradient Richardson number Ri for stable stratification measured by Forrer and Rotach (1997) at 2 m height. The curves represent the non-dimensional gradients calculated using the formulation of Högström (1988), of Webb (1970) and the scheme used in the ECHAM numerical models. The Figure was kindly supplied by A. Ohmura.

measurements averaged over stability classes. The error bars show the standard deviation of the averaged values within the stability classes, individual measurement errors are much smaller. The scaled σ_w follow the local similarity behavior, that is an increase for small stabilities and constant values for large stabilities (z-less scaling). The saturation value lies slightly above the value of 1.4 found by Nieuwstadt (1984), but is within the error bars. However, the KABEG data enable the study of local similarity for much larger stabilities than shown in Nieuwstadt (1984). The error bars are even smaller than in Nieuwstadt (1984), which means that the SBL over the Greenland ice sheet seems to behave in a more consistent way than nighttime mid-latitude SBLs.

Previous field studies   During the last ten years, two larger field experiments were conducted over Greenland to investigate the surface energy balance and PBL structure.

The first was the Greenland Ice Margin Experiment (GIMEX, Oerlemans and Vugts (1993) in conjunction with the ETH Greenland Expedition 1990-1993 (Forrer and Rotach, 1997). This experiment was conducted during summer conditions in the ablation zone of the western slope of the inland ice sheet (near Kangerlussuaq and near Ilulissat, see Figure 5). Tethered balloon soundings were per-
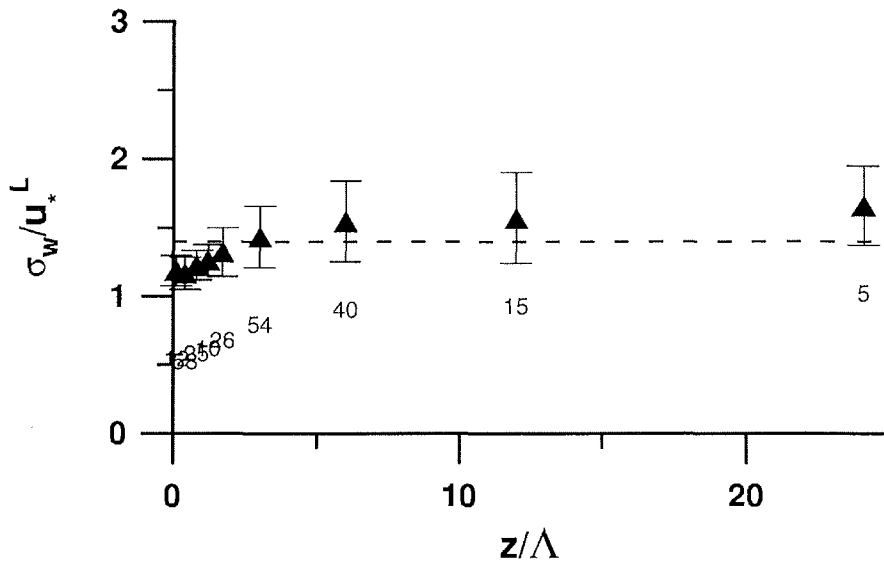
Figure 2.: Standard deviation of the vertical wind scaled with the local shear velocity as a function of local stability from KABEG data. Data points represent averaged values within stability classes, numbers indicate the number of individual measurements (about 250 in total). Error bars show the standard deviation of the averaged values within the stability classes. The dashed line marks a constant value of 1.4 as proposed by Nieuwstadt (1984).

formed near the ice margin (Van den Broeke et al., 1994), mast measurements in the lowest 30 m above the inland ice were made to determine fluxes via the eddy correlation method (Forrer and Rotach, 1997) and remote sensing techniques were applied to investigate the SBL structure over the inland ice (Meesters et al., 1997).

The second field study was the aircraft based experiment KABEG (Katabatic Wind and Boundary Layer Front Experiment around Greenland), which was conducted in April/May 1997 as part of the Arctic Climate SYstems Study (ACSYS). The experimental areas were around Kangerlussuaq, Angmassalik and Ilulissat (Heinemann, 1998). In this experiment, direct turbulence measurements covering the whole boundary layer depth over the ice sheet were made for the first time. Due to the strong katabatic flows during KABEG, only moderate positive Richardson numbers values were encountered in the SBL, and the SBL was found to be fully turbulent.

Besides specially designed experiments, long-term monitoring of the near-surface climate is a valuable source of information. The Greenland Climate Network (GC-Net; Steffen et al., 1996; Steffen and Box, 2001) was set up as a part of PARCA (Project for Arctic Regional Climate Assessment). The automatic weather stations of this network are collecting temperature, radiation, and wind data over the Greenland ice sheet since 1996. The measurements of the PARCA stations

have been used to validate mesoscale models, e.g. in Klein (2000) and Bromwich et al. (2001). The largest differences between simulations and observations occurred over central Greenland, especially during low-wind conditions.

The snow surface The energy budget of a snow surface, in particular under stable PBL conditions with small turbulent fluxes, is significantly influenced by processes inside the snow. If these processes are not adequately considered in numerical models, the snow surface temperature can be over- or underestimated. In turn, this implies wrong results for the simulated exchange processes at the snow-atmosphere interface. For this reason, more complex models of the physical processes in the snow volume recently get more into the focus of atmospheric and glaciologic modelers (Jordan, 1991; Greuell and Konzelmann, 1994; Lehning et al., 1999; Rowe et al., 1995). These snow models again need precisely parameterized turbulent fluxes between the snow surface and the PBL.
Finally, the exchange of momentum between the atmosphere and the snow surface is strongly linked to snow drift. The mass transport by the snow drift significantly contributes to the actual snow accumulation. Water sublimation and the increased specific weight of the ice-in-air suspension potentially even force the katabatic flows (Bintanja, 2000). Current snow drift models are based on surface layer models for different stratification regimes. These are again based on various SBL parameterizations.

Benefits from the IGLOS experiment The current deficits in SBL data sets and parameterizations demand for further studies of the SBL and the overlying lower portion of the free atmosphere over snow surfaces. Since the expected results are rather basic, undisturbed conditions over flat homogenous terrain are desirable. Such terrain is found in central Antarctica or, much better accessible, around the Greenland summit. As will be pointed out in detail in the following sections, the ETH Zürich has run radiation flux measurements on a 50 m mast at Summit Camp that allow the determination of the radiation flux divergences during the occurrence of strongly stable PBL situations. Vertical profiles of mean and turbulent quantities measured by the ETH 50 m tower in the same place yield excellent opportunities to understand and quantify the turbulent processes in the SBL. Combining these efforts with an aircraft-based experiment offers the opportunity to directly record turbulence structures and mean quantities at the same time in the SBL and in the lower free atmosphere, where they are inaccessible even with the most advanced ground instrumentation. The IGLOS experiment has the potential to yield a significant contribution to SBL research, since it was designed as a coordinated experiment of different international research groups at Summit Camp. The combination of snow physics measurements, stationary high-precision radiation and turbulence measurements, and aircraft data will yield high-quality dataset for the SBL over Greenland, which may be used for the validation and the improvement of SBL parameterizations for regional and climate numerical models and of the turbulence statistics from large eddy simulations (LES).

1.3   Participants and acknowledgments

IGLOS was an experiment of the Meteorologisches Institut der Universität Bonn (MIUB) in cooperation with the Alfred-Wegener-Institut Bremerhaven (AWI). The aircraft measurements were coordinated with the Institute for Atmospheric and Climate Science (IACETH) of the Eidgenössische Technische Hochschule Zürich (ETH). The research aircraft POLAR2 was operated by the Deutsches Zentrum für Luft- und Raumfahrt (DLR). The aircraft instrumentation was operated by Optimare, Bremerhaven. The mission freight logistics were organized by DLR. The Greenland Summit Camp is funded by the United States National Science Foundation (NSF) and is operated by VECO Polar Resources, Boulder.

Thanks go to Dr. Jörg Hartmann (AWI) and Heinz Finkenzeller (DLR) for help and support during the preparation phase. Stefan Schröder from DLR is acknowledged for organizing the experiment logistics. Thanks are expressed to Prof. Dr. Atsumu Ohmura of IACETH for enabling the ETH measurements during IGLOS. Thanks go to Optimare for making the experiment possible despite an extremely tight schedule.

The IGLOS field experiment participants were the DLR pilots Martin Hinterwaldner (until 05 July), Hans-Jürgen Berns (after 05 July) and Phillip Weber, the DLR flight engineers Siegfried "Siggi" Judt (until 05 July) and Jens Hammer (after 05 July), the Optimare instrument operators Dr. Axel Bochert, Dr. Thomas Garbrecht and Henning Hinrichs (until 10 July), and the MIUB researchers Prof. Dr. Günther Heinemann (mission leader) and Dr. Clemens Drüe (starting 30 June).

For support during the experiment, thanks go to:
- VECO Polar Resources Camp Crew for smooth handling of the POLAR2 visits at Summit Camp and for all their additional help,
- the Danish Meteorological Institute (DMI) in Copenhagen and Kangerlussuaq for comprehensive weather information and satellite data,
- the ETH Summit Crew (Sebastian Hoch and Saskia Bourgeois) for help with the surface instrumentation,
- VECO Polar Resources Kangerlussuaq Crew for various practical help,
- Bernd Maurer at MIUB for help preparing the sonic anemometer,
- Greenlandair and SFJ Air Traffic Control (ATC) for assistance accomplishing the flight operations, and
- The Danish Polar Center (DPC) for giving all necessary permits.

Until end of 2002, a considerable amount of data has been supplied by different groups and organizations, which we would like to acknowledge:
- Prof. Dr. Atsumu Ohmura and his group at ETH Zürich (in particular Sebastian Hoch and Peter Schelander) for processing and supplying the tower, radiosonde, and radiation data collected at Summit Camp,
- Konrad "Koni" Steffen from the Cooperative Institute for research in environmental sciences (CIRES) in Boulder, Colorado for the data from the automatic weather stations (AWS) of the GC-Net,

- the Danish Meteorological Institute at Kangerlussuaq (DMI-Nord) for supplying the High Resolution Picture Transmission (HRPT) satellite data received at Kangerlussuaq,
- Simon Ekholm and Kort & Matrikelstyrelsen for supply of the high resolution digital elevation model (DEM) of Greenland (Ekholm, 1996), obtained from the NSIDC-DAAC, University of Colorado in Boulder (NSIDC, 1997),
- The GLOBE Project at NGDC for publicly publishing their global high resolution DEM (Hastings and Dunbar, 1998),
- the U.S. National Oceanic and Atmospheric Administration (NOAA) for making the Global Area Coverage (GAC) satellite data accessible via the Satellite Active Archive (SAA), and
- Wetteronline (Bonn, Germany) for collecting and supplying the WMO Global Telecommunication System (GTS) weather report data.

2   Experiment setup

2.1   Experimental area

During IGLOS, the research aircraft POLAR2 was based at Kangerlussuaq (for-
merly known as Søndre Strømfjord; 67.0° N, 50.7° W; see Figures 3 + 5) in West
Greenland. This place was chosen, because it provides good logistic conditions.
Among these are heated aircraft hangars, daily flights to and from Europe, of-
fice space and storage facilities. Furthermore, the Greenland dependency of the
Danish Meteorological Institute (DMI-Nord) is located at Kangerlussuaq airport,
providing first-hand weather information and real-time polar orbiter satellite data.
The POLAR2 was temporarily transferred from Kangerlussuaq to Summit camp for
special observation periods (SOPs), when adequate conditions for flight missions
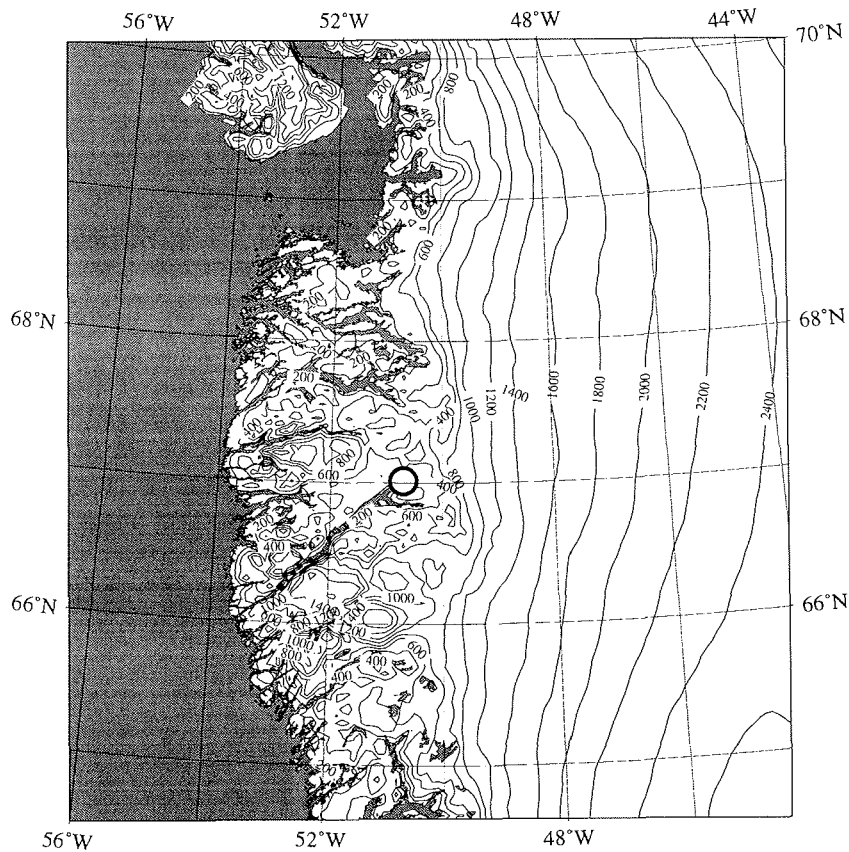in the summit area were expected.

Figure 3.: West Greenland topography (Ekholm dataset; NSIDC, 1997). The circle marks Kanger-
lussuaq, the elevation contour interval is 200 m, sea level surfaces are displayed as grey areas.

The actual flight missions to investigate the SBL were launched from Summit Camp (72.6°N, 38.5°W; see Figures 4 + 5). The Greenland summit region provides an area of roughly 200 x 300 km² with almost perfectly homogeneous surface properties and virtually no gradients in topography (easily seen by comparing the local maps of the West Greenlandic tundra in Figure 3 and of the summit region in Figure 4; note the contour intervals). Because of its elevation of more than 3000 m, this region is also comparable to the inner Antarctic. Due to these properties, the summit region is a unique region on the northern hemisphere to study the SBL. Summit Camp is located in the heart of this region and offers full expedition support like a huge plane fuel depot, the longest prepared skiway worldwide, guest housing opportunities (tents) and fixed satellite communication links that allow the acquisition of updated weather information during stays away from Kangerlussuaq.
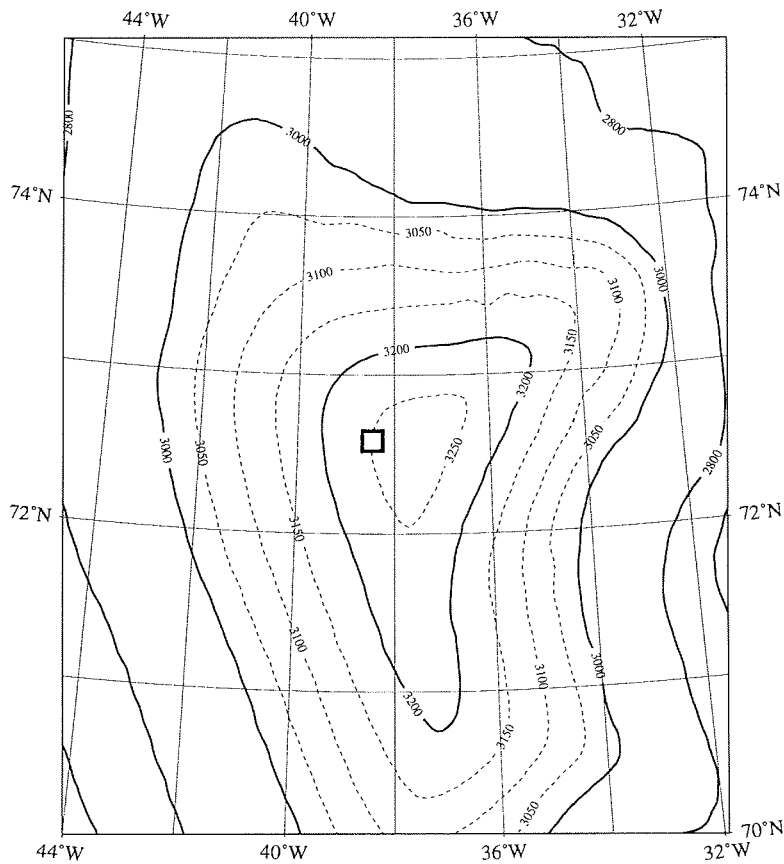

Figure 4.: Topography of the Greenland summit region (Ekholm dataset; NSIDC, 1997). The square marks Summit Camp, the elevation contour interval is 200 m (50 m levels are dashed above 3000 m).
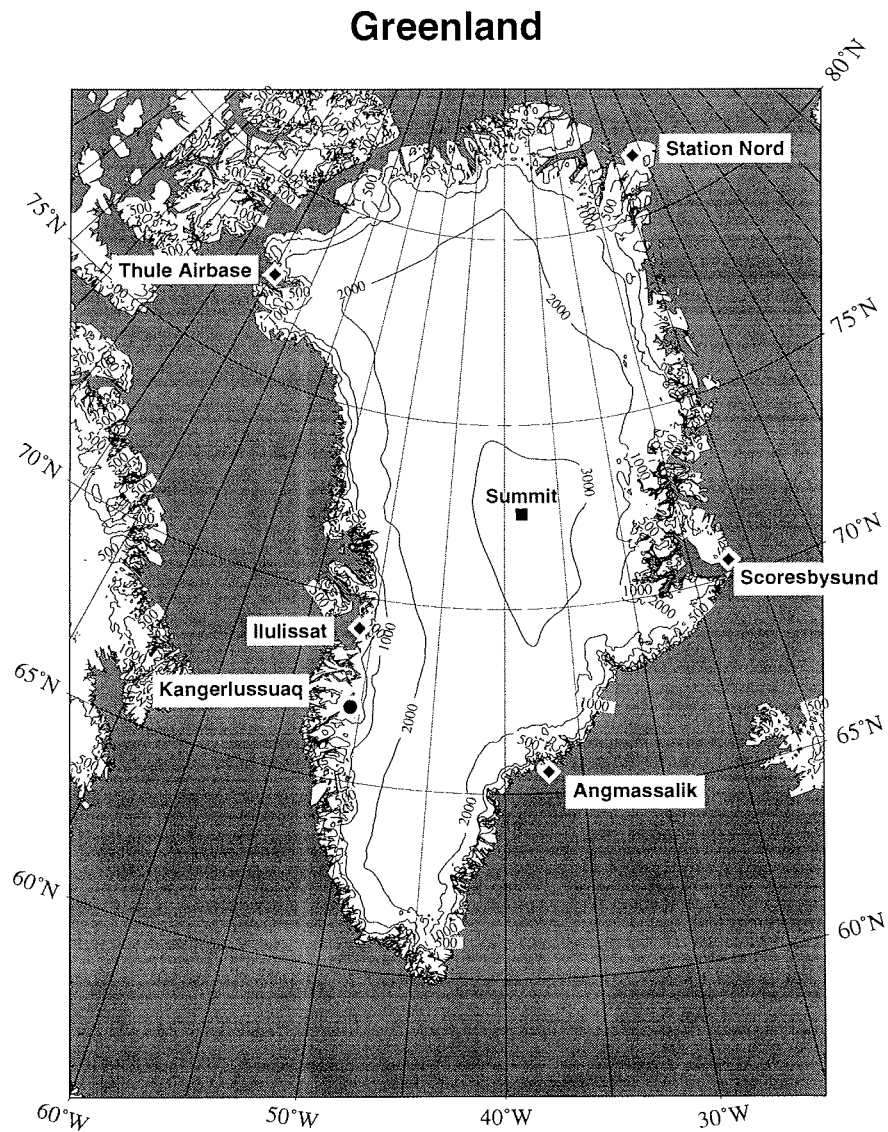
Greenland

Figure 5.: Greenland topography (GLOBE dataset; Hastings and Dunbar, 1998). The circle marks Kangerlussuaq, the square marks Summit Camp. Selected other places are marked by diamonds. The elevation contour interval is 1000 m; sea level surfaces are displayed as grey areas.

2.2   Field phase chronology

Preparation phase

10 Oct 2001:	Preparation meeting at AWI in Bremerhaven
14 Feb 2002:	Preparation meeting at AWI in Bremerhaven
12 Mar 2002:	Application forms sent to DPC
22 Mar 2002:	Received radio permit for Greenland from DPC
29 May 2002:	Preparation meeting at AWI in Bremerhaven
31 May 2002:	Received scientific expedition permit from DPC
May-Jun 2002:	Integration of the aircraft instrumentation, installation of ski gear and ground tests
07 Jun 2002:	Surface station equipment sent from MIUB to Bremerhaven
12-14 Jun 2002:	Test flights with POLAR2 in Bremerhaven
18 Jun 2002:	Equipment sent to Kangerlussuaq

Experiment phase

21 Jun 2002:	Arrival of airfreight at Kangerlussuaq
24 Jun 2002:	Arrival of POLAR2 at Kangerlussuaq
25 Jun 2002:	Installation of the full aircraft instrumentation
26+28 Jun 2002	Inspection flights with full instrumentation
29 Jun 2002:	Calibration flight CAL1
02-04 Jul 2002	First SOP of POLAR2 at Summit Camp (SOP1):
02 Jul 2002	Installation of station S9
04 Jul 2002	Flight mission SBL1, partial data loss by computer trouble
05 Jul 2002	POLAR2 crew changed
08-12 Jul 2002	Second SOP of POLAR2 at Summit Camp (SOP2):
09 Jul 2002:	Flight mission SBL2
10 Jul 2002:	Flight missions SBL3 and SBL4
11 Jul 2002:	Flight mission SBL5
12 Jul 2002:	Flight mission SBL6 and dismount of station S9
16-22 Jul 2002	Third SOP of POLAR2 at Summit Camp (SOP3):
18-22 Jul 2002	No takeoff possible (see Section 3.2).
23+24 Jul 2002	Removal of ski gear from POLAR2 and inspection flight

25 Jul 2002	Calibration flight CAL2, removal of the scientific equipment from the plane and departure of POLAR2 from Kangerlussuaq
26 Jul 2002	All equipment sent back to Germany

Wrap-up phase

03 Sep 2002:	Preliminary data processing by Optimare completed
16-20 Sep 2002:	Post calibration of all sensors at DLR in Oberpfaffenhofen
26 Sep 2002:	De-briefing of IGLOS at AWI in Bremerhaven
Jan 2003:	Final data processing by Optimare completed

2.3 Aircraft and instrumentation

The research aircraft used for IGLOS was the German POLAR2 (Figure 64 in Appendix C), a Dornier Do228 of 6 ton maximum weight and 17 m wingspan. The plane was equipped with skies for the flights at Summit Camp. The skies were mounted to the plane's landing gear that was locked in downward position. It is possible to land on fixed runways by hydraulically pulling up the skies. Hence, the plane could start and land at Summit Camp skiway as well as at Kangerlussuaq airport. All service and maintenance needed during IGLOS was done at the parking position in the Greenlandair hangar at Kangerlussuaq. When the plane was parked at Summit Camp, the engines were wrapped with thermal insulating boots and the plane was electrically re-heated prior to any takeoff.

Besides navigational and basic meteorological instrumentation the aircraft was also equipped with upward and downward looking sensors for solar and terrestrial radiation, a downward looking radiation thermometer and a high precision laser altimeter to determine surface roughness (Table I). The aircraft was carrying the turbulence measurement system METEOPOD (Figure 65 in Appendix C) under the right wing. The METEOPOD allows high-resolution measurements of turbulence spectra and statistic quantities like variances and turbulent heat, moisture, and momentum fluxes (Table II).

Table I: POLAR2 aircraft instrumentation

Quantity	Sampling	Sensor, manufacturer
Position	1 Hz	GPS, Garmin
Position/orientation	45Hz	INS, Honeywell Lasernav
Height	20 Hz	Radar altimeter
	2000 Hz	Laser altimeter, Ibeo
Pressure/airspeed	20 Hz	Pitot tube and static pressure sensor, Rosemount
Surface temperature	20 Hz	KT-4, Heimann
Radiation fluxes	20 Hz	2 Pyranometer, Eppley PSP
		2 Pyrgeometer, Eppley PIR
Temperature	20 Hz	Pt100, Rosemount
Humidity	20 Hz	Humicap + Pt100, Aerodata

Table II: METEOPOD turbulence measurement system instrumentation

Quantity	Sampling	Sensor, manufacturer
Orientation	60 Hz	INS, Litton LTR81
Height	100 Hz	Radar altimeter, TRT
3D airspeed	100 Hz	5-hole probe, Rosemount
Temperature	100 Hz	Pt100 open wire, Rosemount modified by AWI
	100 Hz	Reverse Flow open wire, AWI
Humidity	100 Hz	Lyman-α, AIR
	100 Hz	Humicap/Pt100, Vaisala/Aerodata
	100 Hz	Dew point mirror, General Eastern

2.4 Surface based measurements

At Summit Camp, the ETH Zürich did operate a 50 m profiling mast ("Swiss Tower", ST) from July 2001 to August 2002. (Operation will presumably continue in summer 2003.) This tower is equipped with cup anemometers, wind vanes, temperature, and humidity sensors at multiple levels between 0.5 and 50 m above ground (Tab. IV). Unfortunately, the wind vanes were not in operation during the IGLOS field phase. The snow temperature was monitored by a thermistor chain at eight levels between 0.3 and 15 m below the snow surface. Data from this instrumentation are supplied by the ETH Zürich for a period covering all IGLOS flight missions (01 July 2002 - 15 July 2002).

In addition to these conventional sensors, the mast was equipped with 3D sonic anemometers and Krypton fast hygrometers at four and three levels, respectively (Tab. IV). Furthermore, the radiation balance was measurement by up- and downward looking pyranometers and pyrgeometers at four levels. The uppermost of these levels was variable between 35 and 50 m.

The ETH also regularly launched rawinsondes from Summit every 12 hours from July 2001 through the end of August 2002. During intensive observation periods the launch interval was reduced down to three hours. Data from the ascends closest to the IGLOS flight missions were also supplied by the ETH. The available ascends are listed in Table III. Finally, the cloud cover and height was observed and photographed every six hours by the ETH Summit crew.

During the experiment, a supplementary turbulence measurement station was set up by the MIUB 10 km south of Summit Camp. This station is called "S9" and consisted of one 3D sonic anemometer at three meters height. The purpose of this station is to determine horizontal gradients of the low level wind speed and direction and of the turbulent fluxes. It also served as a second, independent

ground truth for the aircraft measurements. This station was operational during two periods covering IGLOS flight missions (02-04 July, 08-12 July).

The Cooperative Institute for research in environmental sciences (CIRES) in Boulder, Colorado operates the GC-Net, a network of currently 18 surface stations all over Greenland (Steffen et al., 1996). These stations are measuring basic quantities like air temperature, wind speed, wind direction, humidity and pressure, but also accumulation rate, radiation fluxes and snowpack conductive heat fluxes. Data from the summer season 2002 are still being processed and will be supplied for all 18 operational stations.

All available METAR and Synop Reports from Greenland were collected and supplied by WetterOnline.

Table III: List of the available Radiosonde Ascends

date	time (UTC)	top in hPa	Asc. Nr (ETH)
03 Jul 2002	2339	286	603
04 Jul 2002	0256	54	604
04 Jul 2002	1140	590	605
08 Jul 2002	2340	35	618
09 Jul 2002	0300	36	619
09 Jul 2002	0550	38	620
09 Jul 2002	0839	64	621
09 Jul 2002	1145	46	622
09 Jul 2002	2340	35	625
10 Jul 2002	0251	36	626
10 Jul 2002	0550	45	627
10 Jul 2002	0840	33	628
10 Jul 2002	1140	39	629
10 Jul 2002	2032	73	630
10 Jul 2002	2340	54	631
11 Jul 2002	0240	75	632
11 Jul 2002	1140	43	633
11 Jul 2002	2340	41	634
12 Jul 2002	0240	39	635
12 Jul 2002	1140	90	636

Table IV: List of the operational surface stations around Summit Camp

Site	measured quantity	height in m	instrumentation
	wind speed	0.5, 1, 2, 5, 10, 20, 35, 50	cup anemometer, Aanderaa
	wind direction	10, 35, 50	wind vane, Aanderaa
	3D wind vector	2, 5, 10, 50	sonic anemometers, Gill R2
Swiss Tower 72° 34.6' N 38° 27.3' W	humidity fluctuations	2, 10, 50	Krypton hygrometers, Campbell KH2O
	long and shortwave radiation fluxes	0.5, 2, 10, 35-50 (lift)	ventilated Eppley PIR and Kipp & Zonen CM21/11
	snow temperature	-0.3, -0.5, -1, -2 -7.5, -10, -15	Thermistor chain
	local pressure	0	digital microbarograph
S9 72° 28.9' N 38° 27.8' W	3D wind vector, virt. temperature (+ fluctuations)	3	3D sonic anemometer, METEK USA-1
Summit AWS 72.5794 N 38.5042 W	Wind Speed + direction, air temperature, pressure and radiation balance	2 levels, height is constantly monitored and recorded	see: Steffen et al. (1996) or: Steffen and Box (2001)

2.5 Satellite data

The DMI-Nord at Kangerlussuaq operates a receiving station for High Resolution Picture Transmissions (HRPT) from the NOAA (U.S. National Oceanic and Atmospheric Administration) satellites. These data were recorded at DMI-Nord and supplied specifically for the IGLOS flight missions. The HRPT records contain full resolution data from the Advanced Very High Resolution Radiometer (AVHRR) on board of the NOAA satellites. These data have a maximum nadir resolution of 1.1 km. From additional orbits, Global Area Coverage (GAC) data were acquired after the end of the field phase from the NOAA Satellite Active Archive (SAA) (http://www.saa.noaa.gov/). These GAC data have a maximum nadir resolution of 4 km.

The operational NOAA satellites during IGLOS were NOAA-11, 12 and 14 trough 16. The AVHRR sensor on NOAA-11 is broken, the AVHRR sensors on NOAA-14 and 15 are retroactively classified as degraded due to problems with the scan motor. NOAA-14 data are not usable at all, while NOAA-15 data can be usable after quality control.

The available HRPT data for the IGLOS flights are listed in Tables V + VI:

Table V: List of available HRPT-Transmissions recorded by DMI Nord for IGLOS

Case	Date	UTC time	Lines	Filename (Sat.-Name)
SBL1	04 Jul 2002	0255	3610	0207040255.NOAA16.185
	04 Jul 2002	0436	4848	0207040436.NOAA16.185
	04 Jul 2002	0549	2851	0207040549.NOAA12.185
	04 Jul 2002	0617	3964	0207040617.NOAA16.185
	04 Jul 2002	0727	4672	0207040727.NOAA12.185
	04 Jul 2002	0758	4894	0207040758.NOAA16.185
	04 Jul 2002	0908	4927	0207040908.NOAA12.185
	04 Jul 2002	0938	4647	0207040938.NOAA16.185
	04 Jul 2002	1048	4705	0207041048.NOAA12.185
	04 Jul 2002	1118	4294	0207041118.NOAA16.185
SBL2	08 Jul 2002	1906	4976	0207081906.NOAA12.189
	08 Jul 2002	2006	5134	0207082006.NOAA14.189
	09 Jul 2002	0521	5074	0207090521.NOAA16.190
	09 Jul 2002	0702	5123	0207090702.NOAA16.190
	09 Jul 2002	0814	4439	0207090814.NOAA14.190
	09 Jul 2002	0847	4964	0207090847.NOAA12.190
	09 Jul 2002	0955	5040	0207090955.NOAA14.190
	09 Jul 2002	1028	4806	0207091028.NOAA12.190
	09 Jul 2002	1135	4959	0207091135.NOAA14.190

Table VI: Continuation of (Table V)

Case	Date	UTC time	Lines	Filename (Sat.-Name)
SBL3	09 Jul 2002	1703	4205	0207091703.NOAA16.190
	10 Jul 2002	0329	4099	0207100329.NOAA16.191
	10 Jul 2002	0510	5017	0207100510.NOAA16.191
	10 Jul 2002	0651	2598	0207100651.NOAA16.191
	10 Jul 2002	0702	1205	0207100702.NOAA16.191
SBL4	10 Jul 2002	0832	4844	0207100832.NOAA16.191
	10 Jul 2002	1012	4393	0207101012.NOAA16.191
	10 Jul 2002	1152	4258	0207101152.NOAA16.191
	10 Jul 2002	1331	4931	0207101331.NOAA16.191
	10 Jul 2002	1510	5167	0207101510.NOAA16.191
	10 Jul 2002	1652	4980	0207101652.NOAA16.191
SBL5	10 Jul 2002	1818	5070	0207101818.NOAA12.191
	11 Jul 2002	0318	3841	0207110318.NOAA16.192
	11 Jul 2002	0459	4981	0207110459.NOAA16.192
	11 Jul 2002	0619	3801	0207110619.NOAA12.192
	11 Jul 2002	0640	2668	0207110640.NOAA16.192
	11 Jul 2002	0651	1133	0207110651.NOAA16.192
	11 Jul 2002	0759	4890	0207110759.NOAA12.192
	11 Jul 2002	0821	4873	0207110821.NOAA16.192
	11 Jul 2002	0939	5003	0207110939.NOAA12.192
SBL6	11 Jul 2002	1754	5003	0207111754.NOAA12.192
	11 Jul 2002	1934	4870	0207111934.NOAA12.192
	12 Jul 2002	0307	3761	0207120307.NOAA16.193
	12 Jul 2002	0448	4918	0207120448.NOAA16.193
	12 Jul 2002	0629	2223	0207120629.NOAA16.193
	12 Jul 2002	0639	1735	0207120639.NOAA16.193
	12 Jul 2002	0700	1735	0207120700.NOAA16.193
	12 Jul 2002	0735	4743	0207120735.NOAA12.193
	12 Jul 2002	0810	4885	0207120810.NOAA16.193
	12 Jul 2002	0915	4967	0207120915.NOAA12.193
	12 Jul 2002	0950	4659	0207120950.NOAA16.193
	12 Jul 2002	1131	4269	0207121131.NOAA16.193

3 Flight mission overview

3.1 Flight strategy
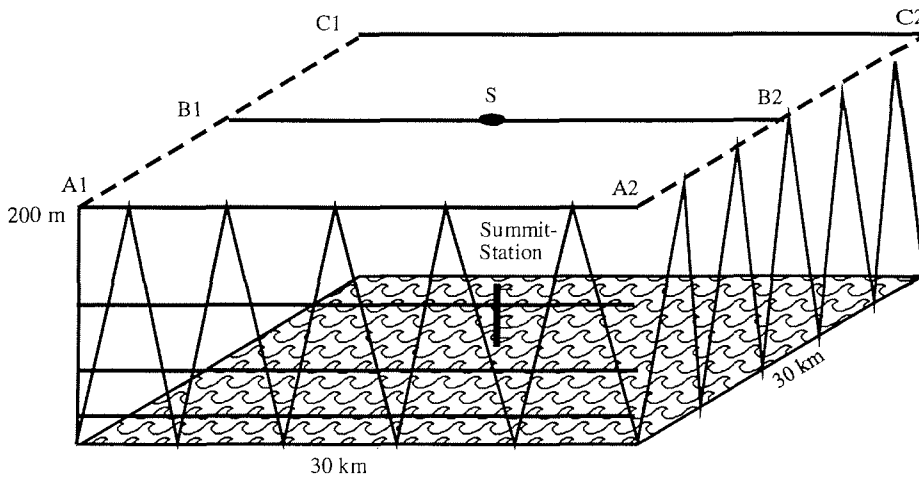
Figure 6.: SBL flight strategy: The geographical positions of the corners and intersections are marked by A1 to C2; S denotes the position of Summit Camp. For clarity, vertical profiles and constant level runs are displayed on the front sides of the box only.

The basic flight pattern to investigate the SBL structure is a box with 30 km by 30 km base and typically 200 m height (Figure 6). The orientation of the box depends on the low-level flow direction. The actual box height is determined according to the vertical PBL structure found during an initial high aircraft temp flown right after takeoff.

The flight pattern itself consists of two main elements:

- A series of vertical profiles ("temps") between the minimum flight level and the box ceiling, flown around the box and along the central leg. These vertical profiles are intended to acquire the 3D structure of the PBL in a short period of time. In Figure 6 the series of profiles is displayed only on the front sides of the box, but a full series e.g. is flown along the positions A1-A2-C2-C1-A1-A2-B2-B1.

- Constant level runs at various heights above ground, typically 30, 60, 100 and 200 m, on one or multiple legs (A, B or C). These runs allow the determination of turbulent fluxes and fine scale variations such as gravity waves. In Figure 6 such runs are only displayed for leg A (connecting positions A1-A2).

To assess the temporal evolution of the PBL structures, parts of these patterns are repeated after full completion of one pattern.

The pattern is located above or in close vicinity to the present surface stations, which yield ground truth for the aircraft measurements. Especially the 50 m Swiss Tower is used to assess the contrasts between the minimum flight level and the surface.

To encounter the most stable PBL stratification in the Arctic summertime, the pattern needs to be flown during clear nights, and the takeoff time has to be close the occurrence of the daily temperature minimum.

The incidence of such clear weather has to be forecasted over at least 36 hours in Kangerlussuaq, mainly based on the model predictions of the DMI. If convenient conditions are expected, the plane is transferred to Summit Camp.

The final decision whether a flight mission is performed, has to be made immediately prior to the scheduled take-off, depending to the local weather conditions (fog or low clouds).

3.2   Overview of the flight missions

As mentioned before, the flight missions were in general performed in clear nights to find situations with the most stable PBL stratification. For three periods, such conditions were expected for the Greenland summit region and the POLAR2 was transferred from Kangerlussuaq to Summit Camp.

Since the Swiss Tower is higher than the lowest scheduled flight levels, the pilots preferred to move the flight pattern away from it. Hence, the whole pattern was shifted in up-wind direction by approximately 20 km to keep at least the station S9 inside the boundaries of the pattern. The orientation was chosen in a way that one of the legs (A, B or C) always was pointing to S9 and (except one case) also to the Swiss Tower. This leg in effect represented the flow upstream of the surface stations.

A total of six flight missions could be performed during the experiment. One flight (SBL1) took place during the first period lasting from 02 July to 05 July, five flights (SBL2-6) were performed during the second period between 07 July and 13 July and no flights could be performed during the last period between 16 July and 22 July.

The last period turned out to be especially problematic. Beginning on 17 July, the air temperature in the summit region rose almost to the freezing point and did not sink below roughly -10° before 22 July. The high temperatures cause the snow surface to get very soft, which strongly increases the friction of the aircrafts skis. Due to this effect, the plane was not able to reach takeoff speed and neither flight missions nor a return to Kangerlussuaq were possible for five consecutive days.

Table VII: Overview of the flight missions: ΔT_0 denotes the difference between the temperature maximum in the inversion to the radiometrically measured surface temperature, ΔT_{mfl} denotes the temperature difference between the temperature maximum and temperature at the minimum flight level (radiation temperatures for SBL1 are not yet available). The upper air flow information is determined from the high aircraft temps. The LLJ was below the minimum flight level during SBL5; the corresponding values are derived from the Swiss Tower measurements.

Flight	Time	characteristics					
		general	inversion		low level jet		upper air flow
			height	$\Delta T_{0/mfl}$	height	max.	
	UTC		m	K	m	m/s	m/s (dir)
CAL1	29 Jun 2002, 1620-1830	Sc	–	–/–	–	–	9 (170)
SBL1	04 Jul 2002, 0350-0630	surface fog, approach-ing Ac, Ci	100	– / 7	45, 80	9, 12	12 (200)
SBL2	09 Jul 2002, 0345-0700	surface fog, Ci	300	20 / 8	50	7	5 (290)
SBL3	10 Jul 2002, 0315-0555	6/8 Ac, Ci	100, 250	11 / 8, 11 / 9	45, 200	9, 9	7 (220)
SBL4	10 Jul 2002, 0715-1005	some Ac, Sc	250	11 / 9	203	9	7 (220)
SBL5	11 Jul 2002, 0010-0230	growing Ac	100	17 / 2	(10)	(4.5)	2.5 (260)
SBL6	11 Jul 2355-12 Jul 0310	surface fog, approa-ching low-level Sc	100	11 / 8	85, 120	13, 12	12 (140)
CAL2	25 Jul 2002, 1230-1415	thin Sc	–	–/–	–	–	7 (350)

3.3   Flight missions in detail

3.3.1   SBL1: 04 July 2002

During SBL1 the flight program (see Figure 9) started with a high (to 900 m) aircraft temp on the central leg (B1-B2, for positions see Table VIII and Figure 7), followed by a series of shallow aircraft temps (to 450 m) around three quarters of the outer rectangle of the flight pattern (B2-C2-C1-A1-A2). Then two constant level runs at 30 and 75 m height were flown along A2-A1-B2-B2-C2-C1 and back, respectively. Next, a constant level run at 150 m height was flown along A2-A1-C1. The flight pattern ended after another high temp between C1 an Summit Camp. Unfortunately a significant fraction of the data from this flight (approximately the first hour) were lost due problems with the data acquisition system. The available data of the majority of the sensors start during the last descent on (B1-A1), see Figure 9.

Table VIII: Geographic positions of the waypoints for the flight pattern during SBL1.

| Position name	Lat	Lon
	in deg	
A1	72.4917	-39.2983
A2	72.2433	-39.3550
B1	72.4816	-38.4633
B2	72.2467	-38.5200
C1	72.4633	-37.6483
C2	72.2150	-37.7067
S9	72.4816	-38.4633
Summit	72.5800	- 38.4567
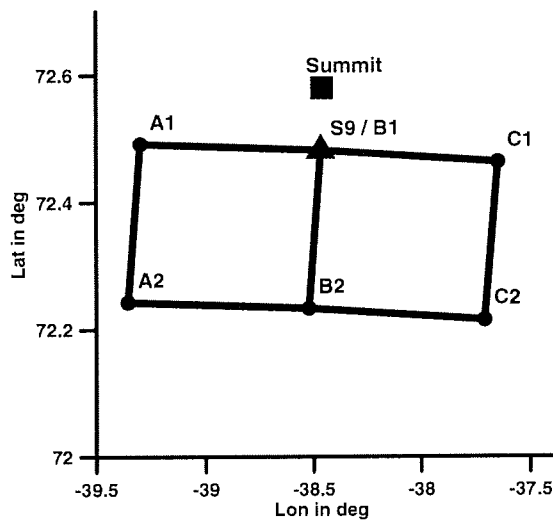
Figure 7.: Schematic plot of the flight pattern orientation during SBL1.

Figure 8.: Photo taken during SBL1 (04 Jul 2002, approx. 0400 UTC): The surface is covered by surface fog, note the wave structures of the fog top. No clouds were present at the beginning of the flight mission.
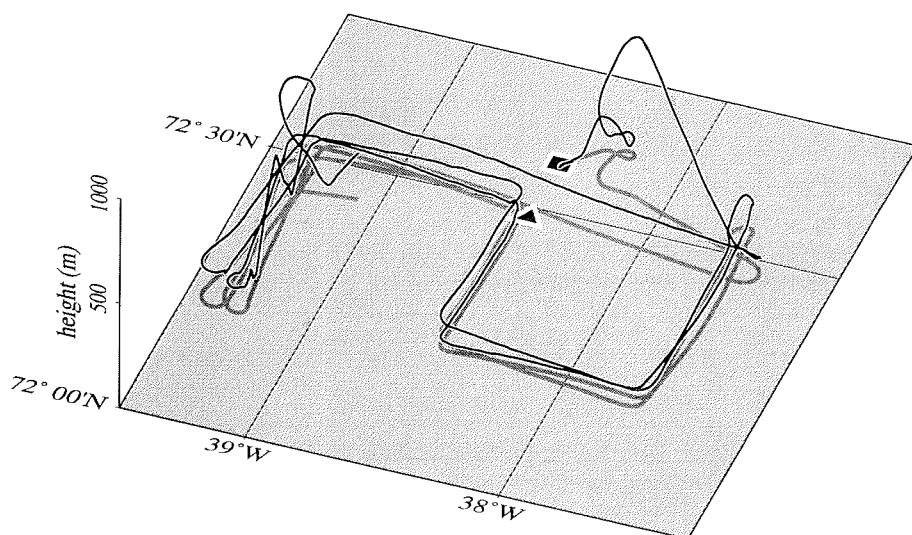
Figure 9.: SBL1 recorded flight path: perspective view from southeast. The square represents Summit Camp, the triangle marks position S9. The gray line depicts the projection of the 3D trajectory onto the ground. The horizontal axes give geographic latitude and longitude, respectively; the vertical axis gives the height (above ground level).
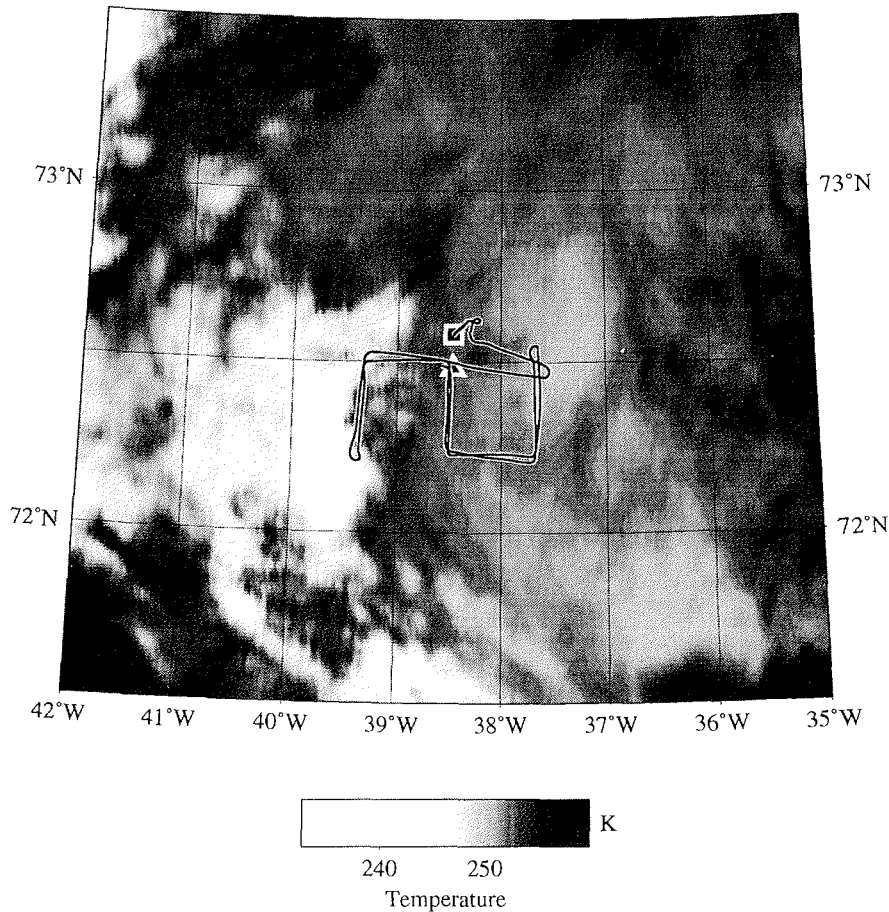
Figure 10.: SBL1 flight path (0350 - 0630 UTC) superimposed to the infrared satellite image taken during the flight (NOAA16, Ch.4, 04 July 2002, 0436 UTC).

The synoptic situation during SBL1 was characterized by a system of high pressure over Northeast Greenland, a trough over the Davis strait and a low over Southwest Greenland (marked by a cloudy area in the satellite picture; Figure 11). The resulting moderate pressure gradient over Central Greenland led to winds of around 5 ms^{-1} from S to SSE in the Greenland summit region according to the NCEP analysis (Fig. 12). In the measurement area, patches of surface fog were present throughout the flight SBL1 (visible in Figure 10). The photo taken shortly after takeoff (Figure 8) shows such a path that exhibits clear signatures of wave motions.. The high clouds visible in Figure 11 over west Greenland extended just to the measurement area.

NOAA 16 Channel 4
04.07.2002 04:36 UTC

K

230 240 250 260 270 280
Temperature
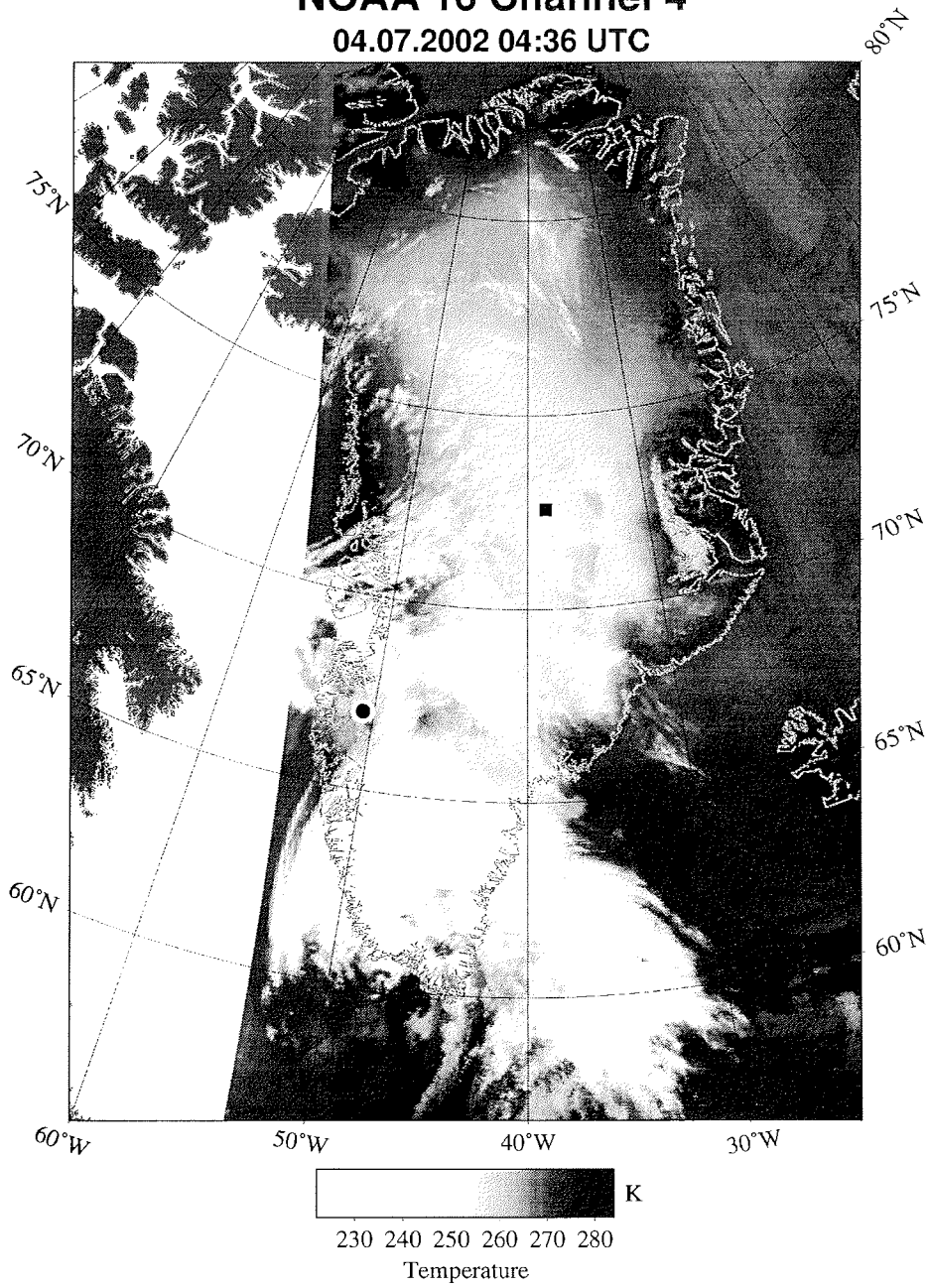
Figure 11.: NOAA 16 channel 4 infrared image 04 July 2002, 0436 UTC: Brightness temperature in K. The square marks Summit Camp, the circle marks Kangerlussuaq.
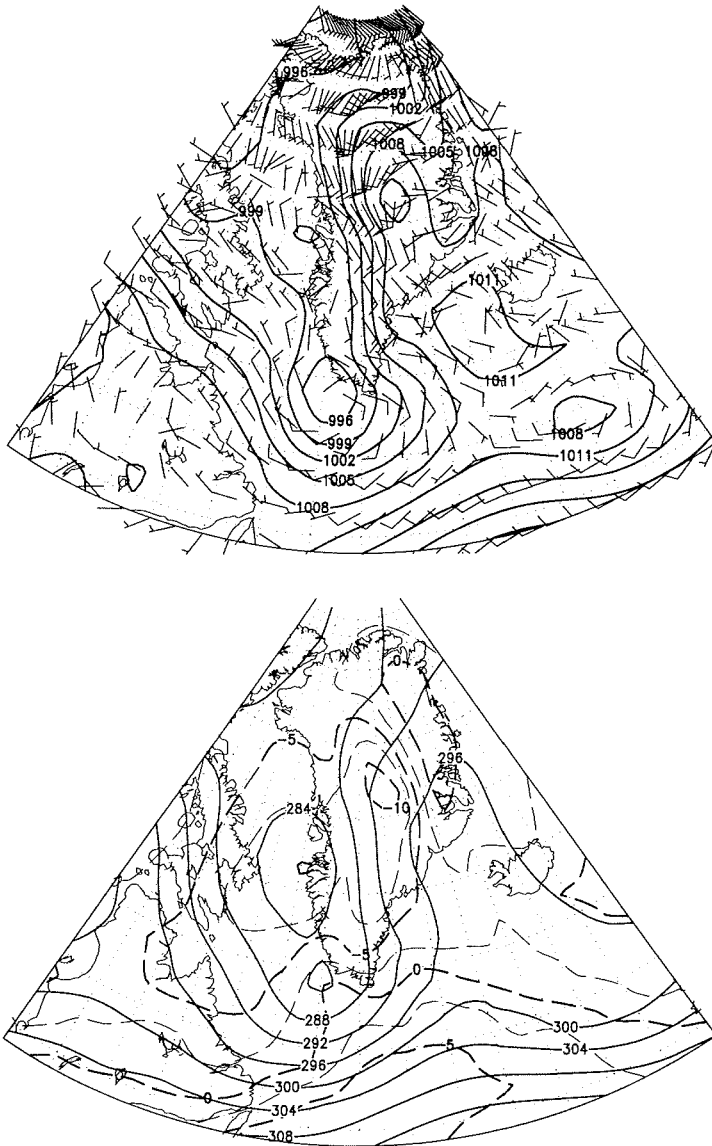
Figure 12.: NCEP Analysis 04 July 2002: The displayed fields represent the arithmetic mean (supplied by NCEP) of the 00 and 12 UTC operational analyses. **Upper panel:** MSLP (isolines every 3 hPa) and surface wind (vectors, half barb: 2.5 ms^{-1}, full barb: 5 ms^{-1}) **Lower panel:** 700 hPa geopotential height (isolines every 4 gpdm) and air temperature (dashed isolines every 2.5 °C)

3.3.2 SBL2: 09 July 2002

The flight program during SBL2 (see Figure 15) started with a high aircraft temp (to 800 m) diagonal to the flight pattern (C1-A2, for positions see Table IX and Figure 13), followed by a series of 450 m-high aircraft temps, first along the central leg (B2-B1) and then around the outer legs of the flight pattern (B1-A1-A2-C2-C1-B2). Then constant level runs were flown along the central leg (B1-B2) at four different heights ($\approx$ 30, 60, 120, 180 m). Next, the aircraft temps along the leg (B1-B2) were repeated, followed again by four constant level flights along (B1-B2) at the same levels as before. The pattern was finished after another high aircraft temp (to 800 m) along (B1-B2). Before landing, the plane went around Summit Camp to thoroughly check the visibility, because of the present light surface fog.

Table IX: Geographic positions of the waypoints for the flight pattern during SBL2.

| Position name	Lat	Lon
	in deg	
A1	72.2483	-39.0833
A2	72.1133	-38.2366
B1	72.3650	-38.7866
B2	72.2300	-38.0167
C1	72.4816	-38.5617
C2	72.3467	-37.7900
S9	72.4816	-38.4633
Summit	72.5800	- 38.4567
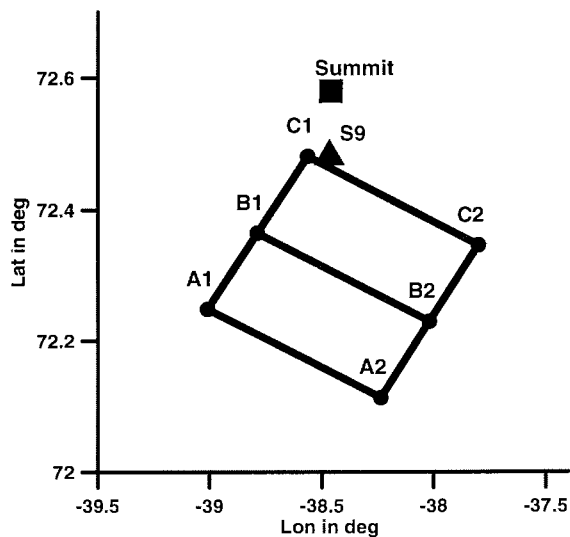
Figure 13.: Schematic plot of the flight pattern orientation during SBL2.

Figure 14.: Photo taken during SBL2 (09 Jul 2002, 0426 UTC): The snow surface is covered with a thin translucent fog layer.
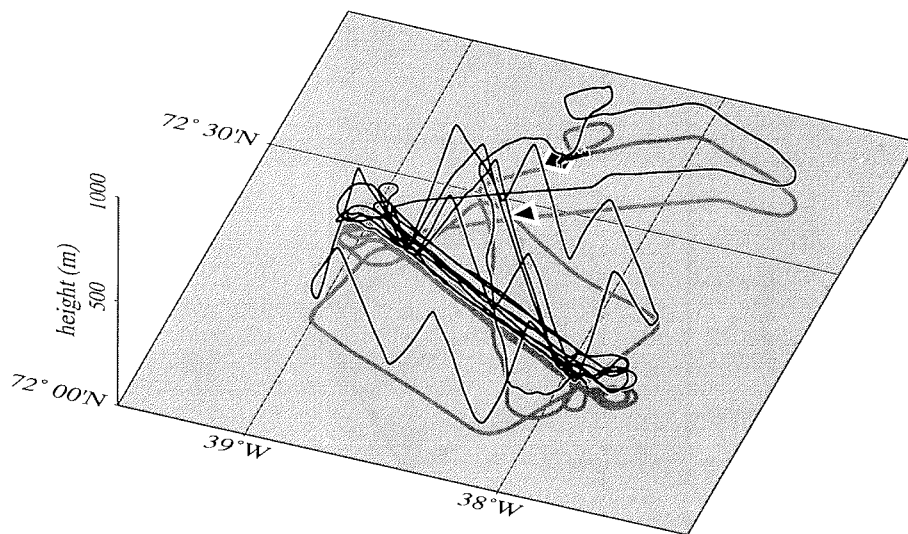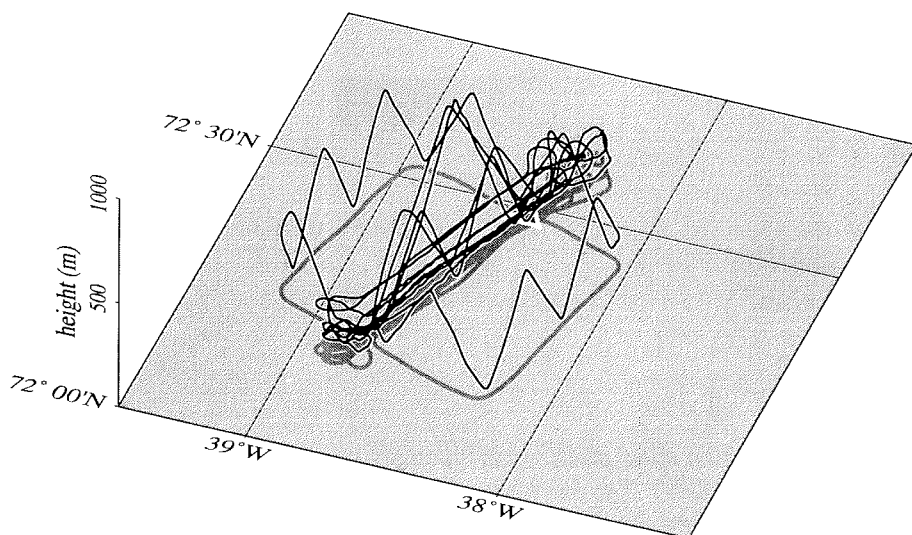

*Figure 15.*: SBL2 flight path, same representation as Figure 9.
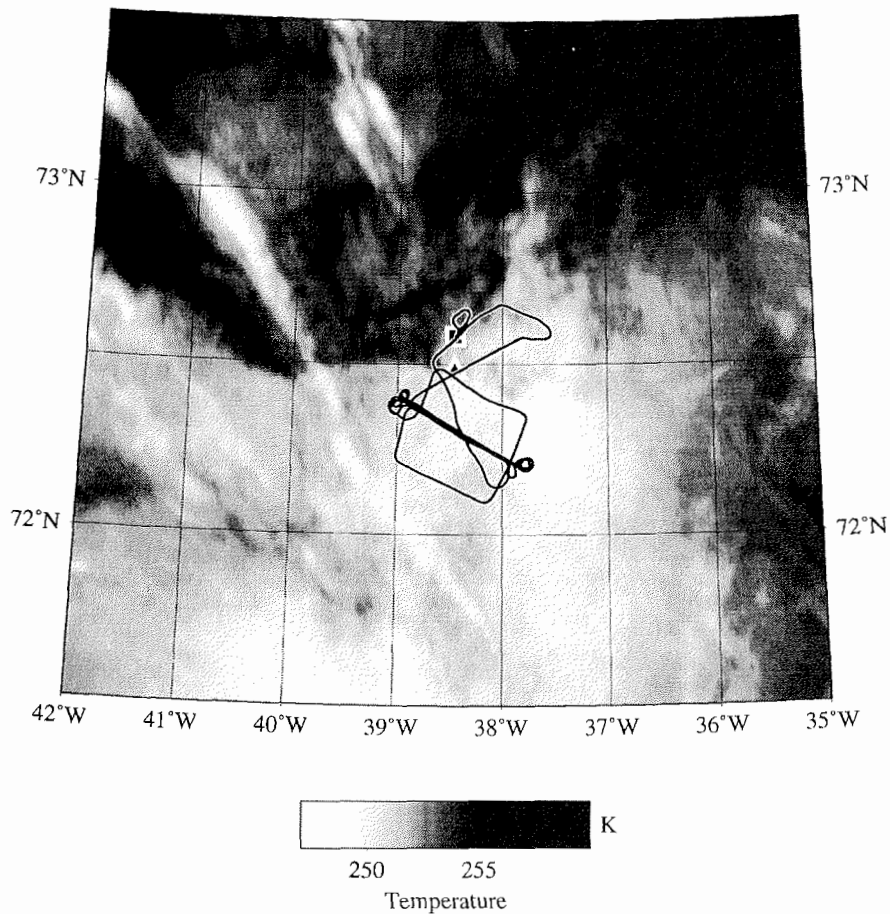
Figure 16.: SBL2 flight path (0345 - 0700 UTC) superimposed to infrared satellite image (NOAA16, Ch.4, 09 July 2002, 0521 UTC).

The synoptic situation during SBL2 is dominated by a high over Central Greenland and strong pressure gradients over the northern slope of the inland ice cap. The NCEP analyses surface winds near the summit to be around 2.5 to 5 ms^{-1} from NNW (Figure 18). The eastern slope of the inland ice was cloud free, while on the western side high clouds developed during the night (Figure 17). The clouds visible in the satellite picture over Southwest Greenland are associated with a low over Labrador. North of the investigation area, vast patches of surface fog are visible in the satellite image (Figure 16). A light surface fog extended even south to Summit Camp. The fog was rather thin, as can be seen in Figure 14.
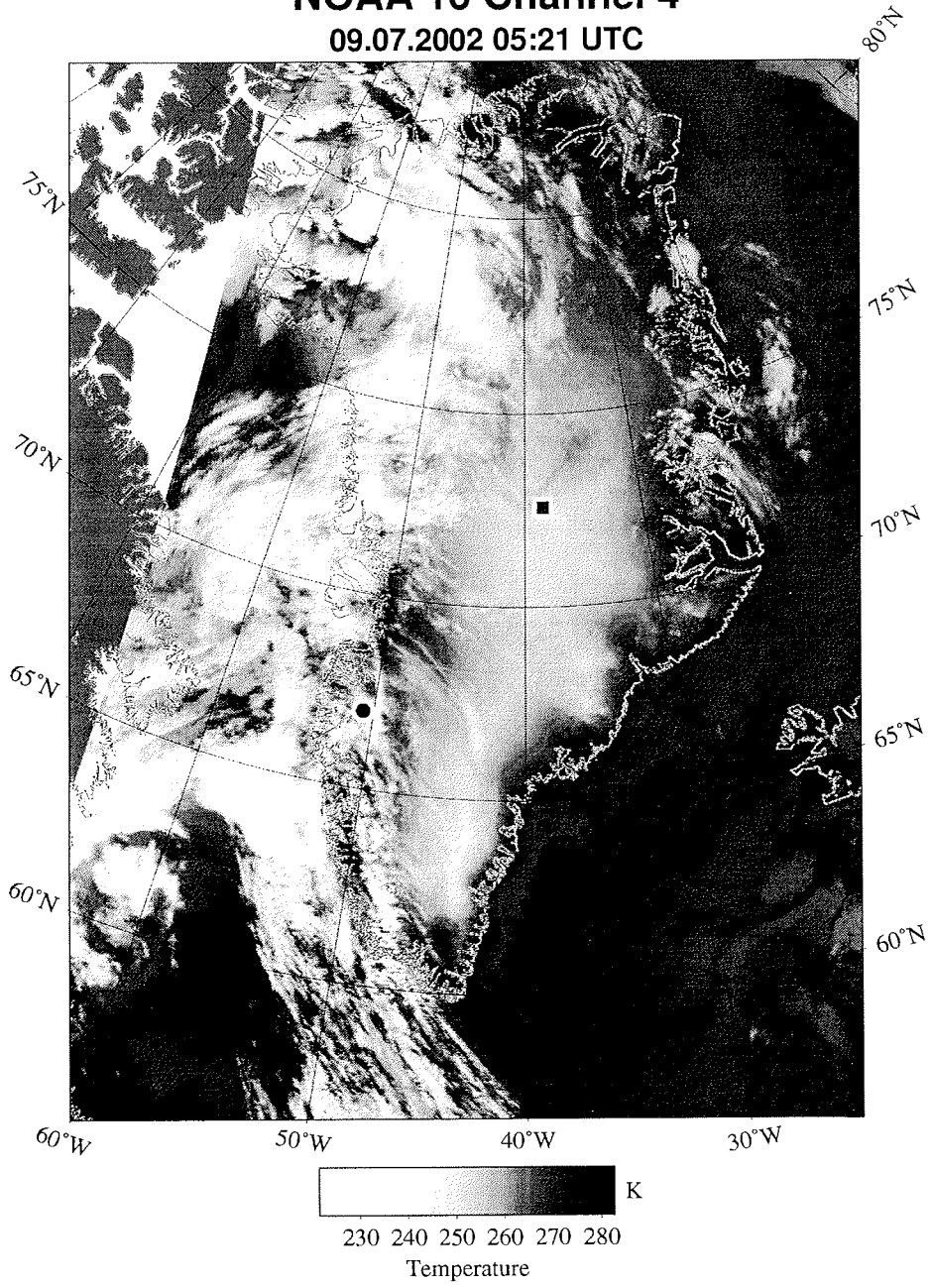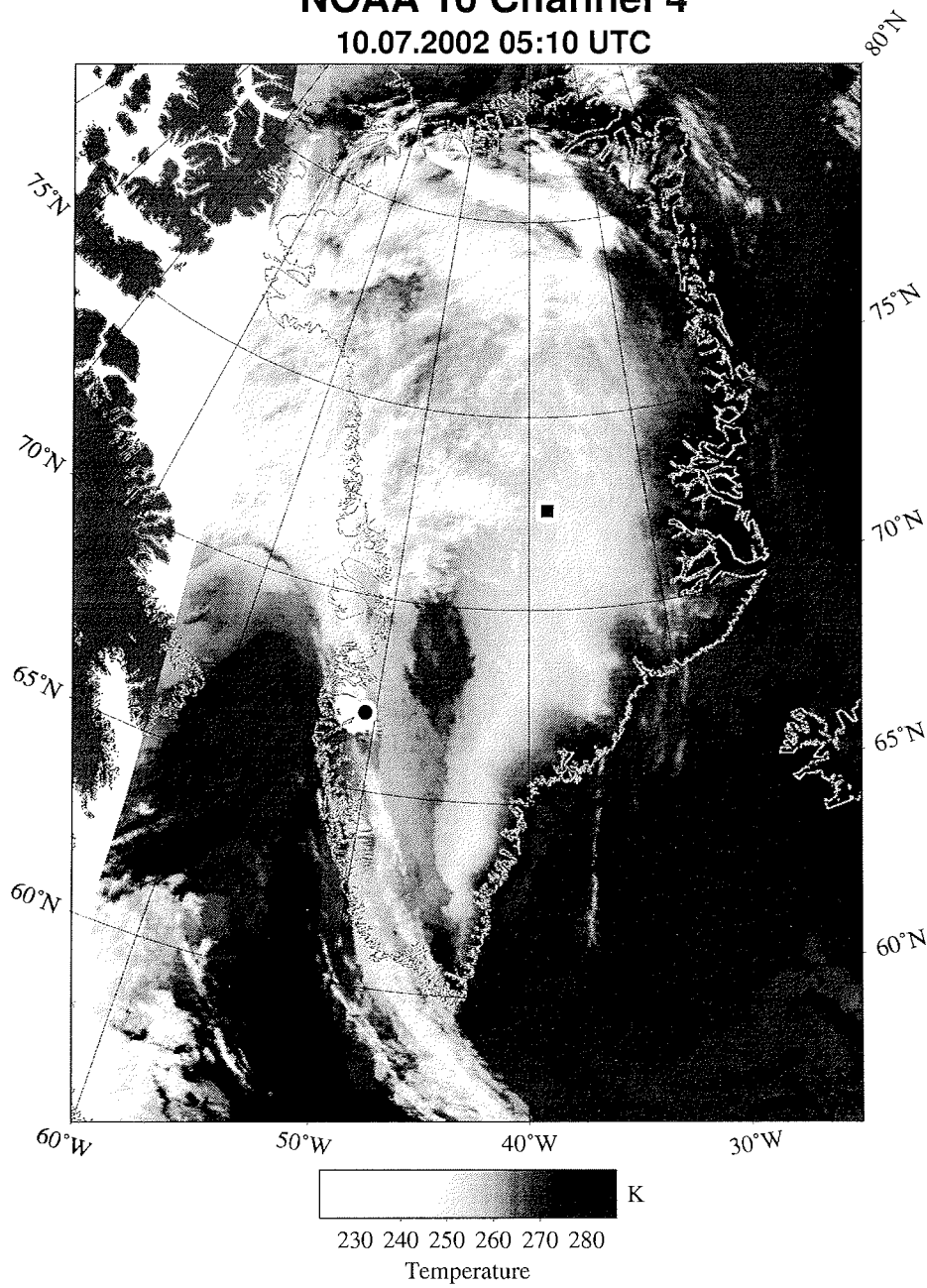
Figure 17.: NOAA 16 channel 4 infrared image 09 July 2002, 0521 UTC, same representation as Figure 11.
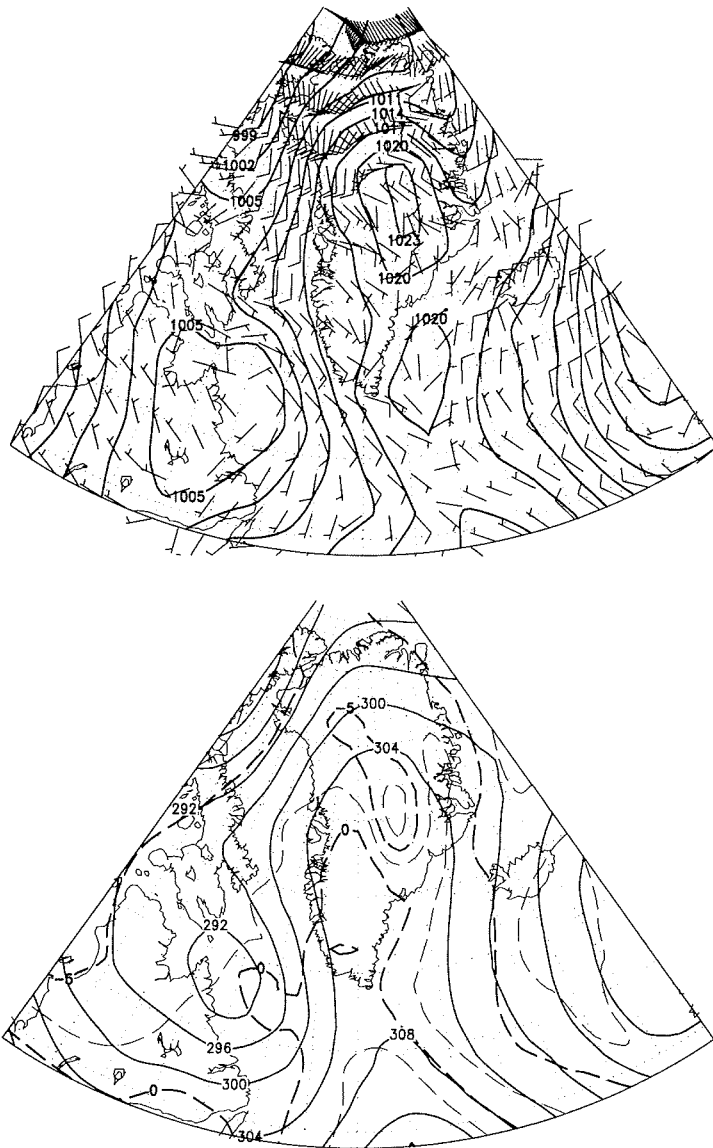
Figure 18.: NCEP Analysis 09 July 2002, 00/12 UTC, same representation as Figure 12

3.3.3   SBL3: 10 July 2002

The flight program during SBL3 (see Figure 21) started with a high aircraft temp (to 900 m) on the central leg of the flight pattern (B1-B2, for positions see Table X and Figure 19), followed by a series of 450 m-high aircraft temps around the outer legs of the flight pattern (B2-C2-C1-A1-A2-B2). Then constant level runs were flown along the central leg (B1-B2) at four different heights ($\approx$ 30, 60, 120, 200 m), followed by a series of aircraft temps (to 450 m) along this leg (B1-B2). Next, the constant level runs as well as the temps on the central leg (B1-B2) both were repeated. The pattern was finished by a high aircraft temp (to 900 m) along (B1-B2).

Table X: Geographic positions of the waypoints for the flight pattern during SBL3.

| Position name	Lat	Lon
	in deg	
A1	72.5117	-38.8850
A2	72.2567	-39.1816
B1	72.4650	-38.4633
B2	72.2117	-38.7650
C1	72.4183	-38.0417
C2	72.1650	-38.3500
S9	72.4816	-38.4633
Summit	72.5800	- 38.4567
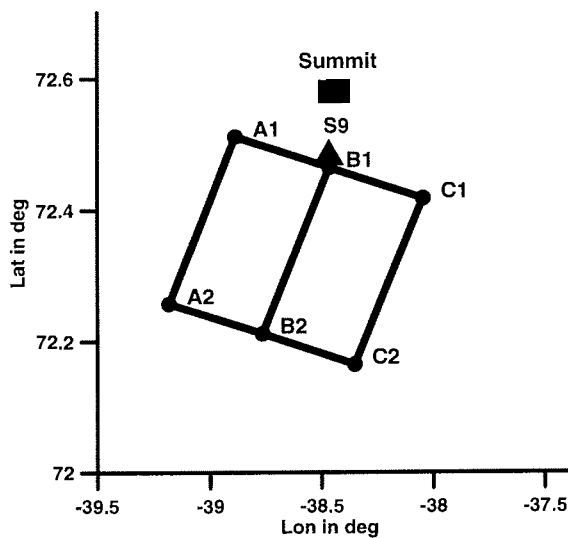
Figure 19.: Schematic plot of the flight pattern orientation during SBL3.

Figure 20.: Photo taken during SBL3 (10 Jul 2002, 0507 UTC): The sky is partly covered by high clouds, the snow surface is well visible.
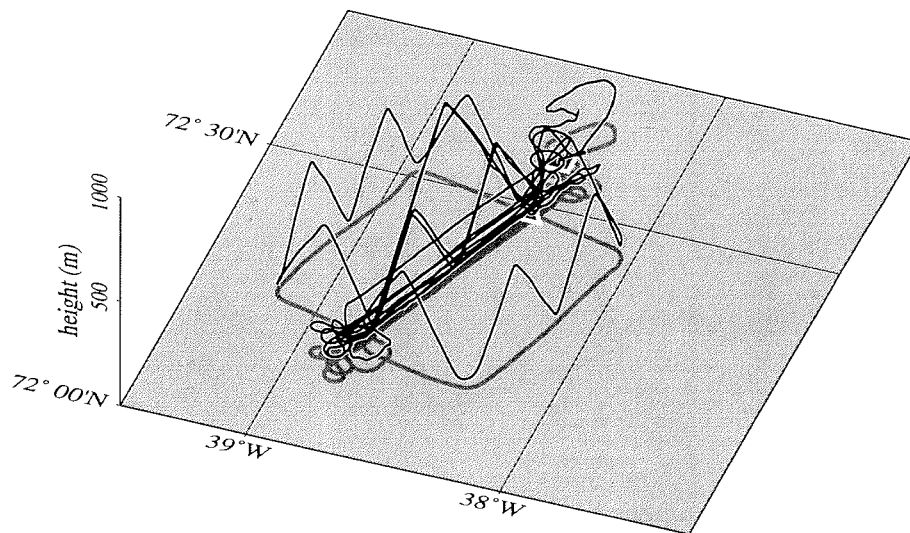

Figure 21.: SBL3 flight path, same representation as Figure 9.
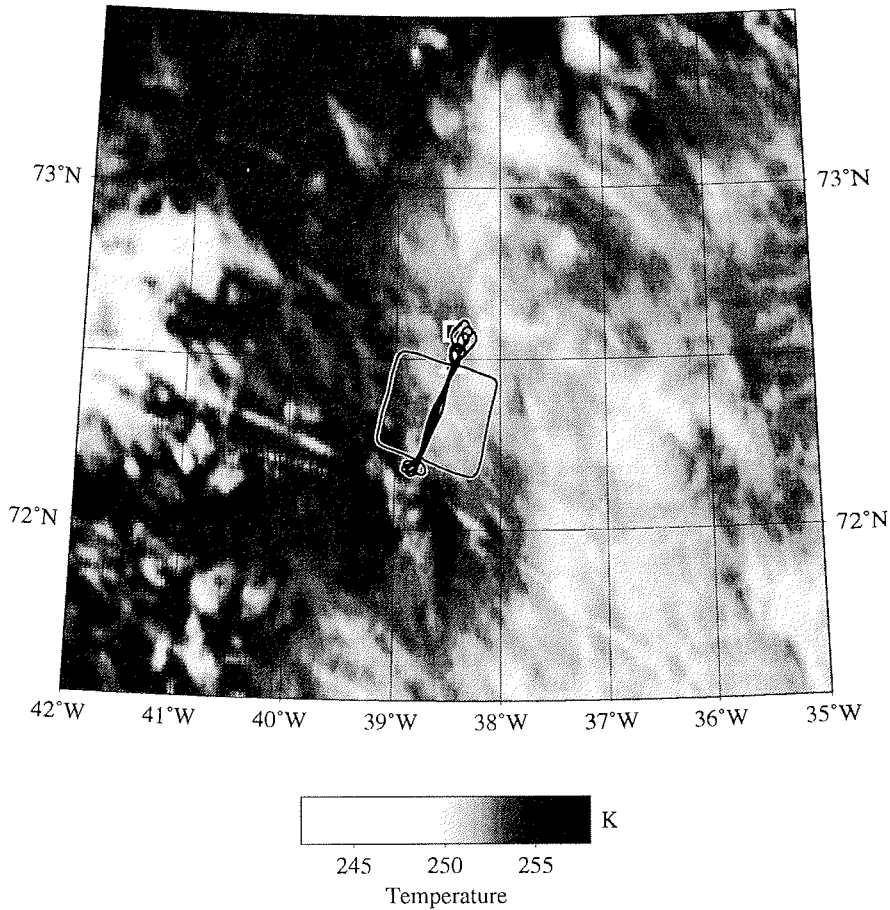
Figure 22.: SBL3 flight path (0315 - 0555 UTC) superimposed to infrared satellite image (NOAA16 Ch.4, 10 July 2002, 0510 UTC).

The synoptic situation during SBL3 was dominated by high pressure of moderate strength over Greenland. Two lows over Canada and Labrador did cause slight warm air advection over the western slope of Greenland. In the large-area satellite image (Figure 23), this advection is associated with a dense cover of low and medium level clouds over the southwestern slope of the inland ice sheet The surface wind in the measurement area is analyzed to be around 2.5 ms^{-1} from SW through NW (see Figure 24). The measurement area at the Greenland summit was 6/8 covered by Ac and Ci clouds (Figure 20). In the satellite image (Figure 22), some of the Ci clouds can be identified as contrails.

NOAA 16 Channel 4
10.07.2002 05:10 UTC

230 240 250 260 270 280
K
Temperature

Figure 23.: NOAA 16 channel 4 infrared image 10 July 2002, 0510 UTC, same representation as Figure 11.
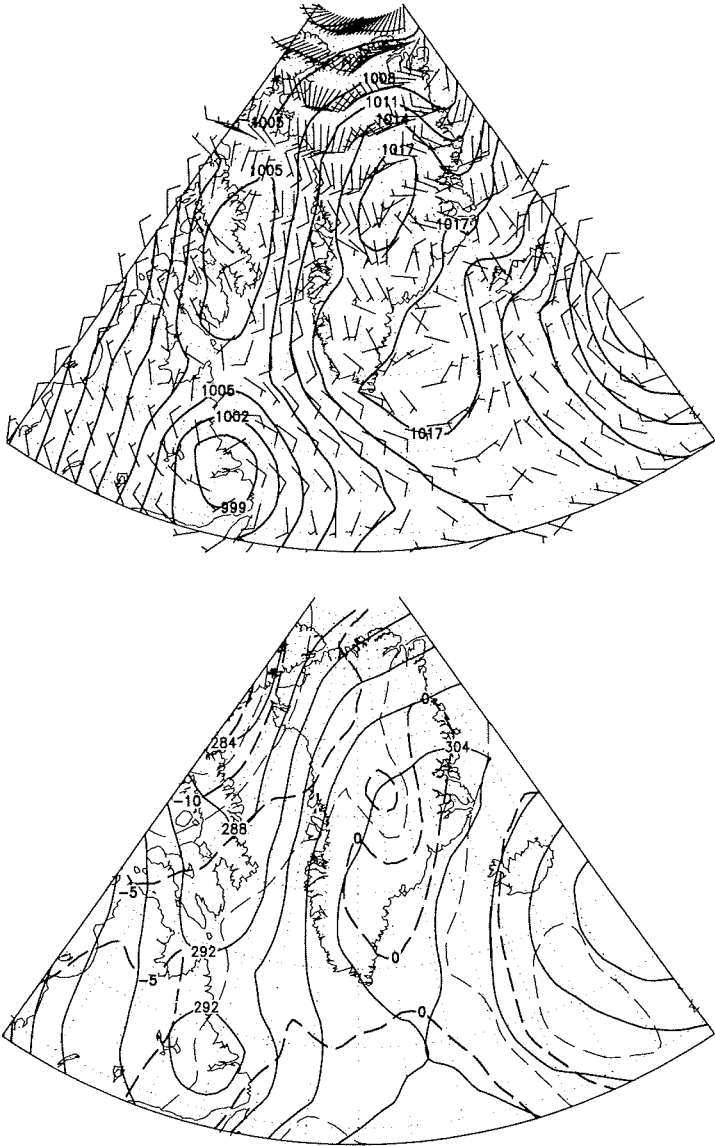
Figure 24.: NCEP Analysis 10 July 2002, 00/12 UTC, same representation as Figure 12.

3.3.4 SBL4: 10 July 2002

SBL4 was flown about two hours after SBL3 in order to measure the development of the PBL in the morning hours. For SBL4, the flight program (see Figure 27) started with a high aircraft temp (to 900 m) on the central leg of the flight pattern (B1-B2, for positions see Table XI and Figure 25). Then a series of 450 m-high aircraft temps followed around the outer legs of the flight pattern (B2-C2-C1-A1-A2-B2). Next, constant level runs were flown along the central leg (B1-B2) at four different heights ($\approx$ 30, 60, 120, 200 m), followed by a series of aircraft temps (to 450 m) along this leg (B1-B2). After these, the constant level runs and the temps on the central leg (B1-B2) both were repeated. The pattern was finished by a high aircraft temp (to 900 m) along (B1-B2).

Table XI: Geographic positions of the waypoints for the flight pattern during SBL4.

| Position name	Lat	Lon
	in deg	
A1	72.5117	-38.8850
A2	72.2567	-39.1816
B1	72.4650	-38.4633
B2	72.2117	-38.7650
C1	72.4183	-38.0417
C2	72.1650	-38.3500
S9	72.4816	-38.4633
Summit	72.5800	- 38.4567
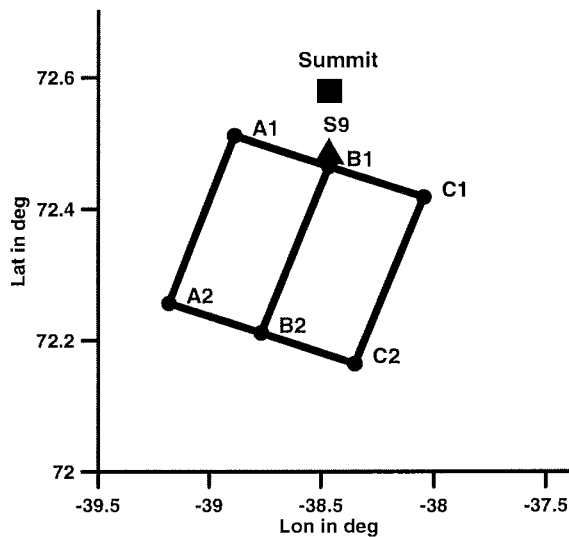
Figure 25.: Schematic plot of the flight pattern orientation during SBL4.

Figure 26.: Photo taken during SBL4 (10 Jul 2002, 0920 UTC): Sparse Ac clouds are visible near the horizon. The air near the surface was very clear, note the sharp shadow of the plane at the bottom.
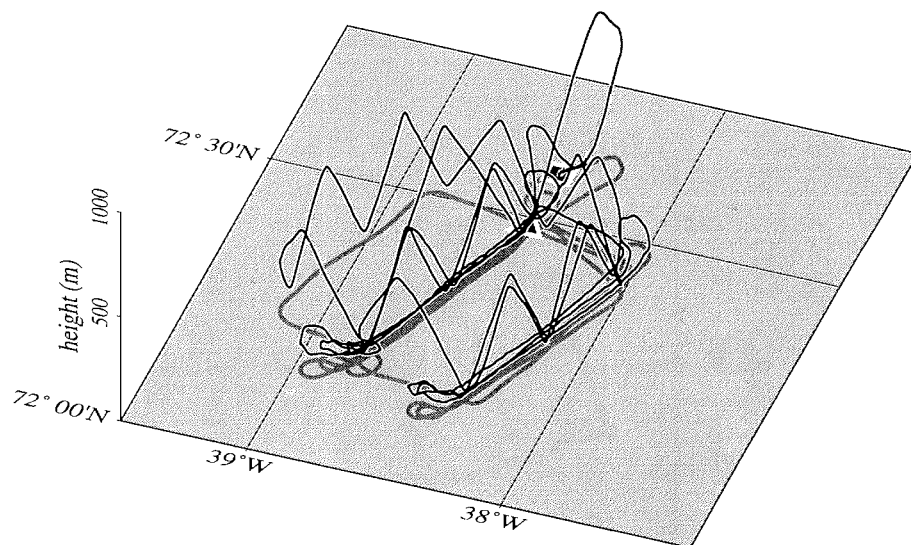

Figure 27.: SBL4 flight path, same representation as Figure 9.
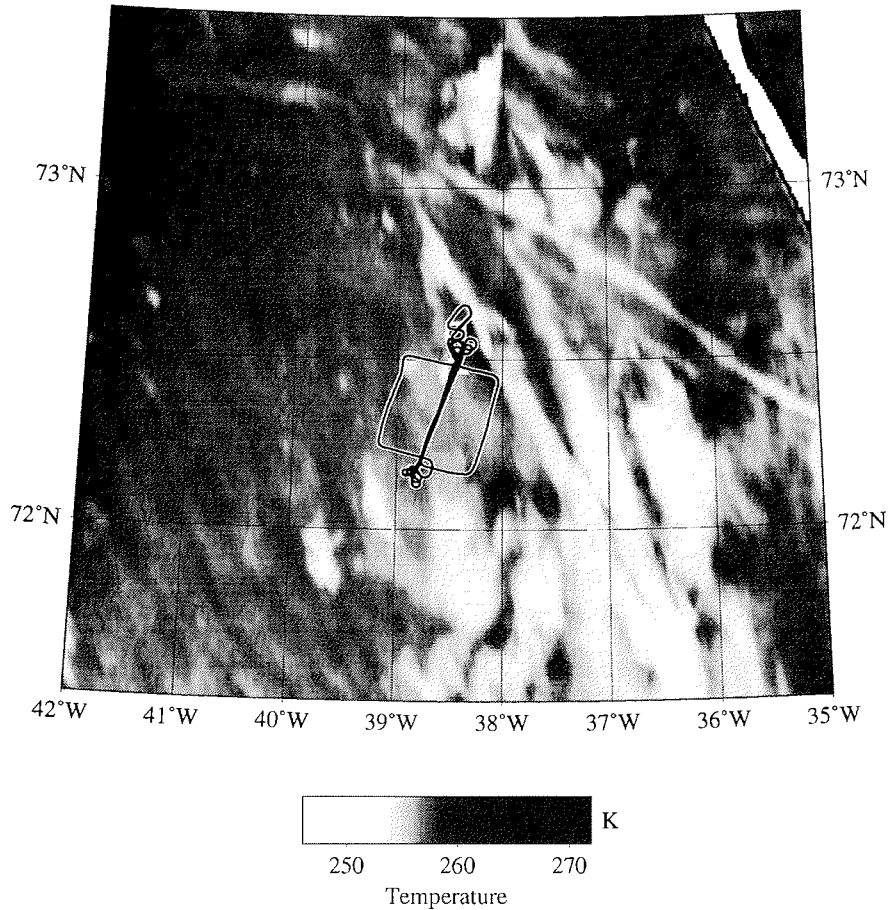
Figure 28.: SBL4 flight path (0715 - 1005 UTC) superimposed to infrared satellite image (NOAA16, Ch.4, 10 July 2002, 0832 UTC). The white bar in the upper right corner is caused by a corruption in the satellite data (not visible in the large image in Figure 29).

The synoptic situation on the 10 July 2002 was already described above (see Figures 23 + 24) with flight SBL3 that was performed earlier in the same morning. However, the amount of clouds covering the measurement area had decreased, compared to SBL3. This is well visible in Figure 26 (compared to Figure 31). From Figures 29 and 23 it can be seen that the area of high clouds present west of the investigation area had moved to the northwest, while the low clouds over the western slope of the Greenland ice sheet had moved northwards. As seen from Figure 28, mostly contrails were present in the measurement area during SBL4.
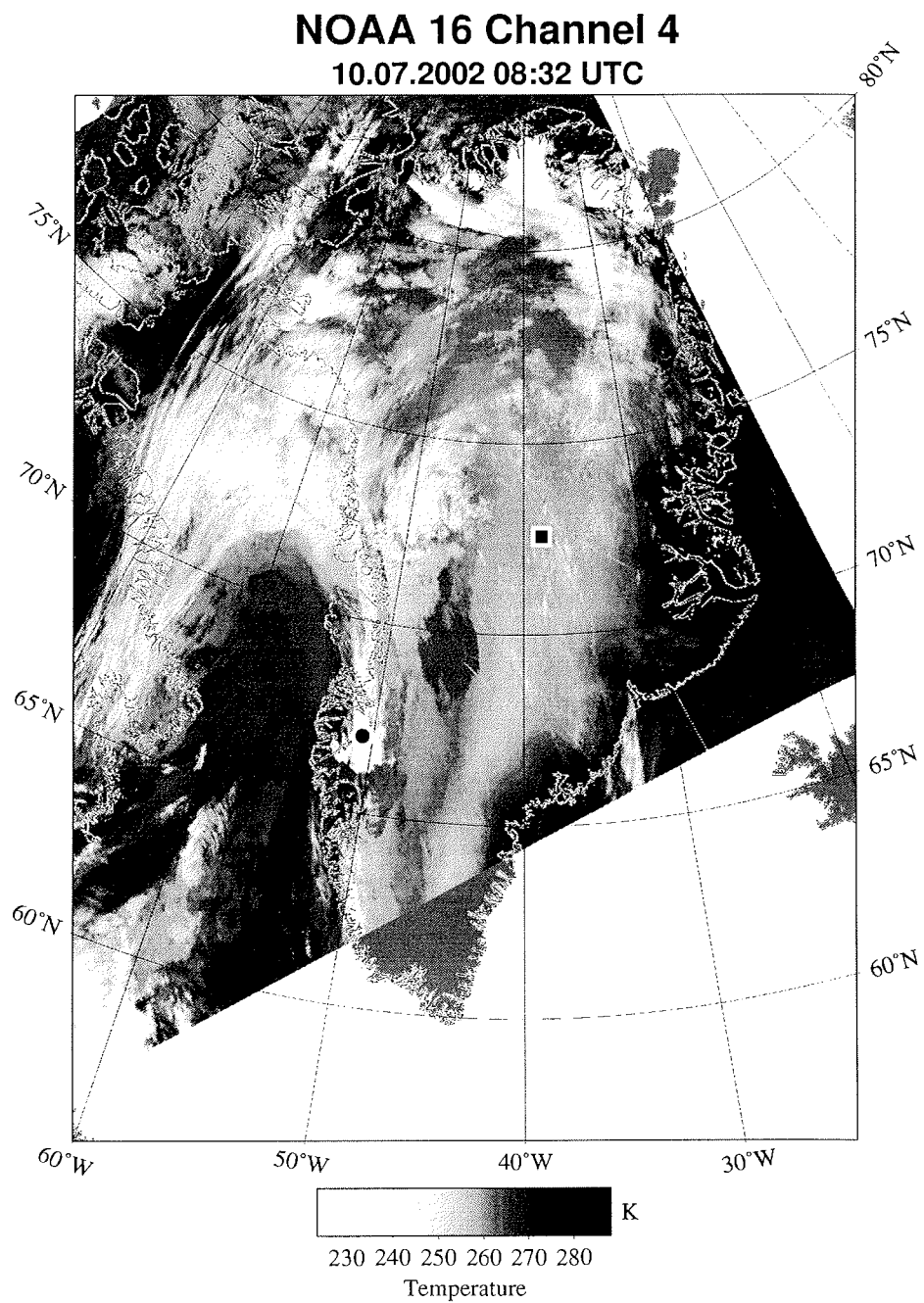
Figure 29.: NOAA 16 channel 4 infrared image 10 July 2002, 0832 UTC, same representation as Figure 11.

3.3.5 SBL5: 11 July 2002

During SBL5, the flight program (see Figure 32) started with a high (to 900 m) aircraft temp on the central leg (B1-B2, for positions see Table XII and Figure 30), followed by a series of temps (to 450 m) around the flight pattern (B2-C2-C1-A1-A2-B2). Then constant level runs were flown along leg (B1-B2) at levels of ca. 30 and 60 m. Since clouds were approaching from the west (see Figure 33), it was decided to repeat the shallow temps and the constant level runs on the eastern (C) instead of the central leg (B). Hence, the row of shallow (to 450 m) aircraft temps was extended along (B2-B1-C1-C2), followed by constant level runs at ca. 30, 15, and 60 m along (C1-C2). The clouds did approach slower than expected. Hence, the flight was continued with a transfer at 60 m height from position C1 to B1, a row of shallow (to 450 m) temps along (B1-B2) and a constant level run at 60 m height back on the same leg (B2-B1). A final aircraft temp (to 900m) between position B1 and Summit Camp concluded the flight for SBL5.

Table XII: Geographic positions of the waypoints for the flight pattern during SBL5.

Position name	Lat	Lon
	in deg	
A1	72.5117	-38.8850
A2	72.2567	-39.1816
B1	72.4650	-38.4633
B2	72.2117	-38.7650
C1	72.4183	-38.0417
C2	72.1650	-38.3500
S9	72.4816	-38.4633
Summit	72.5800	- 38.4567
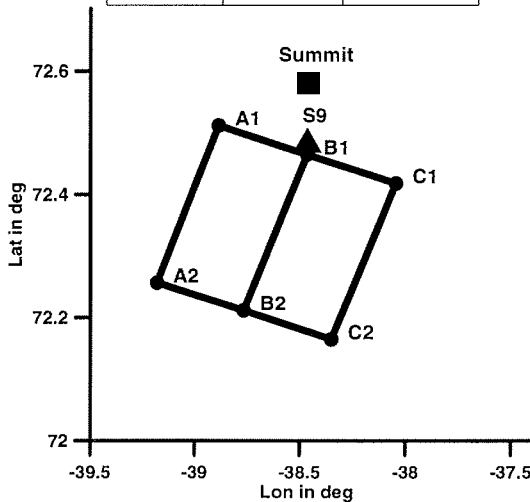
Figure 30.: Schematic plot of the flight pattern orientation during SBL5.

Figure 31.: Photo taken during SBL5 (11 Jul 2002, approx. 0200 UTC): The surface is clearly visible from the plane, Ac clouds are approaching the measurement area.

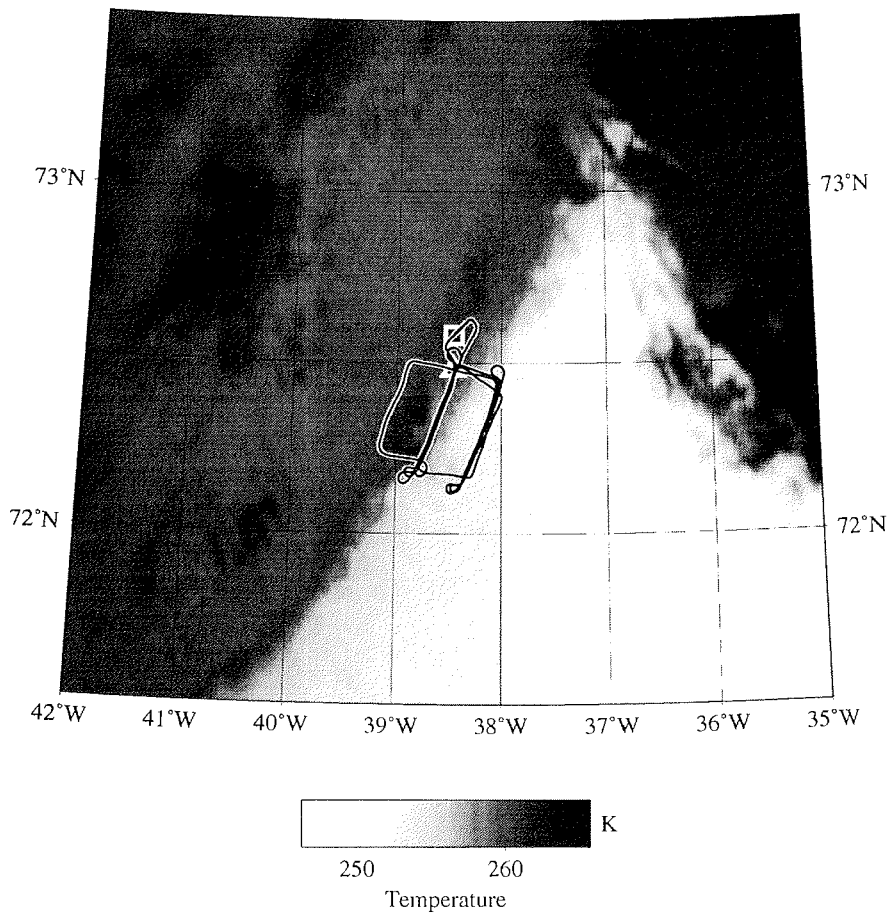*Figure 32.*: SBL5 flight path, same representation as Figure 9.

Figure 33.: SBL5 flight path (0010 - 0230 UTC) superimposed to infrared satellite image (NOAA16, Ch.4, 11 July 2002, 0459 UTC). Note: this satellite image is valid for 2.5 hours *after* the end of the flight mission. Hence, the approaching clouds already cover the flight pattern.

The synoptic situation during SBL5 was characterized by a high over East Greenland and weak pressure gradients over the rest of Greenland (Figure 35). The clouds visible west of Greenland in the satellite picture (Figure 34) are associated with a weak trough over the Baffin Bay and North Canada. The western slope of Greenland was covered with clouds of various levels, while the eastern slope was almost cloud free. Over the summit area, a very slight cold air advection was present. The analyzed winds in the measurement area are weak (< 2.5 ms^{-1}) and the wind direction is almost undetermined. During the actual flight mission, a cover of Ac clouds moved in from the west to the measurement area (see Figure 33). These clouds are depicted in Figure 31 and were observed to be between 620 and 780 m height.

NOAA 16 Channel 4
11.07.2002 04:59 UTC
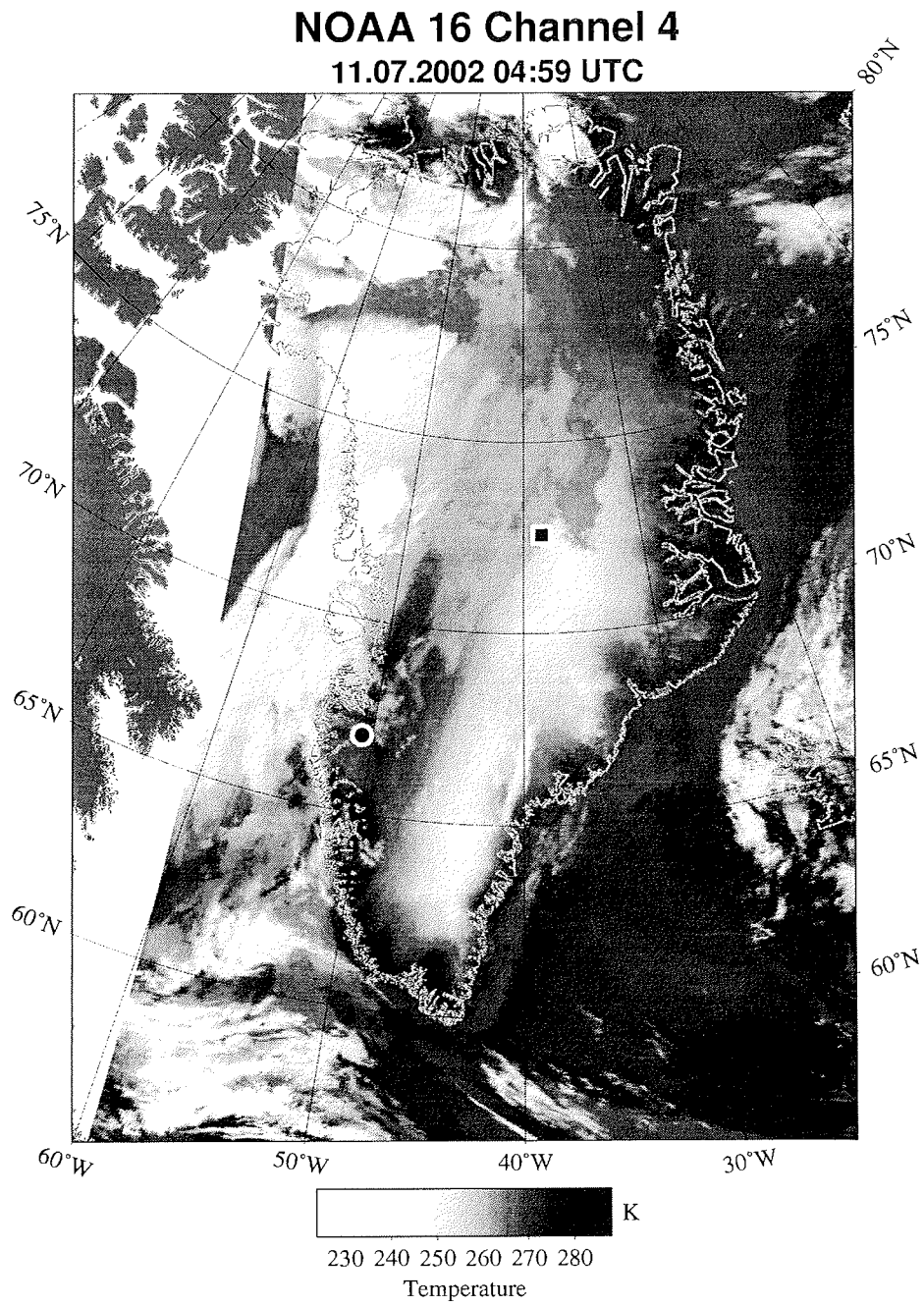
Figure 34.: NOAA 16 channel 4 infrared image 11 July 2002, 0459 UTC, same representation as Figure 11.
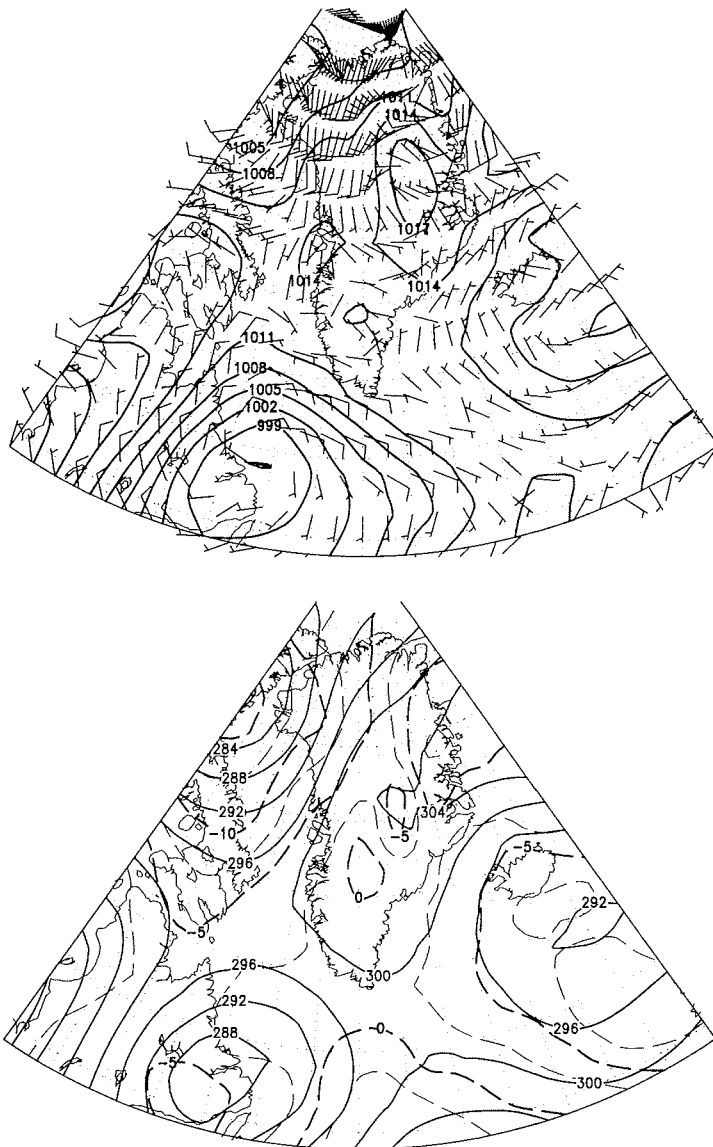
Figure 35.: NCEP Analysis 11 July 2002, 00/12 UTC, same representation as Figure 12.

3.3.6 SBL6: 12 July 2002

The flight program during SBL6 (see Figure 38) began with a high (to 900m) aircraft temp on leg (B1-B2, for positions see Table XIII and Figure 36), followed by a series of shallow temps (to 450 m) around three quarters of the flight pattern (B2-C2-C1-A1-A2). Because of low clouds rising from the east, all further flight elements were concentrated on the westerly leg (A). The purpose was to yield consecutive cross-sections on one leg, in order to capture the rapid destruction of the SBL under the clouds: Constant level runs at four levels (ca. 30, 60, 90 and 120 m) were flown along leg (A1-A2). Next followed a series of shallow temps (to 450 m) on the leg (A2-A1-A2), and a constant level run at 30 m height on the same leg (A2-A1-A2). Finally, a row of shallow aircraft temps was flown on the leg (A2-A1). The return flight to Summit Camp was occupied by thoroughly checking the visibility conditions before landing on the skiway.

Table XIII: Geographic positions of the waypoints for the flight pattern during SBL6.

Position name	Lat	Lon
	in deg	
A1	72.3483	-38.6867
A2	72.2133	-37.9117
B1	72.4650	-38.4633
B2	72.3300	-37.6900
C1	72.5817	-38.2383
C2	72.4467	-37.4667
S9	72.4816	-38.4633
Summit	72.5800	- 38.4567
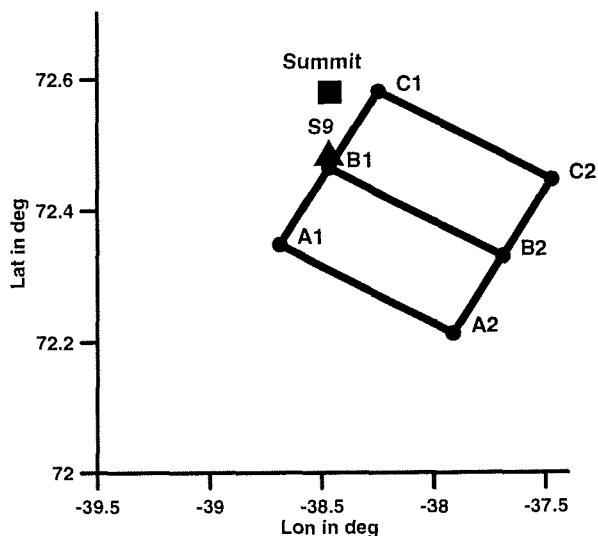
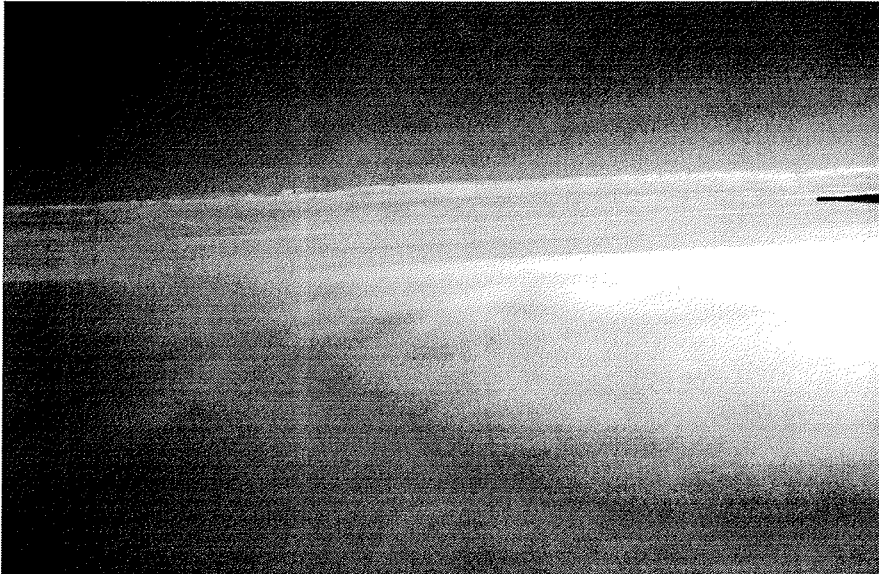Figure 36.: Schematic plot of the flight pattern orientation during SBL6.

Figure 37.: Photo taken during SBL6 (12 Jul 2002, 0005 UTC): At the beginning of the flight, the surface is still covered with fog, but the first low-level clouds have already reached the investigation area.
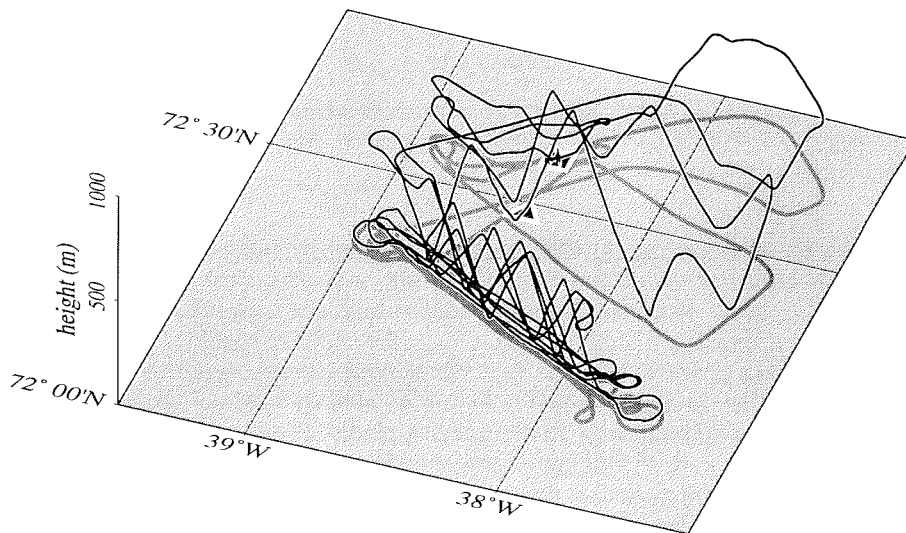

Figure 38.: SBL6 flight path, same representation as Figure 9.
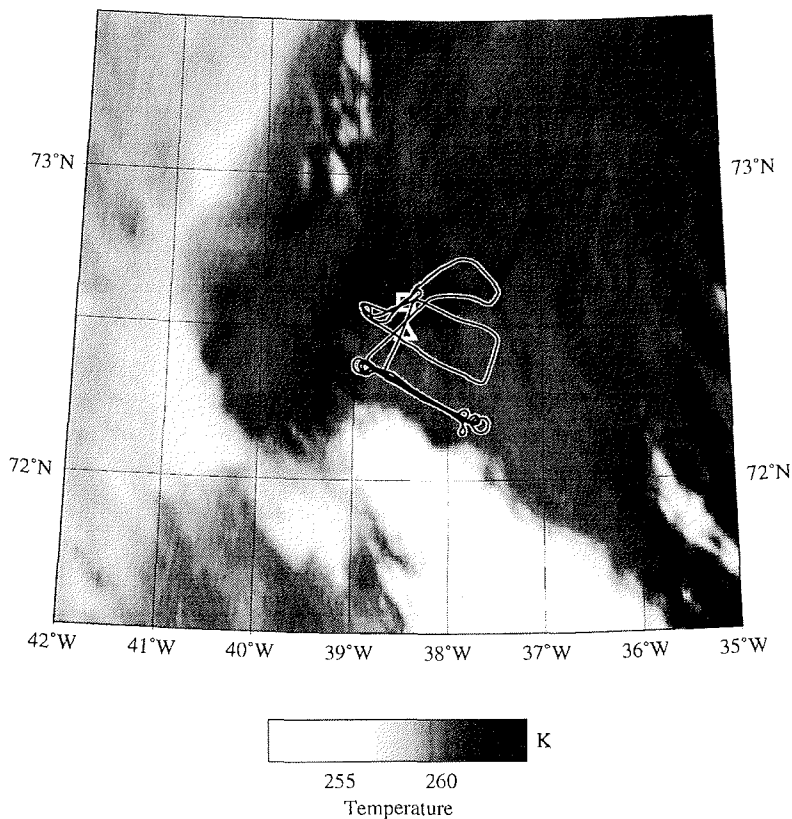
Figure 39.: SBL6 flight path (2355 - 0310 UTC) superimposed to infrared satellite image (NOAA16, Ch.4, 12 July 2002, 0448 UTC). Note that this satellite image is valid for about 2.5 hours *after* the end of the actual measurement pattern.

The synoptic situation during SBL6 was dominated by high over East Green-land, lower pressure over West Greenland, and a strong low east of Labrador. As a result, a zone of a fairly strong pressure gradient was present over Cen-tral Greenland causing a southerly flow over the summit region. Over Iceland, a strong low was present, generating a considerable pressure gradient north of Iceland. The NCEP analysis shown in Figure 41 reveals winds of around 5 ms^{-1} from south for the summit area. In the satellite picture (Figure 40), a dense band of clouds is visible over Northeast Greenland. These clouds are associated with a shallow trough along the west coast of Greenland (see Figure 41). The clouds southeast of the investigation area are associated with the strong pressure gra-dient between Greenland and Iceland. The measurement area was initially cloud free, although some surface fog was present. The top of this fog did show wave-like structures (Figure 37) similar to the ones seen during SBL1 (see Figure 8). During the flight, the Sc cover visible in the satellite image (taken *after* the flight) in Figure 39 moved in a heights between 30 and 300 m.
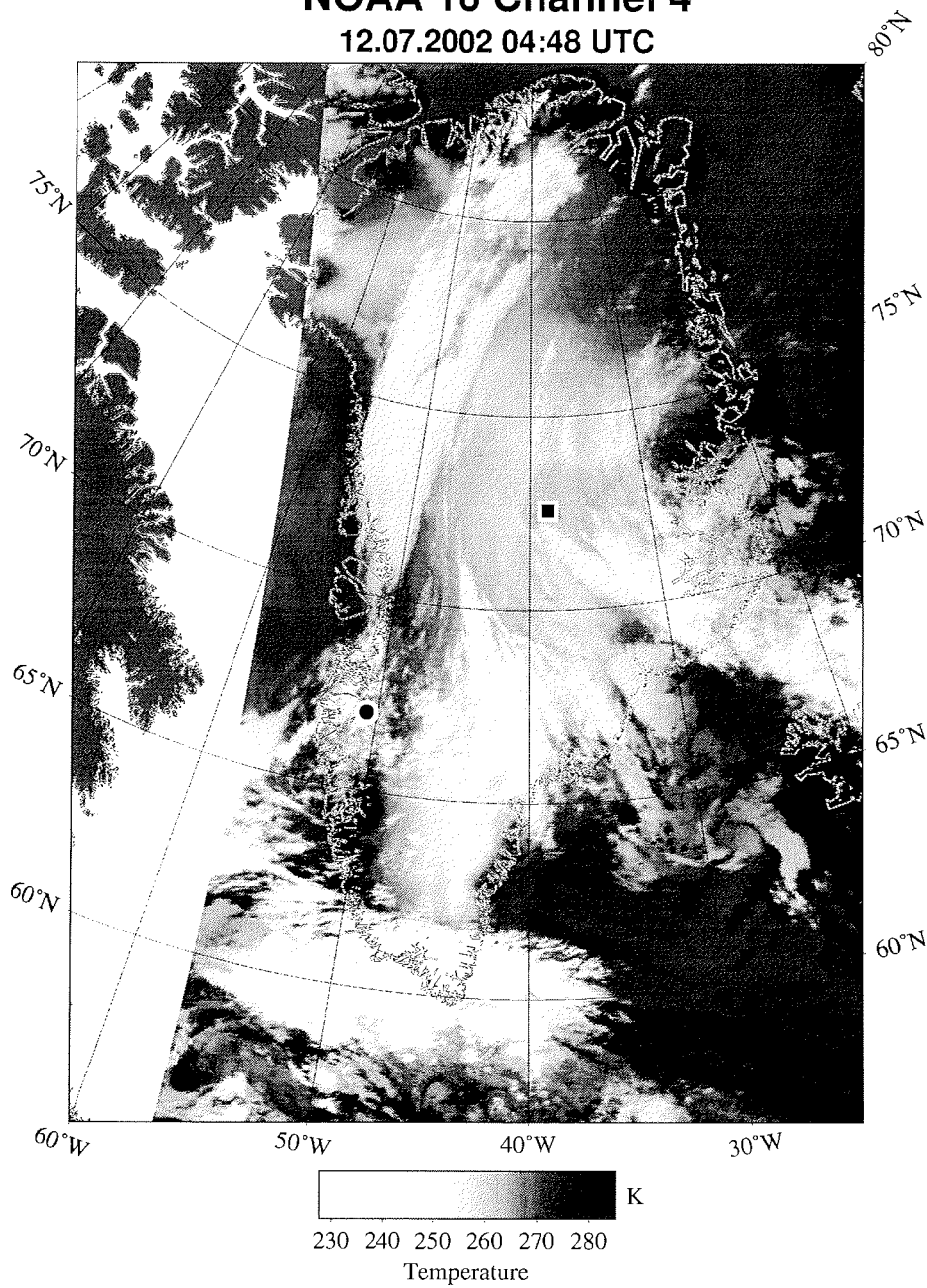
Figure 40.: NOAA 16 channel 4 infrared image 12 July 2002, 0448 UTC, same representation as Figure 11.
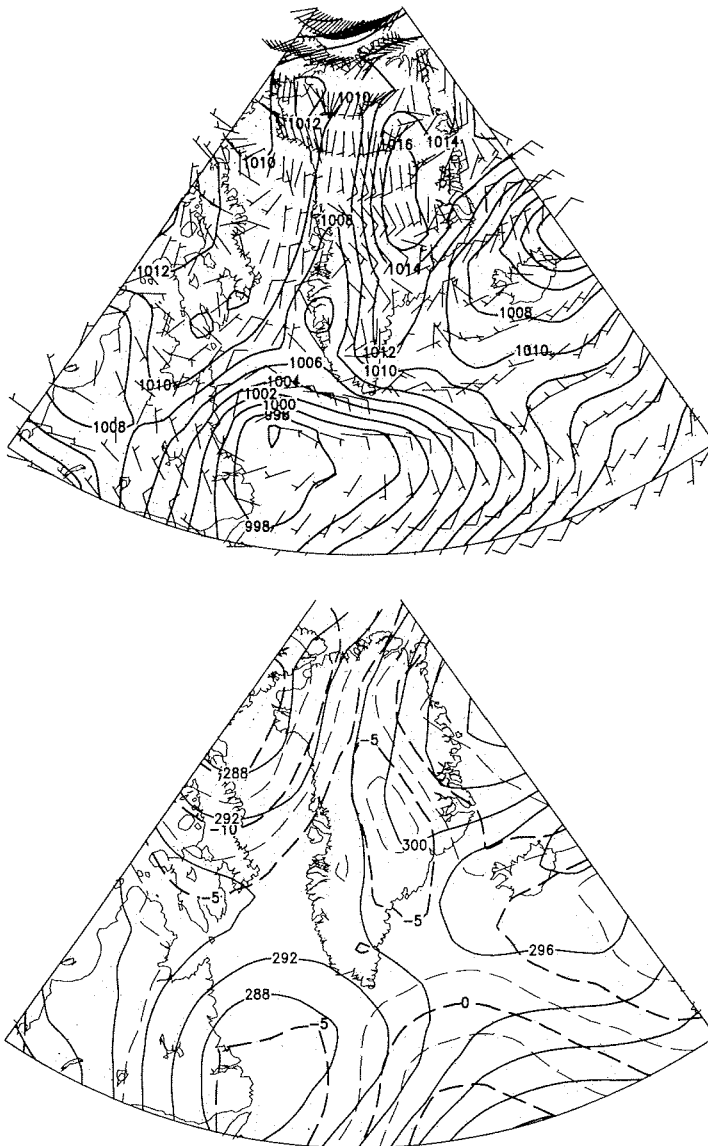
Figure 41.: NCEP Analysis 12 July 2002, 00/12 UTC, same representation as Figure 12.

3.3.7   CAL1: 29 June 2002

The purpose of the flight CAL1 was the in-field calibration of the aircraft instru-
mentation (after mounting the sensors). Among the calibrated quantities are the
actual misalignments of the radiation sensors as well as the current calibration co-
efficients for the five-hole probe. This flight in general has to be conducted prior
to the actual measurement period. For IGLOS, it was carried out around the base
airport at Kangerlussuaq (see Figure 42).
The following list summarizes the flight program during CAL1:

1. low pass at over the Fjord water surface

2. climb to 10.000 ft (3000 m)

3. squared box, on each side:

    (a) five minutes straight flight at constant level

    (b) five oscillations +/- 10° pitch angle

    (c) five oscillations +/- 10° roll angle

    (d) five oscillations +/- 10° bank angle

    (e) 90° right turn to the next side

4. full circle right at 20° roll angle

5. full circle left at 20° roll angle

6. descent to the ice cap surface

7. low pass: two minutes at 45 ft (15 m) above the (melting) snow surface

8. climb to travel altitude and return

The synoptic situation during CAL1 was characterized by generally low pressure
contrasts over Greenland (Figure 45). A trough extending from Canada over the
Davis strait to the south tip of Greenland and an area of slightly higher pres-
sure over northern Greenland resulted in a slight southeasterly flow over the
Kangerlussuaq area. The clouds visible in Figure 44 over southern Greenland
are associated with the front side of this trough. Virtually no temperature advec-
tion took place over West Greenland. The NCEP analysis reveals winds of less
than 2.5 ms^{-1} from southeast to east. The temperature in Kangerlussuaq was
14°C at 1400 UTC. Only some thin low clouds were present in the flight area, a
band of high Ci clouds did approach from northeast during the flight and did cover
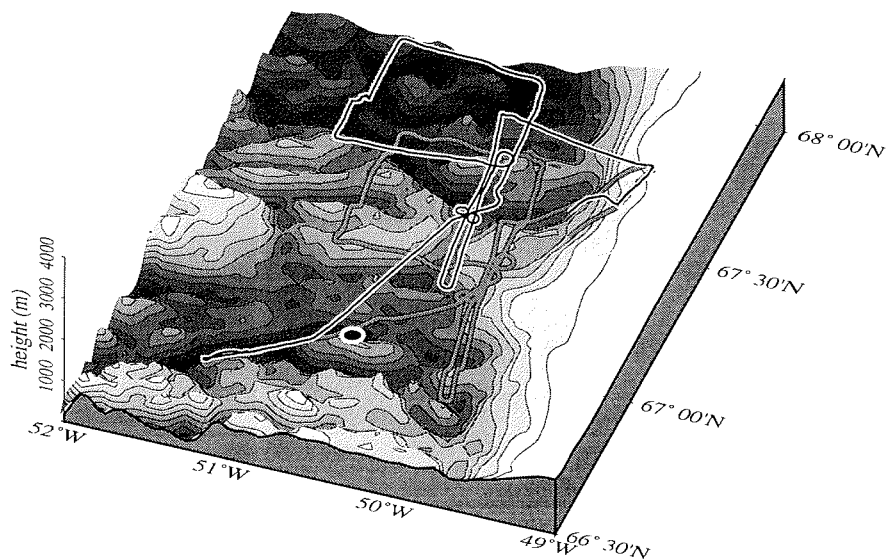the north eastern part of the flight area (Figure 43).

Figure 42.: CAL1 flight path: perspective view from southeast. Topography data are taken from the Ekholm dataset, the elevation isoline spacing is 66 m. The flight path shadow is projected to the topography surface; the circle represents Kangerlussuaq. The vertical coordinate is the altitude in m (above sea level).
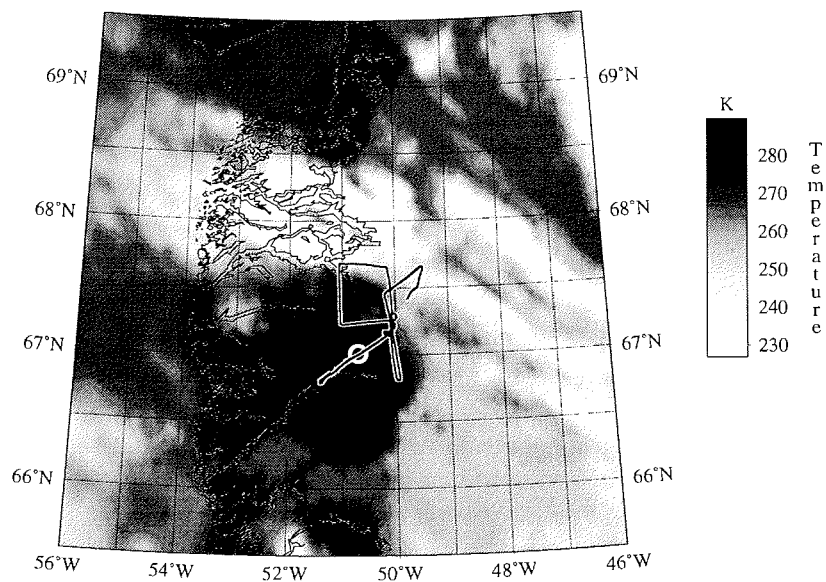

Figure 43.: CAL1 flight path (1620 - 1830 UTC) superimposed to infrared satellite image (NOAA16, Ch.4, 29.06.2002, 1431 UTC; GAC data supplied by NOAA-SAA).
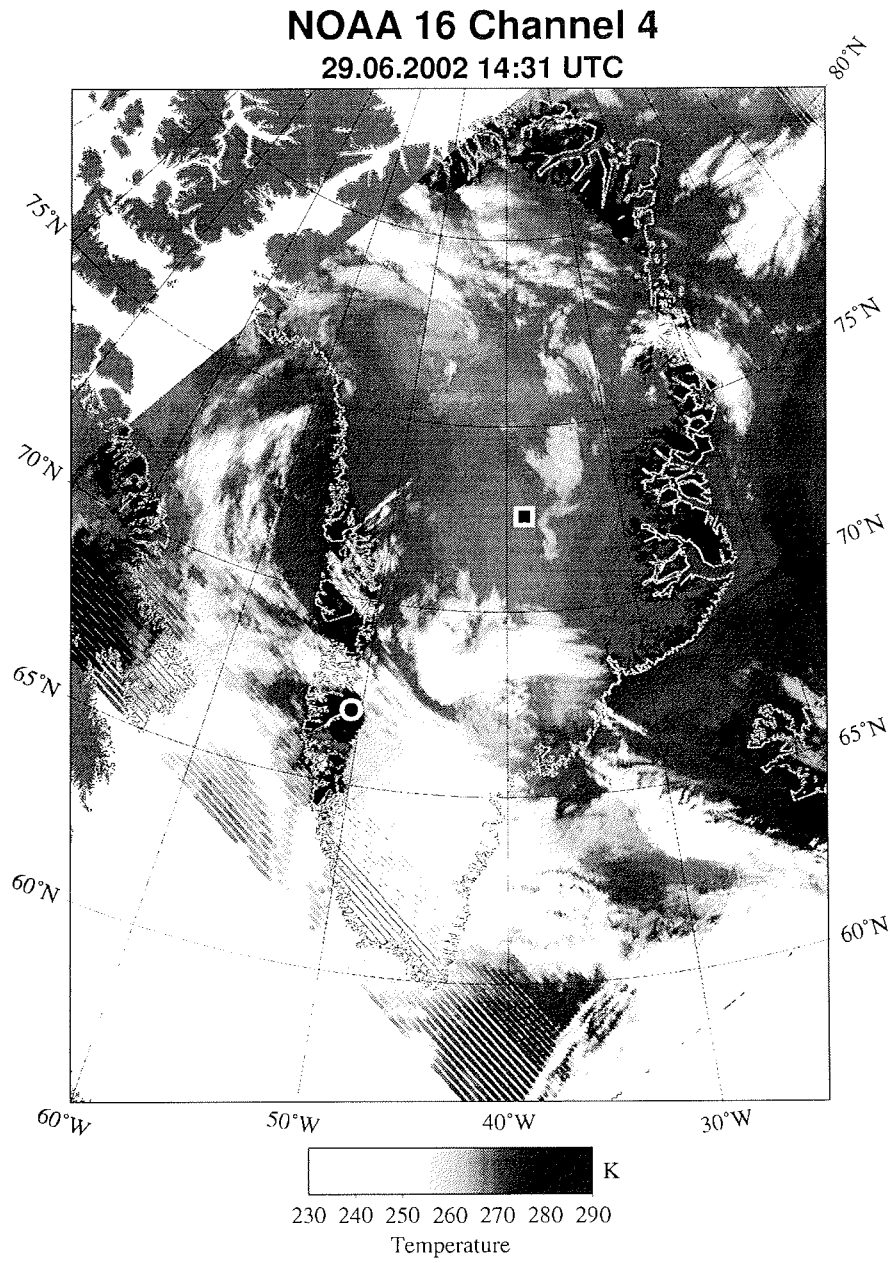
NOAA 16 Channel 4
29.06.2002 14:31 UTC

Figure 44.: NOAA 16 channel 4 infrared image 29.06.2002, 1431 UTC, same representation as Figure 11.
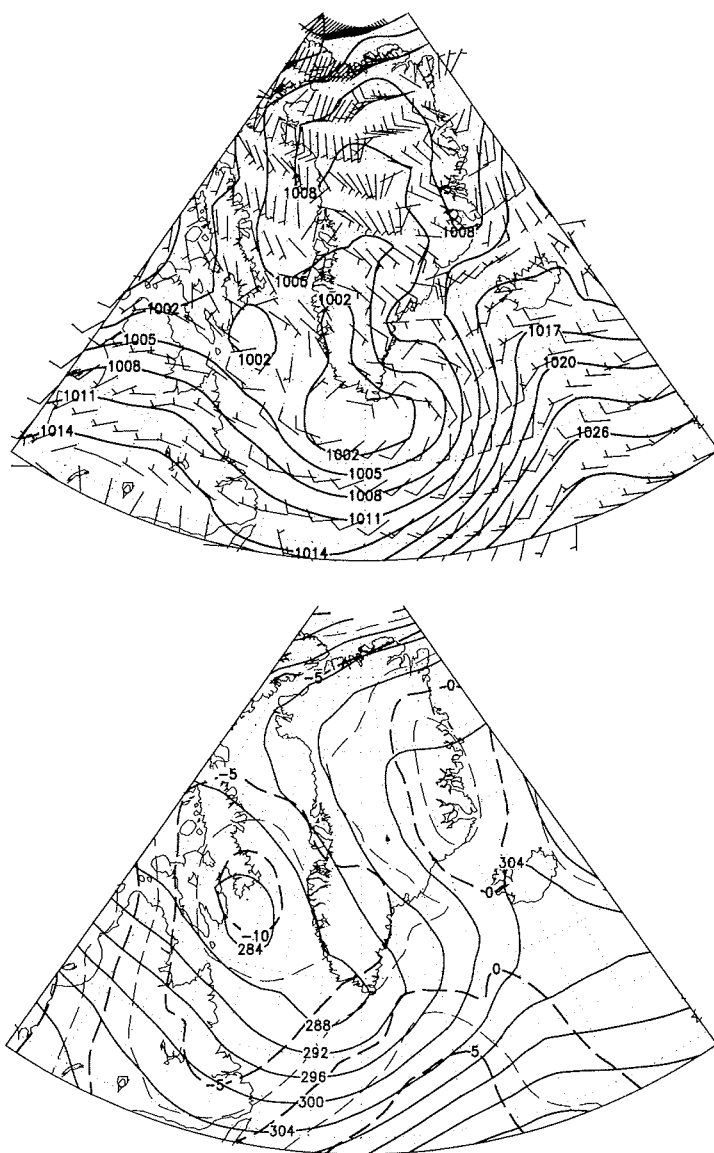
Figure 45.: NCEP Analysis 29.06.2002, 00/12 UTC, same representation as Figure 11.

3.3.8   CAL2: 25 July 2002

The flight CAL2 served two different purposes: One purpose was the re-calibration of the wind measurement instrumentation after removing the skis. The other purpose was the verification of the radiation sensor misalignment angles determined during flight CAL1.

CAL2 was carried out around the base airport at Kangerlussuaq after the end of the actual measurement period.

The following list summarizes the flight program during CAL2 (Figure 46):

1. low pass at over the airport runway at 45 ft (15 m)

2. climb to 10.000 ft (3000 m)

3. squared box, on each side:

    (a) five minutes straight flight at constant level

    (b) five oscillations +/- 10° pitch angle

    (c) five oscillations +/- 10° roll angle

    (d) five oscillations +/- 10° bank angle

    (e) 90° right turn to the next side

4. full circle right at 10° roll angle

5. full circle left at 10° roll angle

6. full circle right at 20° roll angle

7. full circle left at 20° roll angle

8. five minutes go-and-return flight in north-south direction

9. five minutes go-and-return flight in east west direction

10. descent and return

The synoptic situation over western Greenland during CAL2 was characterized by very weak pressure contrasts (Figure 49). A low located between Greenland and Iceland together with a weak high over northern Greenland lead to a generally north-westerly flow with no significant temperature advection over the West-Greenlandic Tundra. The low over Iceland is visible in the satellite image by a vast cloudy area over the east coast of Greenland.

The NCEP-analysis wind for the region of Kangerlussuaq is around 2.5 ms^{-1} from NW and the temperature in Kangerlussuaq was 7°C at 1500 UTC. The measurement area was covered with thin broken low Sc clouds (well below the flight level). East and west of the calibration area, bands of high Cs were present during the flight (Figure 47).
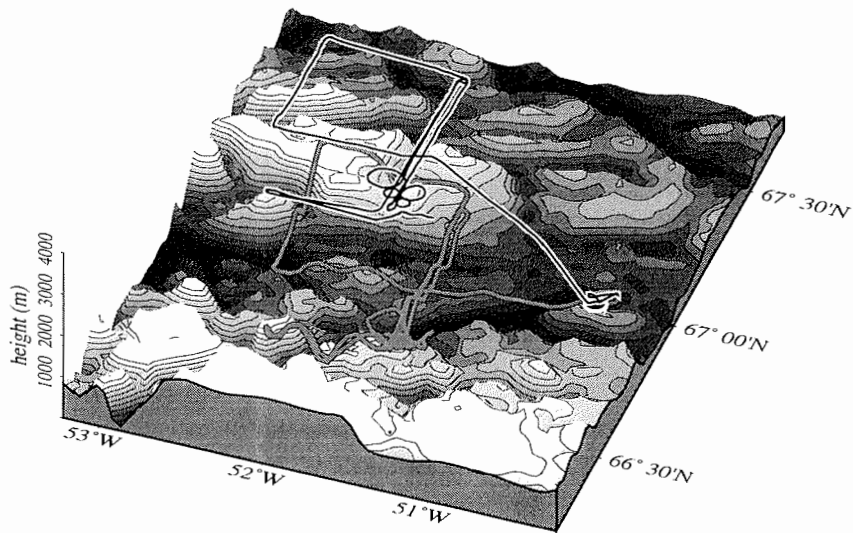
Figure 46.: CAL2 flight path, same representation as Figure 42.
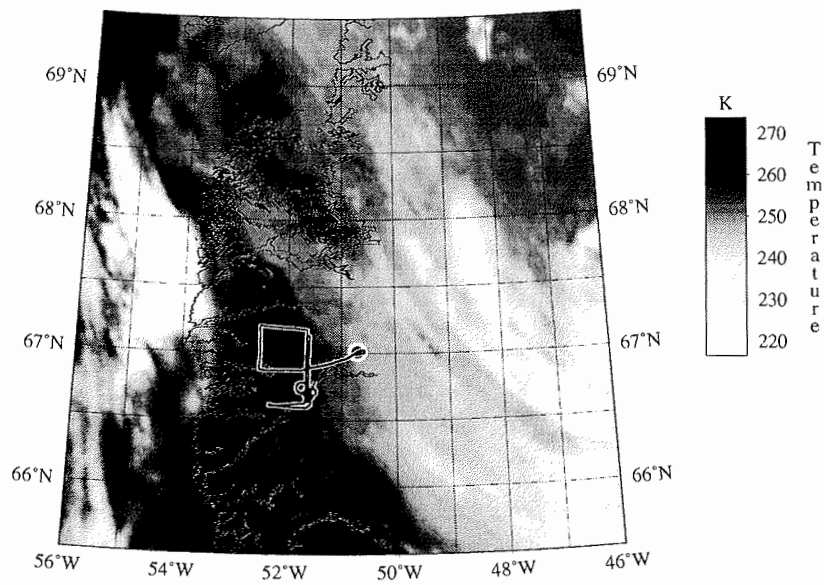

Figure 47.: CAL2 flight path (12:30 - 14:15 UTC) superimposed to infrared satellite image (NOAA16, Ch.4, 25.05.2002, 1219 UTC; GAC data supplied by NOAA-SAA).

NOAA 15 Channel 4
25.07.2002 12:19 UTC
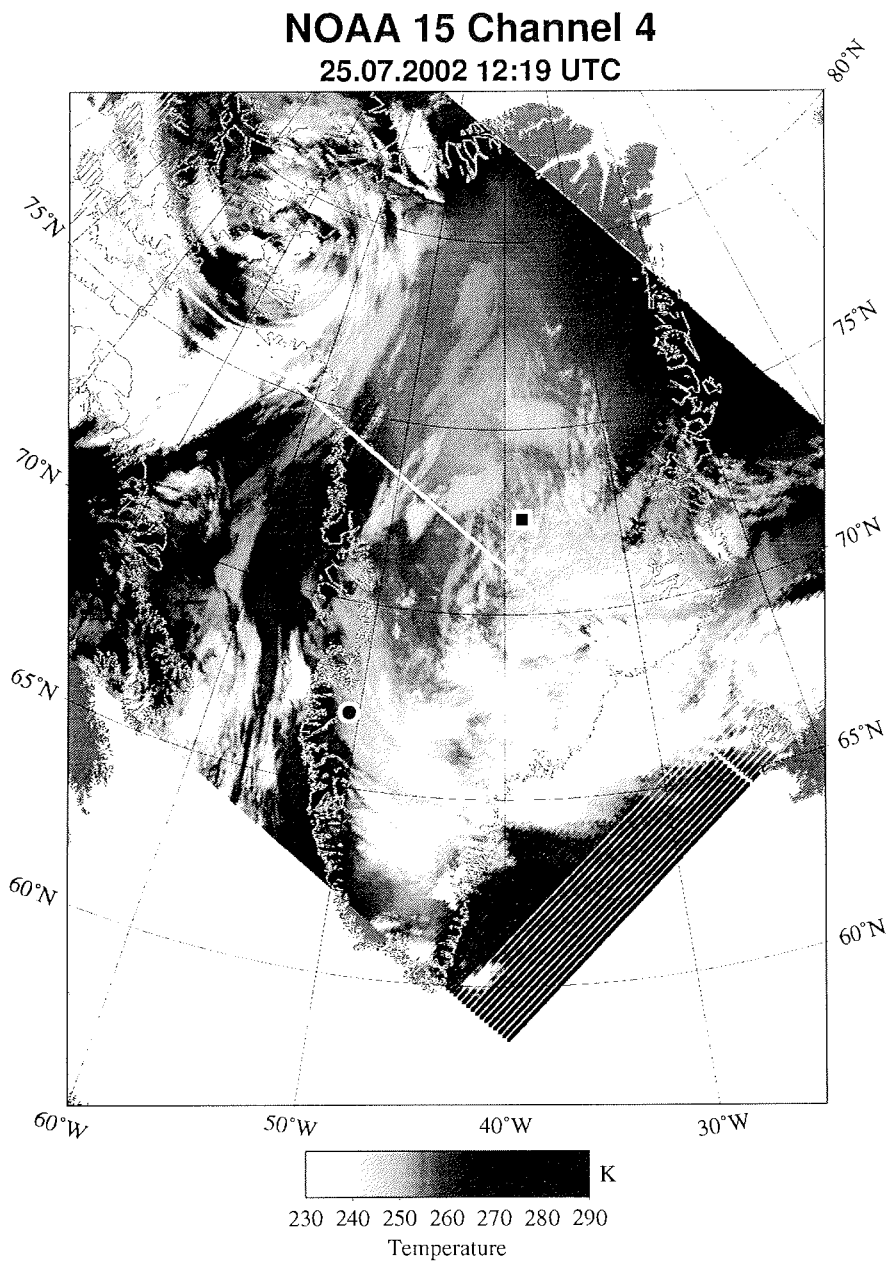

230 240 250 260 270 280 290
Temperature

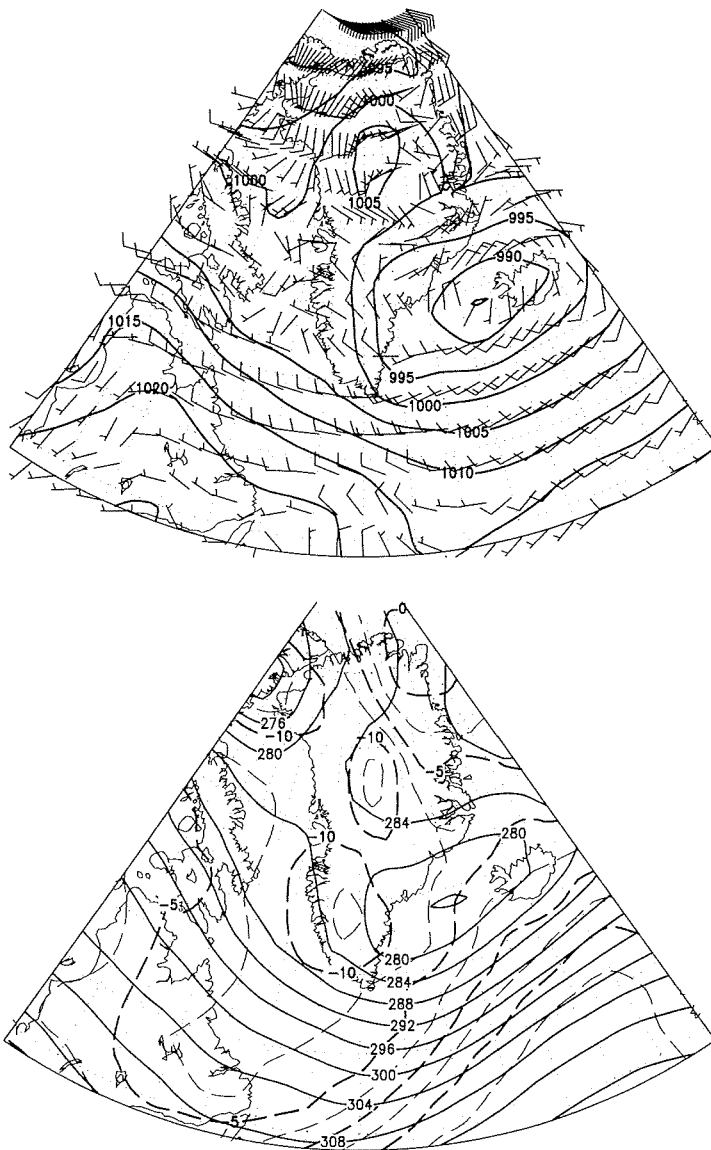*Figure 48.*: NOAA 16 channel 4 infrared image 25 July 2002, 1219 UTC, same representation as Figure 11.

Figure 49.: NCEP Analysis 25 July 2002, 00/12 UTC, same representation as Figure 11.

4 First results

4.1 Weather conditions - operational surface stations

To give an overview of the weather conditions in Greenland during the IGLOS experimental phase, Figures 50 to 52 show the records of the weather stations BGSF (Kangerlussuaq airport, west coast), Scoresbysund (east coast) and Summit Camp (see Figure 5 for positions).

From the pressure records of the two sea level stations, three periods of relative high pressure can be identified. The first, least pronounced one from day 183 to 185 (02-04 July), the second from day 187 to 194 (06-13 July) and the third from day 196 to 198 (15-17 July). These periods coincide with the three SOPs of the POLAR2 at Summit Camp. These periods of relative high pressure are associated with observed sparse or no clouds over Scoresbysund and (at least for SOP2 and SOP3) over Kangerlussuaq. The wind direction at Kangerlussuaq is strongly influenced by topography, but westerly winds during the first period, strictly easterly winds during the second and (local) valley winds during the third period mark the varying nature of the high pressure episodes. At Scoresbysund similarly, winds came from south to west during the first period, turned from east to north during the second, and were low during SOP3. At Summit Camp, the first two periods of high pressure can easily be identified in there pressure record (Figure 52), while the third one is not well represented. However, all three periods correspond to episodes of generally decreased wind speeds. The amount of clouds is mostly high in the summit region (often due to Cirrus clouds), but the lowest daily averages are observed during periods of higher pressure.

The high pressure periods were associated with increasing temperatures at Kangerlussuaq, while the corresponding temperature signal is much less pronounced at Scoresbysund. At Summit Camp, the high pressure periods are linked to increased diurnal temperature variations and low daily temperature minima. After the third period of high pressure, with falling pressure, the temperatures increased at Scoresbysund and - much more - in the summit region due to southeasterly warm air advection.

To summarize, SOP1 was characterized by moderate winds and low temperatures indicating northwesterly advection in Kangerlussuaq and low winds and decreasing temperatures over Summit and Scoresbysund (see Figure 12). SOP2 was characterized by fairly warm easterly winds at Kangerlussuaq (Foehn) and decreasing temperatures, freshening wind turning from west to north, and rapidly rising temperatures at the end of SOP2 at Scoresbysund (see Figure 24). SOP3 exhibited low synoptic forcing on both coasts, leading to the development of local wind systems (in particular at Kangerlussuaq), while on Summit high winds and high temperatures were associated with warm upper air advection (Figure 53, lower panel).

Since no SBL flight missions could be performed during SOP3, the synoptic situation for 19 July 2002 (day 190) is displayed in Figure 53 as an example for the third period of high pressure.
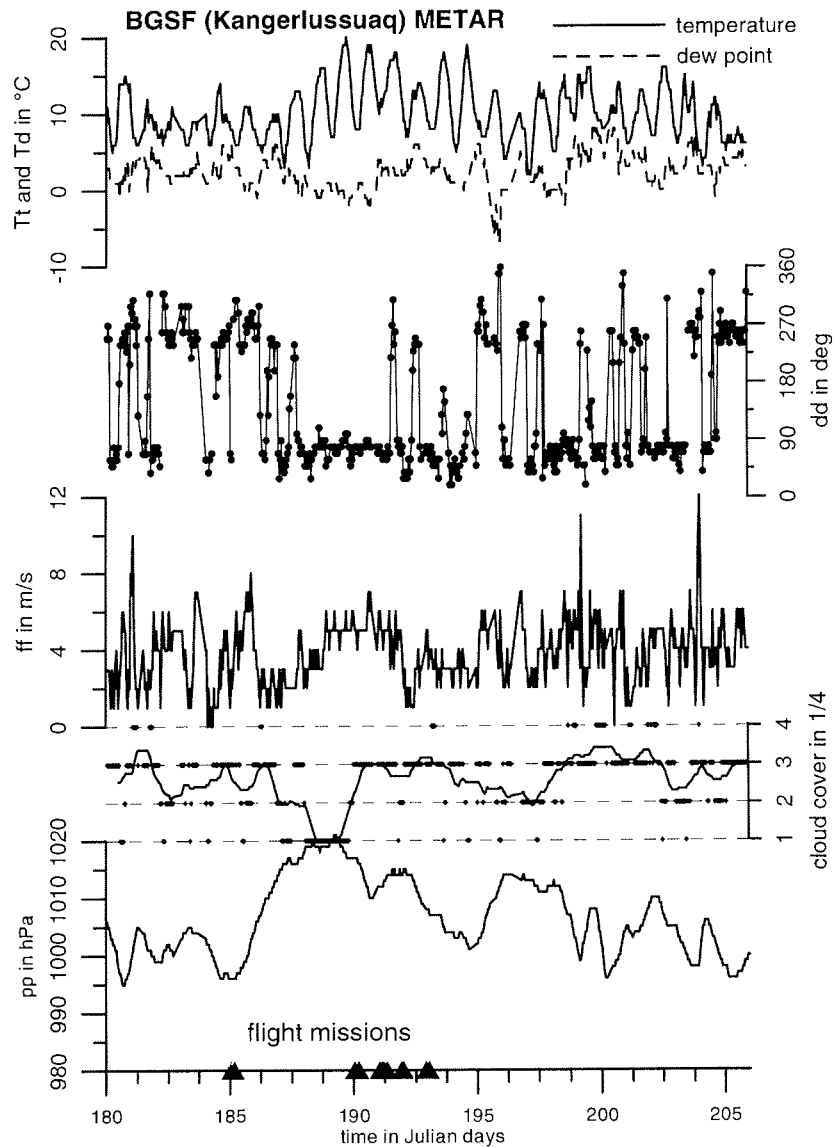
Figure 50.: Weather conditions (hourly data) at Kangerlussuaq (IATA airport code: BGSF) through-
out the IGLOS experimental period from day 180 (29 Jun) to day 206 (25 Jul 2002). The displayed
quantities are from top to bottom: Air temperature (Tt) and dewpoint (Td), wind direction (dd),
wind speed (ff) (all values in the upper three panels are averages between measurements taken
at both ends of the 3 km runway), cloud cover (derived from the cloud layer reports; dots: obser-
vation, line: daily mean), and sea level pressure (pp). SBL flight missions are marked by triangles
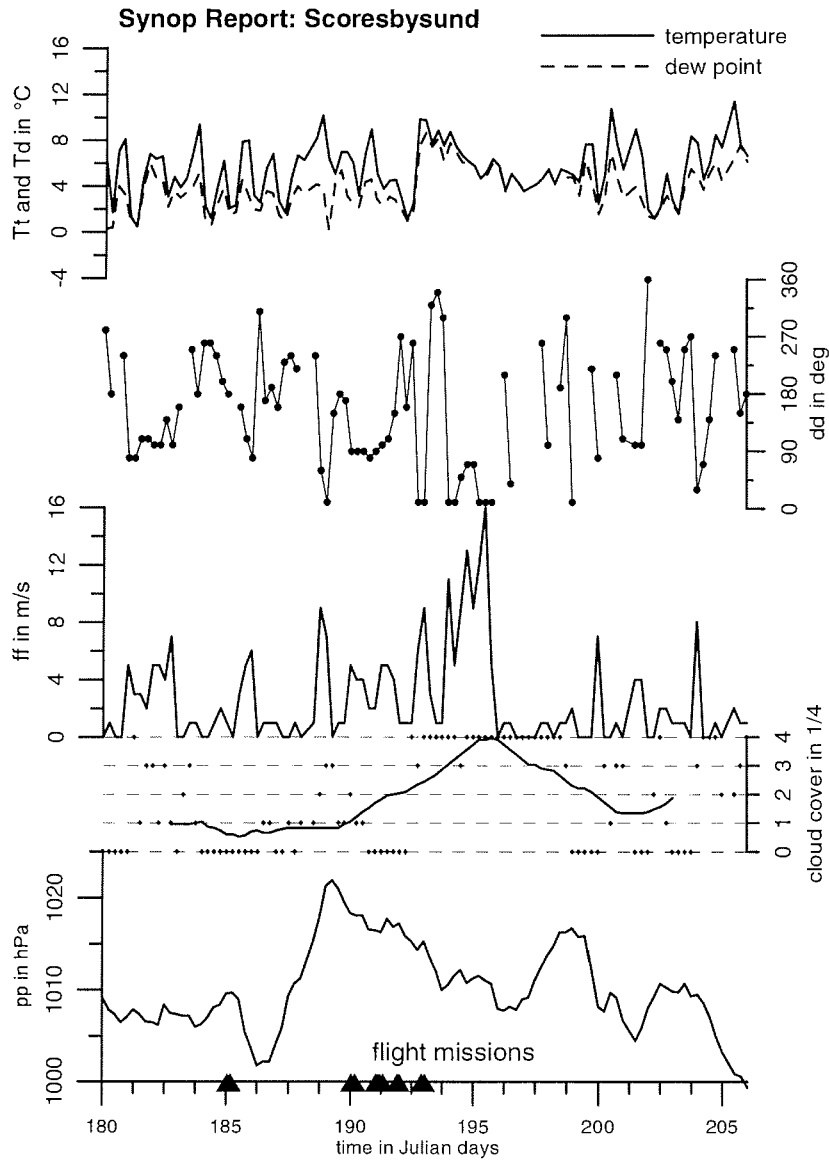on the time axis.

Figure 51.: Weather conditions at Scoresbysund, same representation as Figure 50, but reports were transmitted only every six hours.
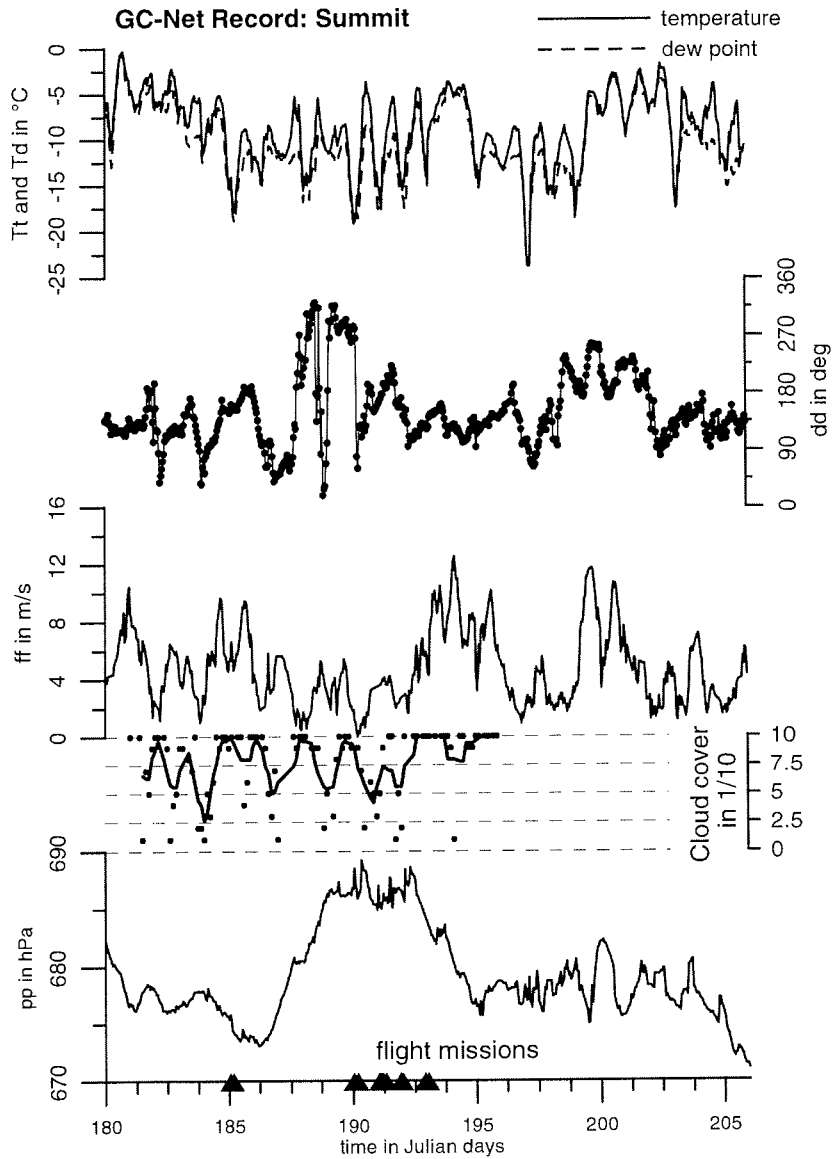
Figure 52.: Weather conditions at Summit Camp; same representation as Figure 50, but data are recorded hourly by the GC-Net Summit AWS, except cloud cover, which was recorded six-hourly by a human observer (from ETH). In case of the Summit AWS data refer to the upper measurement level (at ≈ 4.5 m during IGLOS).
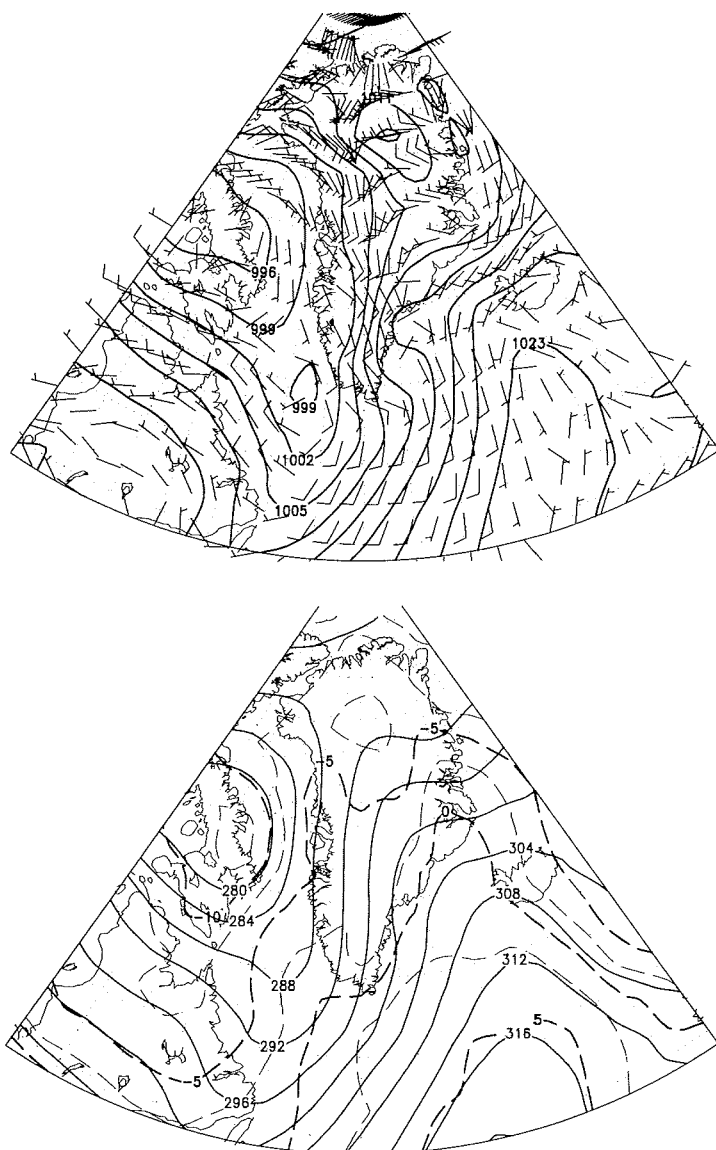
Figure 53.: NCEP Analysis 19 Jul 2002, 00/12 UTC, same representation as Figure 12.

4.2   PBL evolution - surface turbulence measurements

The turbulence activity was mostly weak and the SBL in general was very shallow (see next section, 4.3). The SBL however underwent a variety of turbulence states: Figure 54 depicts the turbulence measurements at position S9 during SOP2 in the summit area, covering the flights SBL2-6. SBL1 is omitted for clarity because of the one-week separation. It is apparent that the diurnal temperature amplitude decreased during the period, while the wind speed increased in general. The wind turned from NW over N to S and back to SSE. This coincides with the observed northeasterly movement of the high pressure system initially found almost over the summit region.

The lowest panel of Figure 54 shows an estimate for the turbulent heat flux and Figure 55 shows estimates for the turbulent momentum flux, for the variances of temperature, horizontal and vertical wind speed and for the stability parameter z/L. Note that the fluxes and all other turbulent quantities in this section have been computed for 15 min intervals using linear detrending and no additional corrections have been applied (like e.g. for device tilt or spurious data, as proposed by Mahrt, 1998). The turbulent fluxes exhibit quite small values during the very calm first day of the period. However, the slight negative values during midnight of day 190 (09 July) was associated with a significant surface fog (Table VII).
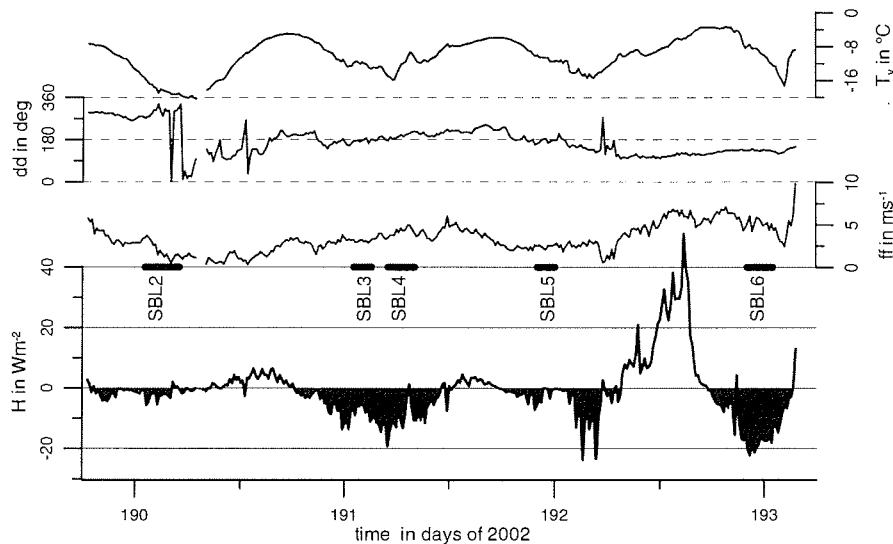

Figure 54.: Mean quantities measured at S9 by the sonic anemometer at 3 m height from 08 Jul 2002 18 UTC to 12 Jul 2002 09 UTC. The horizontal bars at the center of the figure mark the duration of the SBL flight missions. Displayed values are 15 min averages, data gaps result from icing, high snowdrift, or snowfall. Plotted are from top to bottom: virtual temperature (T_v, derived from the speed of sound), horizontal wind direction (dd) and speed (ff), and the turbulent sensible heat flux (H).
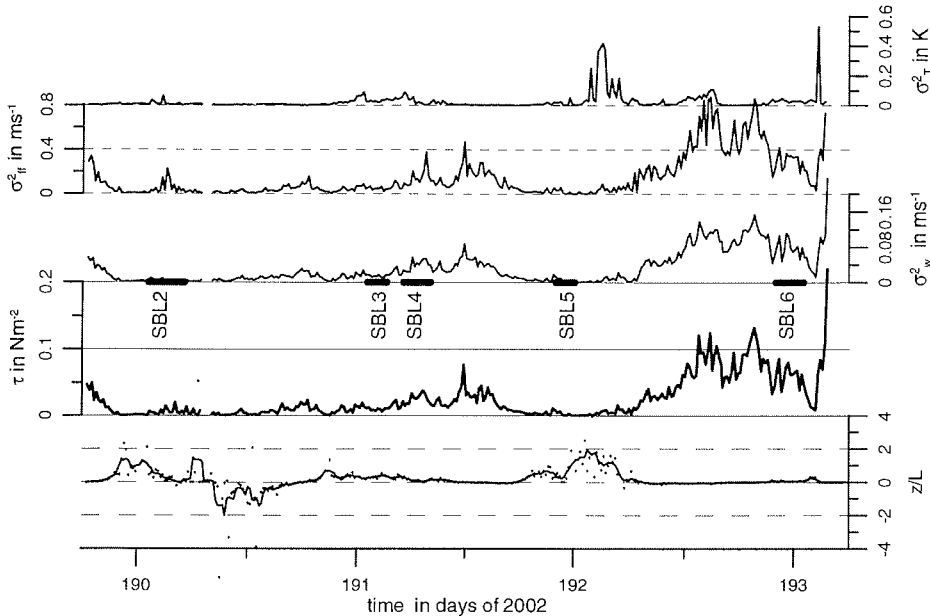
Figure 55.: As Figure 54, but the displayed values are (from top to bottom): variances of air temperature (σ_T^2), horizontal (σ_{ff}^2) and vertical (σ_w^2) wind speed, the turbulent momentum flux (τ), and the stability parameter $(z/L$, dots represent 15 min means, the line depicts a one-hourly running mean).

In general, turbulence was quite weak that night, as indicated by the small wind speed and temperature variances, and by strong stability values $(z/L$ up to $+6)$. One night later (during SBL3/4), the situation was quite different compared to the previous one. With about 4 ms^{-1} average wind speed, a pronounced PBL mixing took place. The result was a much stronger downward heat flux (roughly -10 Wm^{-2}), a higher momentum flux (τ), and considerable turbulence $(\sigma_{ff}^2, \sigma_w^2)$. The same applies for the night from day 192 to 193 (11/12 July), when the wind speed was even about 50% above the values found during the early morning of day 191 (10 July).

The most striking event visible from Figures 54 and 55 presumably is the strong peak in the temperature variance (σ_T^2) during the morning hours of day 192 (11 July), associated with strong stability $(z/L$ hourly average of almost $+2)$ and hardly any turbulence intensity $(\sigma_{ff}^2, \sigma_w^2)$.

To allow a closer look at this event, Figure 56 shows the measured values of the virtual temperature T_v, wind speed (ff) and direction (dd) and the vertical wind speed (w) for one hour (0100 - 0200 UTC) of the morning of day 192 (11 July). The record reveals pronounced intermittent turbulence. During the first twenty minutes (seconds 3600 to 4800), there is almost no turbulence. Suddenly around second 4800 (0120 UTC), the PBL apparently turns turbulent until approximately second 6300 (0145 UTC), when the flow gets near laminar again. Around second
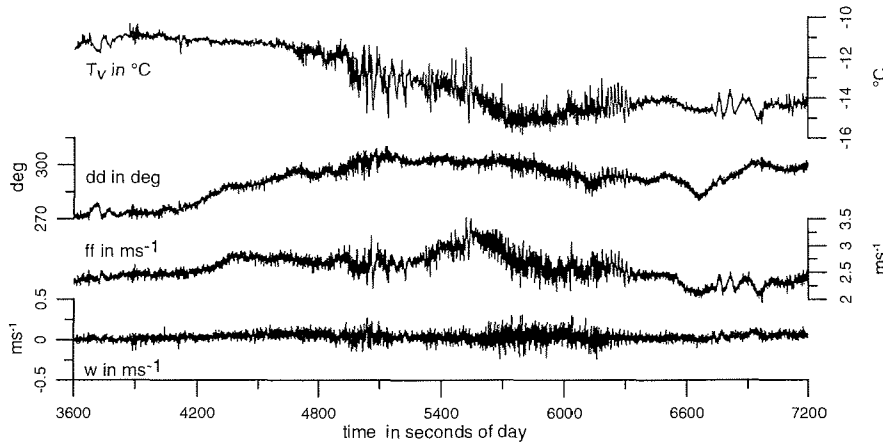
Figure 56.: Sample data of the sonic anemometer at S9 from 11 Jul 2002, 0100 to 0200 UTC. For clarity, only 2 Hz data sampled out of the 20 Hz measurements are plotted. The displayed data from top to bottom: virtual temperature (T_v, derived from the speed of sound), horizontal wind speed (ff) and direction (dd) and vertical wind speed (w). Note the varying states of turbulence.

6800 (0153 UTC) two oscillations in the temperature, horizontal wind and even the vertical wind record are visible. These indicate the presence of SBL waves. A wavelet transform of the temperature record from the most turbulent part of this hour (seconds 4500 to 6300, 0115 to 1045 UTC) is shown in Figure 57. The transform was done using a von-Hann windowed complex 2π-wavelet normalized to unity amplitude. This was chosen for best oscillation detection (Kumar and Foufoula-Georgiou, 1997). The analysis reveals three main episodes of oscillations: Approximately five minutes around second 5100 with an oscillation pe-
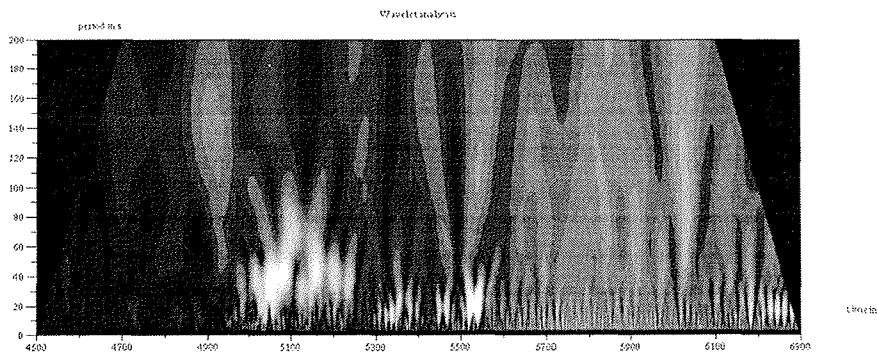

Figure 57.: Wavelet transform of the temperature timeseries measured by S9 during SBL5 (11 Jul 2002). The horizontal axis gives the time in seconds of day (4500 to 6300 s = 0115 to 0145 UTC), the vertical axis gives the oscillation period in seconds (0 to 200 s). The grayshade gives the modulus of the transform in arbitrary units (white = highest values).
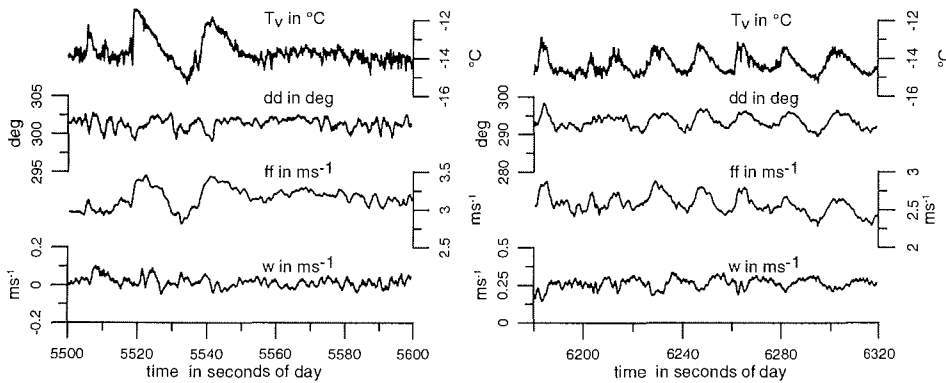
Figure 58.: Surface layer oscillations (right panel), and ramp structures (left panel). Both are enlarged segments from (Figure 56).

riod of 20 to 40 s, around second 5500 and after second 6200, both with periods around 20 s. Although between seconds 5600 and 6200 turbulence is strong (Fig. 56) no pronounced wave activity is detected. This suggest the presence of breaking waves, which would explain the slight decrease of the horizontal wind speed at this time due to increased friction.

An enlarged view of the periods around seconds 5500 and 6200 are shown in Figure 58. The right panel depicts a very clean wave motion, with the major oscillation in w shifted in phase by $\pi/2$ against ff and dd. This represents the signature of a gravity wave (Stull, 1976) with a period of approximately 20 s. A vertical temperature gradient of 5 K over 5 m was measured simultaneously at the Swiss Tower. This gradient implies a Brunt-Väisälä frequency of 0.04 Hz (25 s period), which is close to the period found at S9.

The left panel of Figure 58 shows ramp structures, which are similar to the structures seen at the edges of convective plumes called microfronts. In contrast to a leaving plume, here the ramp is reverse and corresponds to the sensor peeking into a warmer, faster moving portion of the flow. It is striking that there is no matching signal in the record of w. Hence, this feature deserves further inspection in the future.

4.3   Vertical structures - aircraft and tower measurements

As mentioned in the last section, the stable boundary layer turned out to be quite shallow during IGLOS. As an example, Figures 59 and 60 show data from case SBL2, where the winds were moderate and the SBL could be expected to be quite shallow.

The vertical profile of the air temperature T shows the typical behavior for a SBL. A strong vertical temperature gradient is found near the ground, a local temperature maximum near 200 m height and a slight decrease with height above. Note that in this case, the decrease is smaller than the dry-adiabatic temperature gradient, which implies considerably stable stratification even above the actual SBL.
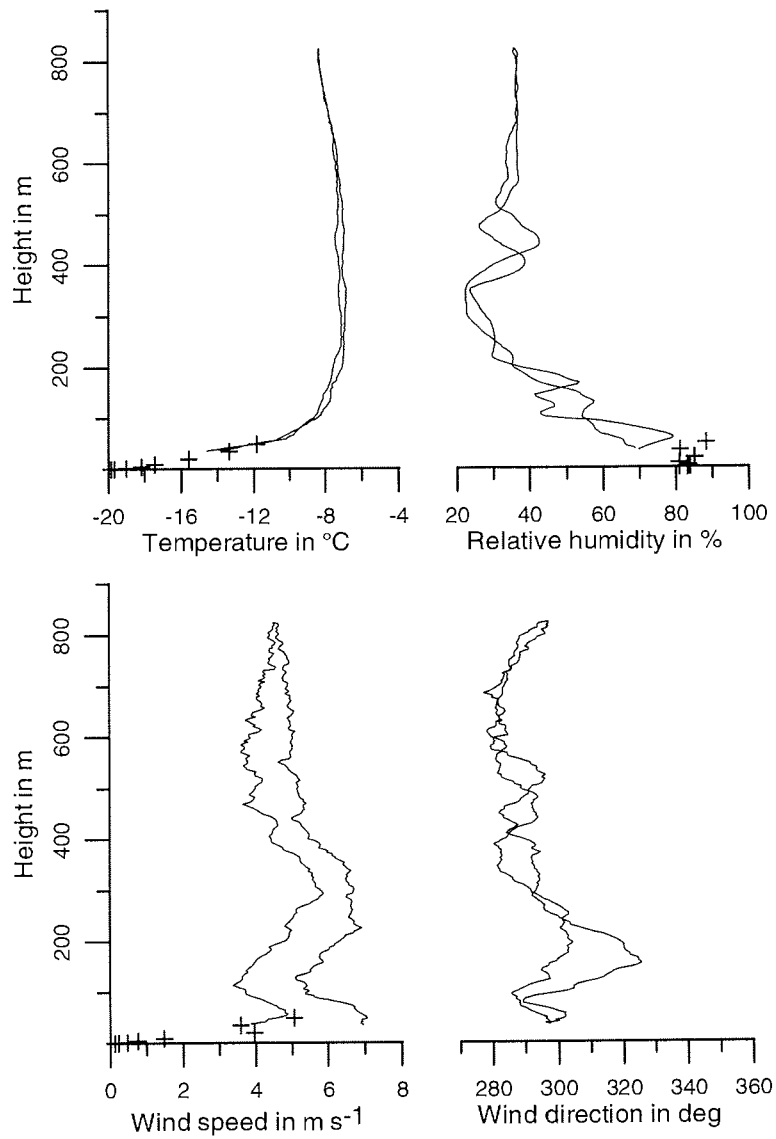
SBL2 Vertical Profiles Polar2 / Swiss tower

Figure 59.: Vertical profiles of mean quantities during SBL2 (09 Jul 2002, 0400 UTC): Lines depict aircraft data sampled at 1 Hz from the full resolution data, crosses mark measurements made by the Swiss Tower (10 min means). Plotted are from top left to bottom right: air temperature (T), relative humidity (rF), horizontal wind speed (ff) and direction (dd). The vertical axes give height (above surface level).
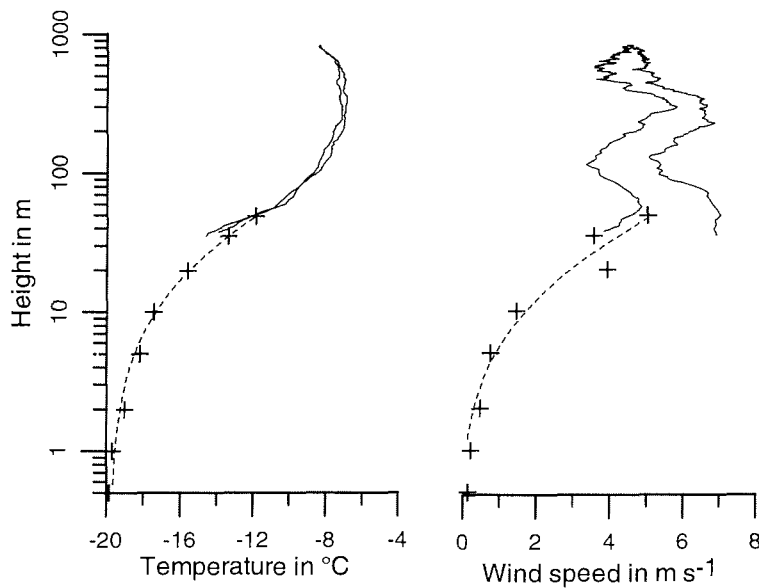
Figure 60.: Same data as Figure 59, except the vertical axis is logarithmic and only air temperature (T) and horizontal wind speed (ff) are displayed. A log-lin function was fitted to the tower data.

The horizontal wind speed (ff) profile shows a low-level jet (LLJ; Figure 59) of 5 to 8 ms^{-1} at 75 m.

Heinemann (2002) found the thermal boundary layer height h_T to be a good estimate for the SBL height, if h_T is defined as the level, where the surface inversion stability falls below 0.015 Km^{-1} (for potential temperature). For katabatic winds associated with pronounced LLJs, h_T corresponds to the height, where the turbulent kinetic energy (TKE) vanishes, while the height of the wind maximum (h_v) is located considerably lower. For SBL2, h_T and hence the thermal SBL height can be estimated to be around 150 m. This height should also correspond to the level of vanishing turbulence generated by the ground friction and/or wind shear. In the SBL2 data, h_v is around 75 m, as mentioned above. Hence both values (h_T and h_v) differ quite strongly in the present case.

The relative humidity (rF) is almost constant around 80% below 50 m (indicating the surface fog), but above it drops quickly to half that value at 200 m height because of the increase in temperature. The wind direction (dd) is in general 290° and veers to 300° in the LLJ (but turns back to 290° above).

One unusual feature is the yet undiscussed second wind speed maximum around 200 to 300 m height, in which the wind veers right to 300 to 320° and turns back to 290° above, like in the LLJ. This layer is topped by a relative humidity increase
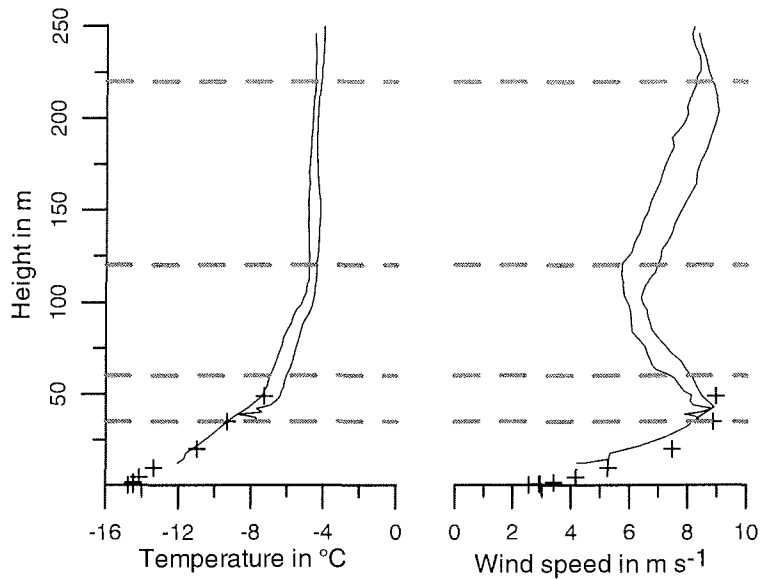
Figure 61.: Vertical profiles from SBL3 (10 Jul 2002, 0320 UTC): left panel gives air temperature (T), right panel gives horizontal wind speed (ff). Thin lines depict aircraft data, crosses mark measurements made by the Swiss Tower, horizontal dashed lines mark the heights of the constant level runs flown during SBL3.

of roughly 10%. The stratification in this layer is still much stronger than above ($\gtrsim 400$ m), but the temperature profile does not reveal any prominent structure at this level. Hence, this upper jet is probably caused by synoptic forcing and is not a part of the SBL.

Despite the height of the 50 m, data measured by the Swiss Tower alone would not be able to reveal such structures. This gets very obvious in semi-logarithmic representation of the same profiles (Fig. 60). No matter, which parameterization scheme will turn out to match best the measurements, most of them yield profiles for wind and temperature in the surface layer that are similar to a log-lin relation with height. Hence, a simple log-lin function is fitted to the data in Figure 60. In the vertical range of the Swiss Tower, the measured data indeed consistently exhibit a log-lin structure. But just above the tower height, at approximately 50 to 75 m, the curvatures of both profiles (T and ff) change abruptly. This impressingly demonstrates, that even in such a not very windy situation like SBL2, the whole SBL could not be explored without the help of a research aircraft.

In the case of SBL3, the wind was $\approx 30\%$ stronger than during SBL2 (Table VII). The lower part of the vertical profiles of T and ff measured during SBL3
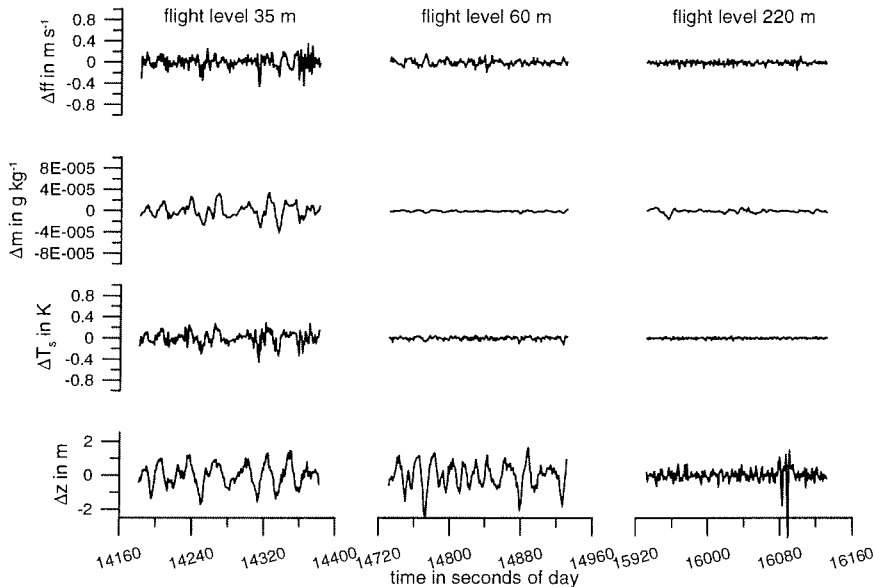
Figure 62.: Horizontal profiles from SBL3 (10 Jul 2002, 0350-0435 UTC): Values are high-pass filtered by an approximative Gauss-filter with 30 s cutoff to eliminate variations by aircraft movements across vertical gradients. The left column shows values from 35 m flight level, the middle one from 50 m and the right column from 220 m. The uppermost row shows horizontal wind speed (ff) variations, the second row shows mixing ration (m) variations, the third row shows static temperature (T_s) variations, and the lowest row shows the remainder of the aircraft movements after filtering. Note that the vertical axes have the same scale for all columns and that the horizontal axes have all the same length.

is displayed in Figure 61. Again, both profiles show a strong vertical gradient in the lowest 50 m. In case of the wind speed, again a log-lin-like structure can be seen. A LLJ of about 9 ms^{-1} is found at 50 m. On top of the LLJ, the temperature shows a weaker gradient, but temperature still increases with height up to roughly 110 m height, where the wind speed reaches a local minimum of approximately 6 ms^{-1}. Above this level, air temperature is almost constant and the wind speed slightly increases with height. Hence, the h_T in this case may be estimated to be about 120 m, which is slightly lower than during SBL2. The strength of the surface inversion is roughly 40 % weaker compared to SBL2, as is expected from to the more intense mechanical mixing done by the stronger wind.

Usually one would expect to find strong turbulence activity at levels of increased wind shear, i.e. where the wind speed gradient is strong. Figure 62 shows measurements made by the aircraft on three of the four constant-level runs done along the leg B1-B2 (Table X). The heights of all four runs are marked in Figure 61. The data were high-pass filtered with a fast, approximative Gauss filter with 30 s cutoff (corresponding to $\approx$ 2 km wavelength) to eliminate variations in the measured quantities caused by aircraft movements across the strong vertical gradients.
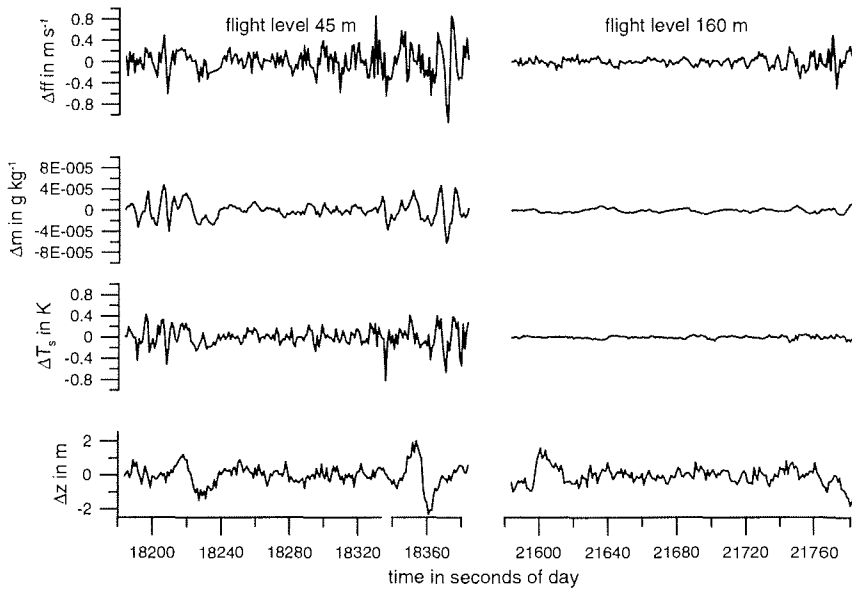
Figure 63.: Horizontal profiles from SBL1 (04 Jul 2002, 0500-0610 UTC): Same representation as Figure 62, except that data are filtered with 60 s cutoff (due to less aircraft movements) and only two flight levels are displayed.

At the lowest level (35 m), the flow is rather turbulent, as expected. The temperature variance is $\sigma_T^2 \approx 0.04$ K^2, the mixing ratio variance is $\sigma_m^2 \approx 2.0 \cdot 10^{-10}$ and the vertical wind variance is $\sigma_w^2 \approx 0.003$ m^2s^{-2}. Just 15 m higher and just above the wind speed maximum, wind shear is approximately as strong as at 35 m, and the temperature gradient is still about half of the gradient at 35 m. The flow, however, turns out to be nearly laminar: The temperature, humidity and wind speed records are almost even. (Note that the aircraft height variations remaining after filtering are of the same order as at 35 m and the vertical gradients are similar.) The temperature variance has dropped by 80% to $\sigma_T^2 \approx 0.0025$ K^2, the mixing ratio variance to $\sigma_m^2 \approx 1.7 \cdot 10^{-12}$ and the vertical wind variance to $\sigma_w^2 \approx 0.002$ m^2s^{-2}. At 220 m, above the SBL, the picture is similar and the variances of T and w are even smaller ($\sigma_T^2 \approx 0.0014$ K^2 and $\sigma_w^2 \approx 0.0009$ m^2s^{-2}), while the mixing ratio variance is slightly increased ($\sigma_m^2 \approx 1.0 \cdot 10^{-11}$), possibly due to humidity advection in the free atmosphere.

This striking behavior of the turbulence almost vanishing even at low heights near the LLJ wind maximum is not unique to the particular case SBL3. For example, it is found during SBL1, too. Figure 63 shows measurements made on the leg B1-B2 (Table VIII) during constant level runs at 45 and 160 m height. In this case, filtering with a cutoff period of 60 s ($\hat{=}$ 4 km) was sufficient to eliminate most of the disturbing influences by vertical aircraft motions. During SBL1, a temperature

maximum of -9° and a local wind speed maximum of 12 ms^{-1} were found at 100 m height. Above, the temperature dropped with height (but again less than dry adiabatic), while the wind dropped to 8 ms^{-1} at 300 m an showed a slight increase with height above that level. Hence, at both levels (45 and 160 m) significant wind shear and a vertical wind gradient were present. At 45 m, turbulence was quite active with $\sigma_T^2 \approx 0.04$ K^2 and $\sigma_w^2 \approx 0.02$ m^{2}s^{-2}. In contrast, at 160 m the turbulence was again very weak ($\sigma_T^2 \approx 0.0006$ K^2 and $\sigma_w^2 \approx 0.008$ m^{2}s^{-2}) indicating an almost laminar flow. Note that in Figure 63 it can be seen, that to the end of the 160 m run, the records of T, m and ff exhibit stronger fluctuations than over the first half of that run. This indicates, that the flow was just at the transition from an almost laminar to a turbulent state.

4.4 Summary

Six SBL flight missions could be performed successfully. Unexpected problems with the aircraft instrumentation at the beginning of the IGLOS period and exceptionally warm weather in the summit region at the end of the period unfortunately did not allow more flight missions. The successful flights, however, cover a quite wide range of different synoptic framework conditions (Table VII). The first results presented in this chapter are based on raw data (without further quality control applied) in the case of surface measurements and are based on 1 Hz quicklook data (sampled from the up to 100 Hz measurements and converted using preliminary calibration parameters) in the case of aircraft data.

Detailed, quantitative studies will be possible as soon as the finally calibrated full resolution data from the aircraft and the quality controlled surface measurements by the Swiss and U.S. research partners become available. The full profile analysis of these data is expected to be a challenging task because most of the available measurement principles and processing methods are pushed to their limits.

In all cases well developed stable boundary layers were found. The thickness of these SBLs were mostly below the values suggested from previous studies (e.g. after Handorf et al., 1999). The SBLs found during IGLOS were also thinner than the SBLs found during KABEG (Heinemann, 1998).

Furthermore, the turbulence activity turned out to become extremely low at very limited heights. The stacked, multistory structures of the PBL in some of the cases suggest that the synoptic situation and possibly even the extremely weak orographic gradient have to be considered interpreting the data.

A   Abbreviations

Abbreviation	Explanation
ACSYS	Arctic Climate Systems Study
ATC	Air Traffic Control
AVHRR	Advanced Very High Resolution Radiometer
AWI	Alfred-Wegener-Institut für Polar- und Meeresforschung
AWS	Automatic Weather Station
BGSF	ICAO code for Kangerlussuaq
CDC	Climate Diagnostic Center
CIRES	Cooperative Institute for Research in Environmental Sciences
DAAC	Distributed Active Archive Center
DEM	Digital Elevation Model
DFG	Deutsche Forschungsgemeinschaft
DLR	Deutsches Zentrum für Luft- und Raumfahrt
DMI	Danish Meteorological Institute
DPC	Danish Polar Center
ECHAM	ECMWF-Model Extended and Modyfied in Hamburg
ECMWF	European Center for Medium Range Weather Forecast
EOSDIS	Earth Observing System Data and Information System
ETH	Eidgenössische Technische Hochschule
GAC	Global Area Coverage
GC-Net	Greenland Climatological (AWS) Network
GLOBE	Global Land One-km Base Elevation
GPS	Global Positioning System (NAVSTAR)
GTS	Global Telecommunication System
HRPT	High Resolution Picture Transmission
IACETH	Institute for Atmospheric and Climate Science of ETH Zürich
ICAO	International Civil Aviation Organization
IGLOS	Investigation of the Greenland boundary Layer Over Summit
INS	Inertial Navigation System
KABEG	Katabatic Wind and Boundary Layer Front Experiment around Greenland
LES	Large Eddy Simulation
LLJ	Low Level Jet
METAR	METeorological report - Aviation Routine
MIUB	Meteorologisches Institut der Universität Bonn
NESDIS	U.S. National Satellite, Data, and Information Service
NGDC	U.S. National Geophysical Data Center
NOAA	U.S. National Oceanic and Atmospheric Administration
NSF	U.S. National Science Foundation
NSIDC	U.S. National Snow and Ice Data Center
PBL	Planetary boundary layer
SAA	Satellite Active Archive

|	
SAR	Synthetic aperture Radar
SBL	Stable boundary layer
SBL1-6	Flight mission 1 to 6 at Summit Camp (dates see Section 2.2)
SFJ	airport code for Kangerlussuaq
SOP1-3	Special Observation Period 1 to 3 (dates see Section 2.2)
ST	Swiss Tower
TKE	Turbulent Kinetic Energy
U.S.	United States of America
WMO	World Meteorological Organization

B   References

References

Andreas, E. L.: 1987, 'A theory for the scalar roughness and the scalar transfer coefficient over snow and ice'. *Boundary Layer Meteorol.* **38**, 159 – 184.

Bintanja, R.: 2000, 'Snowdrift suspension and atmospheric turbulence. Part I: Theoretical background and model description'. *Boundary Layer Meteorol.* **95**, 343 – 368.

Bromwich, D. H., J. J. Cassano, T. Klein, G. Heinemann, and K. M. Hines: 2001, 'Mesoscale Modelling of Katabatic Winds Over Greenland with Polar MM5'. *Mon. Wea. Rev.* **129**, 2290 – 2309.

Cassano, J. J., T. R. Parish, and J. C. King: 2001, 'Evaluation of Turbulent Surface Flux Relationships for the Stable Surface Layer over Halley, Antarctica'. *Mon. Wea. Rev.* **129**, 26 – 46.

Ekholm, S.: 1996, 'A full coverage, high-resolution, topographic model of Greenland, computed from a variety of digital elevation data'. *J. Geophys. Res.* **B10**, 21961 – 21972.

Forrer, J.: 1999, 'The structure and turbulence characteristics of the stable boundary layer over the Greenland ice sheet'. *Züricher Klimaschriften* **75**, 1 – 132.

Forrer, J. and M. W. Rotach: 1997, 'On the structure in the stable boundary layer over the Greenland ice sheet'. *Boundary Layer Meteorol.* **85**, 111 – 136.

Greuell, W. and T. Konzelmann: 1994, 'Numerical modelling of the energy balance and the englcacial temperature of the Greenland ice scheet'. *Glob. and Planet. Change* **9**, 91 – 114.

Handorf, D.: 1996, 'Zur Parameterisierung der stabilen atmosphärischen Grenzschicht über einem antarktischen Schelfeis'. *Reports on Polar Research* **204**, 1 – 133.

Handorf, D., T. Foken, and C. Kottmeier: 1999, 'The stable atmosphere boundary layer over an antarctic ice sheet'. *Boundary Layer Meteorol.* **91**, 165 – 189.

Hastings, D. A. and P. K. Dunbar: 1998, 'Development & Assessment of the Global Land One-km Base Elevation Digital Elevation Model (GLOBE)'. *ISPRS Archives* **32**(4), 218 – 221.

Heinemann, G.: 1989, 'Über die Rauhigkeitslänge z_0 der Schneeoberfläche des Filchner Rønne Schelfeises'. *Polarforschung* **59**, 17 – 24.

Heinemann, G.: 1998, 'Katabatic wind and Boundary Layer Front Experiment around Greenland ("KABEG 97")'. *Reports on Polar Research* **269**, 1 – 94.

Heinemann, G.: 2002, 'Aircraft-based measurements of turbulence structures in the katabatic flow over Greenland'. *Boundary Layer Meteorol.* **103**, 49 – 81.

Högström, U.: 1988, 'Non-dimensional wind and temperature profiles in the atmospheric surface layer: a re-evaluation'. *Boundary Layer Meteorol.* **42**, 55 – 78.

Jordan, R.: 1991, 'One-dimensional Temerature Model for a Snowcover. Technical Documentation for Sntherm'. *CRREL Special Report* **657**, 1 – 136.

Klein, T.: 2000, 'Katabatic Winds over Greenland and Antarctica and their interaction with Mesoscale and Synoptic-scale Weather Systems: Investigations using three-dimensional numerical Models'. *Bonner Meteorologische Abhandlungen* **53**, 1 – 146.

König, G.: 1985, 'Roughness length over an Antarctic ice shelf'. *Polarforschung* **55**, 27 – 32.

Kumar, P. and E. Foufoula-Georgiou: 1997, 'Wavelet analysis for geophysical applications'. *Rev. Geophys.* **35**, 385 – 412.

Lehning, M., P. Bartelt, B. Brown, T. Russi, U. Stöckli, and M. Zimmerli: 1999, 'SNOWPACK model calculations for avalanche warning based upon a new network of weather and snow stations'. *Cold Reg. Sci. Technol.* **30**, 145 – 157.

Mahrt, L.: 1998, 'Flux Sampling Errors for Aircraft and Towers'. *J. Atmos. Ocean. Technol.* **15**, 416 – 429.

Meesters, A., N. Bink, E. Henneken, H. Vughts, and F. Cannemeijer: 1997, 'Katabatic wind profiles over the Greenland ice sheet: observation and modelling'. *Boundary Layer Meteorol.* **85**, 475 – 496.

Nieuwstadt, F. T. M.: 1984, 'The Turbulent Structure of the Stable, Nocturnal Boundary Layer'. *J. Atmos. Sci.* **41**, 2202 – 2216.

NSIDC: 1997, *Digital SAR Mosaic and Elevation Map of the Greenland Ice Sheet*, Digital data available from nsidc@nsidc.org. NSIDC Distributed Active Archive Center, University of Colorado at Boulder, Boulder, Colorado.

Oerlemans, J. and H. Vugts: 1993, 'A meteorological experiment in the ablation zone of the Greenland ice sheet'. *Bull. Amer. Meteor. Soc.* **74**, 355 – 365.

Rowe, C., K. Kuivinen, and R. Jordan: 1995, 'Simulation of summer snowmelt on the Greenland ice sheet using a one-dimensional model'. *J. Geophys. Res.* **D8**, 256 – 273.

Steffen, K. and J. Box: 2001, 'Surface Climatology of the Greenland ice sheet: Greenland Climate Network'. *J. Geophys. Res.* **106**, 33951 – 33964.

Steffen, K., J. E. Box, and W. Abdalati: 1996, 'Greenland Climate Network: GC-Net'. In: S. C. Colbeck (ed.): *Glaciers, Ice Sheets and Volcanoes, trib. to M. Meier*, Vol. 96-27 of *CRREL Special Report*. pp. 98 – 103.

Stull, R. B.: 1976, 'Internal gravity waves generated by penetrative convection'. *J. Atmos. Sci.* **33**, 1279 – 1286.

Van den Broeke, M. R., P. G. Duynkerke, and J. Oerlemans: 1994, 'The observed katabatic flow at the edge of the Greenland ice sheet during GIMEX-91'. *Glob. and Planet. Change* **9**, 3 – 15.

Webb, E. K.: 1970, 'Profile relationships: The log-linear range, and extension to strong stability'. *Quart. J. R. Met. Soc.* **96**, 67 – 90.

Zilitinkevich, S. and P. Calanca: 2000, 'An extended similarity theory for the stably stratified atmospheric surface layer'. *Quart. J. R. Met. Soc.* **126**, 1913 – 1923.

Zilitinkevich, S. and D. V. Mironov: 1996, 'A Multi-Limit Formulation for the Equilibrium Depth of a Stably Stratified Boundary Layer'. *Boundary Layer Meteorol.* **81**, 325 – 351.
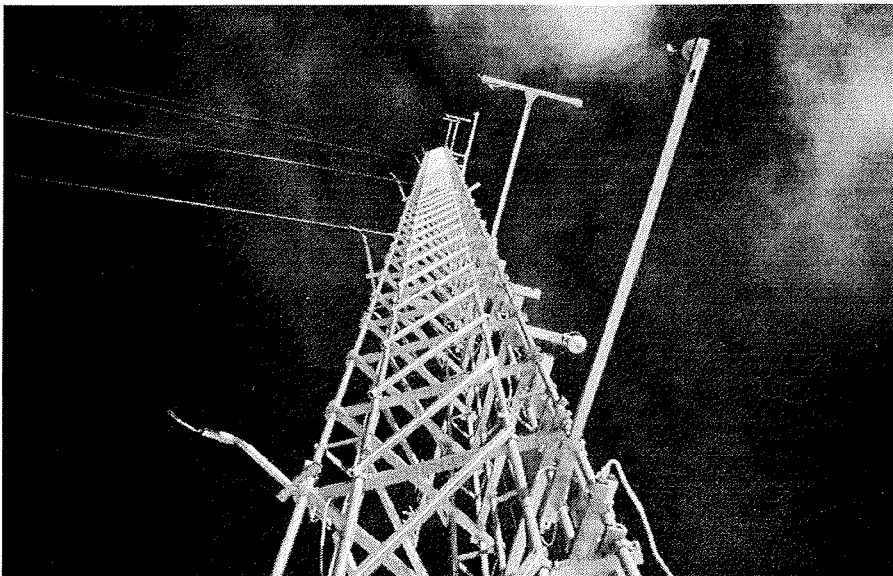
C Pictures

Figure 64.: POLAR2 Research aircraft parked at summit camp
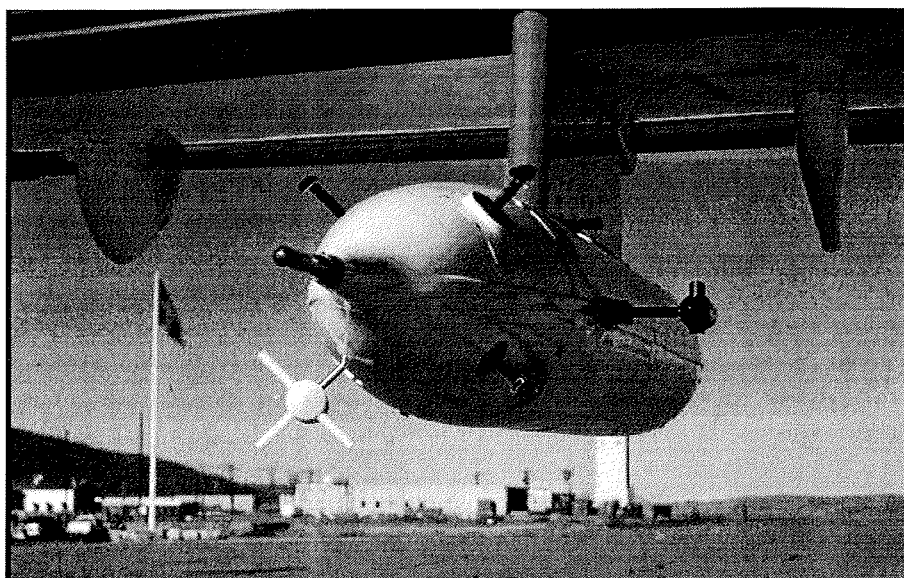
Figure 65.: METEOPOD turbulence measurement system, left front view
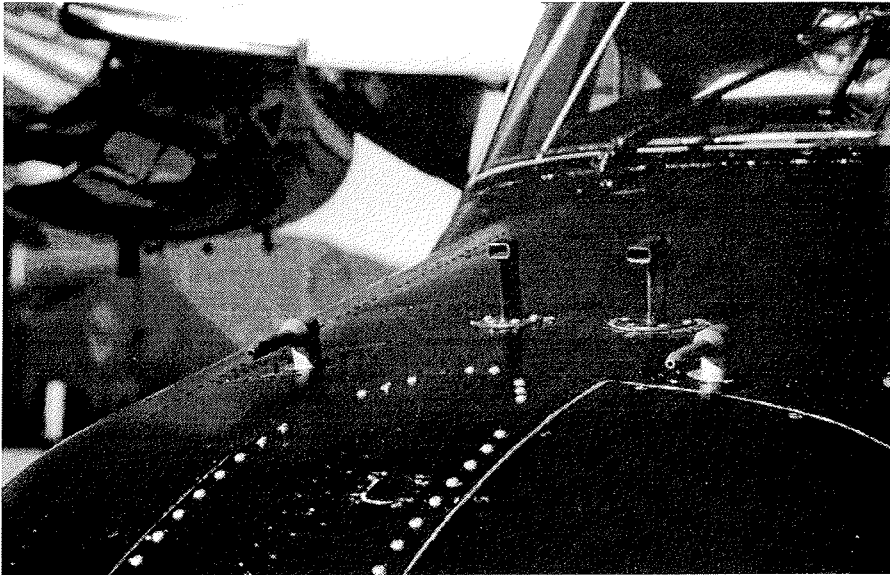
Figure 66.: POLAR2 basic meteorologic instrumentation
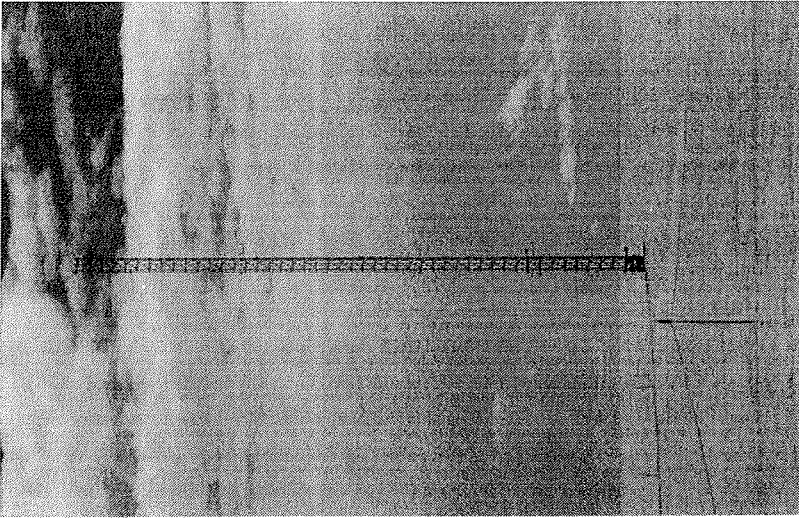

Figure 67.: View up the Swiss Tower at Summit Camp

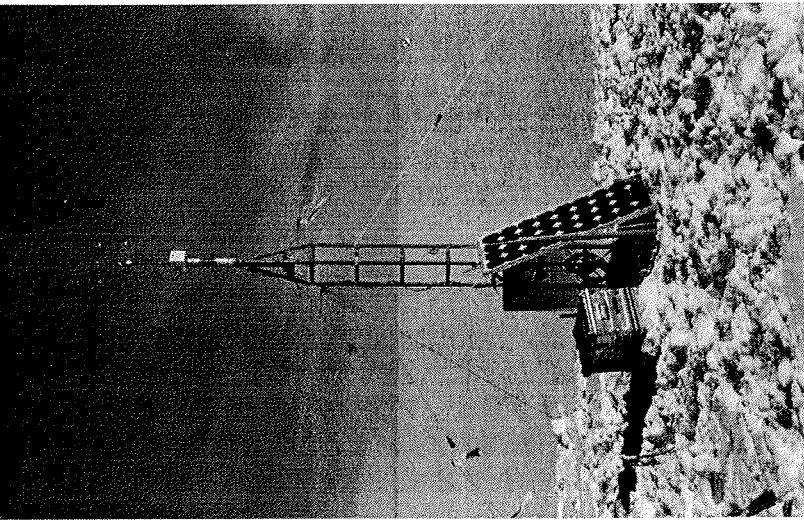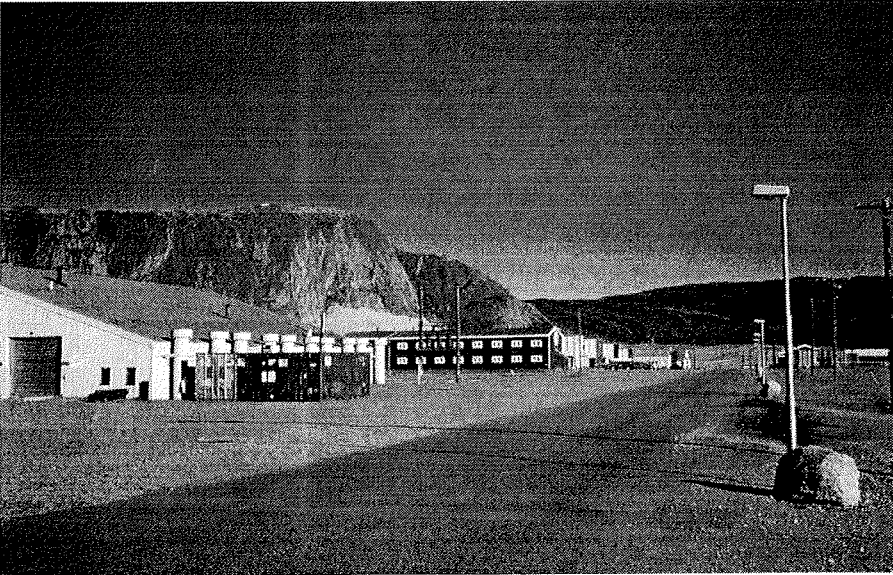*Figure 68.*: Swiss Tower at Summit Camp, seen from northwest

Figure 69.: Station S9, view from northwest

Figure 70.: Kangerlussuaq, accommodation buildings and Black Ridge seen from the airport

Figure 71.: View of the Summit Camp from north (taken from POLAR2 flying at 45 m height)